



Smithian ammonoid faunas from northeastern Nevada: implications for Early Triassic biostratigraphy and correlation within the western USA basin.

Romain Jattiot, Hugo Bucher, Arnaud Brayard, Morgane Brosse, James F. Jenks, Kevin G. Bylund

► To cite this version:

Romain Jattiot, Hugo Bucher, Arnaud Brayard, Morgane Brosse, James F. Jenks, et al.. Smithian ammonoid faunas from northeastern Nevada: implications for Early Triassic biostratigraphy and correlation within the western USA basin.. *Palaeontographica A*, 2017, 309 (1-6), pp.1-89. 10.1127/pala/2017/0070 . hal-01585001

HAL Id: hal-01585001

<https://hal.science/hal-01585001v1>

Submitted on 18 Feb 2025

HAL is a multi-disciplinary open access archive for the deposit and dissemination of scientific research documents, whether they are published or not. The documents may come from teaching and research institutions in France or abroad, or from public or private research centers.

L'archive ouverte pluridisciplinaire **HAL**, est destinée au dépôt et à la diffusion de documents scientifiques de niveau recherche, publiés ou non, émanant des établissements d'enseignement et de recherche français ou étrangers, des laboratoires publics ou privés.



Distributed under a Creative Commons Attribution 4.0 International License

Smithian ammonoid faunas from northeastern Nevada: implications for Early Triassic
biostratigraphy and correlation within the western USA basin.

ROMAIN JATTIOT^{1,2}, HUGO BUCHER¹, ARNAUD BRAYARD², MORGANE BROSSE¹, JAMES F.
JENKS³ and KEVIN G. BYLUND⁴.

¹Paläontologisches Institut der Universität Zürich, Karl Schmid-Strasse 4, 8006, Zürich,
Switzerland; e-mail: roman.jattiot@pim.uzh.ch

²UMR CNRS 6282 Biogéosciences, Université de Bourgogne Franche-Comté, 6 boulevard
Gabriel, 21000 Dijon, France

³1134 Johnson Ridge Lane, West Jordan, Utah 84084, United States of America

⁴140 South 700 East, Spanish Fork, Utah 84660, United States of America

Abstract

Intensive sampling of the lower portion of the Thaynes Group within the Palomino Ridge area (northeastern Nevada) yielded abundant and well-preserved Smithian (Early Triassic) ammonoid faunas. Ammonoid taxonomy and a detailed biostratigraphy for this locality are reported herein. One new genus (*Palominoceras*) and one new species (?*Pseudosageceras bullatum*) are described.

Additionally, based on new data from Palomino Ridge and previous data from neighboring localities in Utah, we provide here the first quantitative Smithian ammonoid biochronological scheme for the western USA basin. This new zonation is based on the Unitary Associations (UA) method. The biochronological sequence comprises five unitary association zones that can be correlated with other localities from the Northern Indian Margin (Salt Range, Pakistan; Spiti northern India; and Tulong, South Tibet). Three unitary association zones (UAZ₁, UAZ₂ and UAZ₃) are defined for the early Smithian, one (UAZ₄) spans the entire middle Smithian

and one (UAZ_5) comes into the first part of the late Smithian. Finally, a provisional UAZ_6 would represent the second part of the late Smithian.

Key words: Ammonoids, Early Triassic, Smithian, Nevada, Biochronology.

Contents

Introduction	3
Geological setting	4
Ammonoid zonation in the western USA Basin.....	6
Quantitative biochronology (Unitary Associations).....	6
Systematic Palaeontology	11
Acknowledgements	68
References	69
List of the described ammonoids	86
Explanation of the plates	88

Introduction

In the aftermath of the Permian-Triassic boundary mass extinction (about 251.9 Ma, BURGESS et al. 2014), ammonoids recovered very fast in comparison with many other marine clades (BRAYARD et al. 2009a, ZAKHAROV & ABNAVI 2013, ZAKHAROV & POPOV 2014, BRAYARD & BUCHER 2015). Following low values in the Griesbachian, taxonomic richness shows 1) a first modest peak in the early Dienerian; 2) low values persisting throughout the middle Dienerian; 3) a very modest increase during the late Dienerian and 4) a first marked increase in the early Smithian (BRÜHWILER et al. 2010a, WARE et al. 2015). The Smithian is a crucial time interval, recording the first global, major diversification-extinction cycle after the Permian-Triassic boundary mass extinction (BRAYARD et al. 2006, BRÜHWILER et al. 2010a). Early and middle Smithian corresponds to the main rediversification of ammonoids and conodonts (e.g., BRAYARD et al. 2006, 2009a, 2011; ORCHARD 2007), whereas the late Smithian (sensu BRÜHWILER et al. 2010a; c. 1.4 myr after the Permian-Triassic boundary mass extinction, OVTCHAROVA et al. 2006, 2015; GALFETTI et al. 2007, BURGESS et al. 2014) witnessed the most severe intra-Triassic crisis for the nekton. This late Smithian extinction as it affected ammonoids and conodonts was of equal or larger magnitude than that of the Permian-Triassic crisis (BRÜHWILER et al. 2010a); and it is concomitant with the inception of a global positive shift of the carbon cycle (Text-fig. 1; GALFETTI et al. 2007) and a quick ecological recovery of gymnosperms that followed the middle Smithian C-isotope negative peak and spore spike, respectively (HERMANN et al. 2011).

Our knowledge of Smithian ammonoids has significantly increased thanks to a number of recent studies from various basins including the Guangxi Province, South China (BRAYARD & BUCHER 2008); South Primorye, Russia (ZAKHAROV et al. 2002, SHIGETA & ZAKHAROV 2009,

SHIGETA et al. 2009, ZAKHAROV et al. 2013, SHIGETA & KUMAGAE 2015); Tulong, South Tibet (BRÜHWILER et al. 2010b); Oman (BRÜHWILER et al. 2012a); the Salt Range, Pakistan (BRÜHWILER et al. 2012b) and Spiti (BRÜHWILER et al. 2012c).

Since the pioneering contributions of SMITH (1904), HYATT & SMITH (1905), MATHEWS (1929) and SMITH (1932), the western USA basin is also recognized as including an excellent record of Early Triassic ammonoids. Numerous more recent studies have especially focused on the description of the abundant and well-preserved ammonoid faunas from the Lower Triassic Thaynes Group (e.g., KUMMEL & STEELE 1962, SILBERLING & TOZER 1968, GARDNER & MAPES 2000, JENKS 2007, BRAYARD et al. 2009b, 2013; GUEX et al. 2010, JENKS et al. 2010, 2013; STEPHEN et al. 2010).

Our recent intensive field investigation of the Lower Triassic Thaynes Group at Palomino Ridge (Elko County, northeastern Nevada) has yielded abundant, well-preserved Smithian ammonoid faunas, and shown that Palomino Ridge probably represents one of the most complete middle-to-late Smithian ammonoid successions in northeastern Nevada.

Understanding the mechanisms underlying the Early Triassic biotic recovery also requires an accurate and robust Smithian regional biostratigraphical framework that likely has worldwide correlation. By means of the Unitary Associations method (GUEX 1991), biochronological data from Nevada (this work) and Utah (BRAYARD et al. 2013) has enabled the construction of a key Smithian ammonoid biochronology for the low latitudes in eastern Panthalassa.

Geological setting

The Sonoma Foreland Basin of western USA represents a unique key study area located at a near-equatorial position in eastern Panthalassa during the Early Triassic (Text-fig. 2). The alternating limestones and shales of the Lower Triassic Thaynes Group (*sensu* LUCAS et al. 2007a) reflect deposition within the relatively shallow Sonoma Foreland Basin and generally

include both the Smithian and the Spathian substages. Smithian marine deposits are widely distributed within a large area covering southeastern Idaho, Utah and northeastern Nevada (Text-fig. 3A), thinning from the northwest to southeast across Utah, where they interfinger with terrestrial sediments of the Moenkopi Group (*sensu* LUCAS et al. 2007a). BRAYARD et al. (2013) recently described Smithian sedimentary successions and associated ammonoid faunas from Utah, thus yielding a new detailed biostratigraphical scheme for this area.

Here, we focus on Smithian exposures from the Palomino Ridge locality, whose stratigraphic successions and associated faunas have never been described till now. Yet, SMITH (1932) first reported Smithian ammonoids from the Phelan Ranch locality, about 5 km SW of Palomino Ridge (Text-fig. 3). The Palomino Ridge locality was discovered in 1967 by SILBERLING (unpublished field notebook), who mentioned *Anasibirites* from this locality.

Palomino Ridge is a ~ 5 km long, ~ 2.5 km wide, NNW-SSE trending monoclonal structure dipping to the east, and is located about 15 km NW of Currie in Elko County (Text-fig. 3).

Overlying the Gerster Formation of Permian age, the Smithian deposits consist of a thick sequence of interbedded shales and thin-bedded limestones, and thicker limestone beds (Text-fig. 4). The base of the Smithian crops out intermittently near the base of the ridge along its northeastern side. Due to the high proportion of shales, exposures of Smithian strata are relatively poor on the gullied eastern slope of Palomino Ridge. Nevertheless, based on bed-by-bed correlation between the main section and PLR9, PLR24, PLR73, PLR87, PLR94 sections (Text-fig. 3B), we constructed a composite section ('Section 1', Text-fig. 4) representing an expanded ammonoid succession with highly fossiliferous strata that resembles the succession described from the Confusion and Pahvant Ranges (Utah) by BRAYARD et al. (2009b, 2013) and STEPHEN et al. (2010), with the exception of the early Smithian beds. In addition, we constructed a second composite section ('Section 2'; Text-Fig. 5), based on bed-by-bed correlation between the PLR43 and PLR34 sections (Text-fig. 3B) that provides a very

detailed late middle to late Smithian succession. We then correlated this ‘Section 2’ with the uppermost part of ‘Section 1’ (Text-fig. 5).

Ammonoid zonation in the western USA basin

Originally described from southeastern Idaho (PEALE in WHITE [1879]) and commonly used as a regional Smithian time-marker, the *Meekoceras gracilitatis* Zone probably represents the most famous Smithian ammonoid fauna of the western USA basin. JENKS et al. (2010) emphasized that the *M. gracilitatis* Zone is essential for correlation between eastern and western Panthalassa (e.g., South China), and between low and high paleolatitudes (e.g., British Columbia and the Canadian Arctic). The co-occurrence of several ammonoid genera on opposite sides of the Panthalassa indicates significant faunal exchanges at that time (BRAYARD et al. 2007b, 2009c; JENKS et al. 2010, BRAYARD et al. 2013, BRAYARD & BUCHER 2015, SHIGETA & KUMAGAE 2015). Recently, BRAYARD et al. (2013) provided a comprehensive distribution of ammonoid faunas throughout the Smithian of the Thaynes and Moenkopi Groups in Utah, encompassing 12 assemblages (BRAYARD et al. 2013, fig. 14). The available zonation for Smithian ammonoid faunas from Nevada by SILBERLING & TOZER (1968) and revised by JENKS et al. (2010) only considered in ascending order, the *Meekoceras gracilitatis* Zone (including most of the middle Smithian), and the *Anasibirites* and *Glyptophiceras* beds (both representing the late Smithian). Biostratigraphical data for Nevada were therefore very scarce and only a few detailed correlations were established between the Utah and Nevada localities.

Quantitative biochronology (Unitary Associations)

We provide here for the first time a quantitative Smithian ammonoid biochronological scheme for the western USA basin (including Utah and Nevada localities) by means of the Unitary Associations method (UAs method, GUEX 1991). This method and its applications are described in detail in GUEX (1991), SAVARY & GUEX (1991, 1999), ANGIOLINI & BUCHER (1999), MONNET & BUCHER (2002), MONNET et al. (2011, 2015), GUEX et al. (2015) and BROSSE et al. (2016). Our data set includes Smithian ammonoid distributions from Palomino Ridge (Nevada), the Confusion Range, Pahvant Range, Mineral Mountains, Star Range, Cedar City, Kanarraville, Torrey and San Rafael Swell (Utah; BRAYARD et al. 2013). Taxonomy was standardized by directly comparing original specimens from Utah and Nevada. For subsequent biochronological analyses, taxa with uncertain taxonomic assignment and endemic species (found in only one locality) have been omitted from the data set. This led to the removal of 42 out of 67 taxa (62.7%), which were reinjected into the data set after the biochronological analyses.

The optimal result (Text-fig. 6A) produces a biozonation with 6 preliminary unitary associations (UAs). However, UA₅ almost entirely includes UA₄, the only difference being that *A. tuberculatum* is present in UA₄ but absent in UA₅ (both UAs of middle Smithian age). Since *A. tuberculatum* is known to occur up to the uppermost part of the middle Smithian at Crittenden Springs, Nevada (JENKS et al. 2010), we consider its absence in UA₅ as a sampling bias and therefore decided to merge UA₄ and UA₅. The initial sequence of six UAs is thus reduced to a sequence of 5 UA zones (UAZs; Text-fig. 6B) of higher lateral reproducibility (Text-fig. 7).

From the composition of the UAZs (Text-fig. 6B), we identify their characteristic species or pair of species and we formally define the UAZs as including the full range of these species. Identifying any characteristic species or pair of species in a given sample allows for identifying unambiguously the corresponding UAZ. Synthetic range charts showing the

biochronological distribution of Smithian ammonoid species (including taxa with uncertain taxonomic assignment and endemic species) and genera of the western USA basin are also given in Text-figure 8.

-UAZ₁

Content: See Text-fig. 8A.

Characteristic species: *Meekoceras olivieri*.

Age: early Smithian. Correlative of the *Meekoceras olivieri* beds from Utah (BRAYARD et al. 2013).

UAZ₁ is composed of only one species (*Meekoceras olivieri*), which is not shared with the Northern Indian Margin (NIM). The genus *Kashmirites* apparently does not occur in UAZ₁. Therefore, we tentatively place UAZ₁ below the first appearance of *Kashmirites* in the NIM (i.e., UAZ S-4; see BRÜHWILER et al. 2010a, fig. 4), but a correlation with a specific UAZ (S-1, S-2 or S-3) is not possible at the present time (Text-fig. 9).

-UAZ₂

Content: See Text-fig. 8A.

Characteristic species: *Kashmirites stepheni*.

Age: early Smithian. Correlative of the *Preflorianites/Kashmirites* beds from Utah (as initially described in BRAYARD et al. 2013).

As it corresponds to the first regional appearance of *Kashmirites*, we only tentatively correlate UAZ₂ with UAZ S-4 that represents the first occurrence of *Kashmirites* in the NIM (Text-fig. 9; see BRÜHWILER et al. 2010a, fig. 4).

-UAZ₃

Content: See Text-fig. 8A.

Characteristic species: *Inyoites beaverensis*.

Age: latest early Smithian. Correlative of the *Inyoites beaverensis* beds from Utah (BRAYARD et al. 2013).

BRAYARD et al. (2013, fig. 14) attributed a latest early Smithian or earliest middle Smithian age to their *Inyoites beaverensis* beds (= UAZ₃). Noteworthy, the species *Kashmirites utahensis*, BRAYARD et al. 2013 is found in this UAZ₃. As the genus *Kashmirites* is not known from the middle Smithian, UAZ₃ is likely of latest early Smithian age. Therefore, it correlates with UAZ S-7 from the NIM (Text-fig. 9).

-UAZ₄

Content: See Text-fig. 8A.

Age: middle Smithian. Correlative of the *Meekoceras gracilitatis* interval Zone from Nevada (KUMMEL & STEELE 1962, JENKS et al. 2010) and the *Owenites* beds from Utah (BRAYARD et al. 2013).

Characteristic species: *Juvenites thermarum*, *Dieneroceras dieneri*, *Guodunites hooveri*, *Owenites carpenteri*, *O. koeneni*, ?*Kashmirites cordilleranus*, *Parussuria compressa*, *Churkites noblei*, *Inyoites oweni* and *Lanceolites compactus*.

The UA biostratigraphical analysis confirms the previously established succession for the middle Smithian in western USA (see BRAYARD et al. 2013). After removing endemic species (found in only one locality), the western USA basin exhibits a peculiar middle Smithian diversity pattern, characterized by the occurrences of mostly cosmopolitan, rather long-ranging genera, which continually becomes more diverse with additional taxa through time.

Consequently, the maximum set of species for the middle Smithian is observed in the late middle Smithian (see Text-figs. 4, 5 and BRAYARD et al. 2013), and includes all previous middle Smithian sets of species. It therefore leads to the creation of a single UAZ for the entire middle Smithian in the western USA basin. This pattern of diversity is unique compared with diversity patterns observed in other basins. For instance, high turnover rates during the middle Smithian in the NIM led to the creation of a biochronological scheme of much higher resolution for this time interval (BRÜHWILER et al. 2010a, see Text-fig. 9).

Pseudosageceras multilobatum, *Aspenites acutus*, *Juvenites spathi*, *Meekoceras gracilitatis*, *Owenites koeneni* and *O. carpenteri* is a set of species from UAZ₄ that are also found in the NIM. Considering this set of shared species, it appears that UAZ₄ correlates with UAZs S-8 to S-12 from the NIM (Text-fig. 9). A more accurate correlation is not possible at this time. It is also worth noting that *M. gracilitatis* is here shown to be a long-ranging species that also occurs in the early Smithian (UAZ₂ and UAZ₃; Text-fig. 8A). Thus, this emblematic Smithian species is not of any use for precise biostratigraphical zonation (see discussion in BRAYARD et al. 2013). We therefore recommend not using the long-recognized *Meekoceras gracilitatis* Zone but instead, suggest the use of the newly defined UAZ₄ and its characteristic set of species (e.g., *Owenites koeneni*, *Churkites noblei*, *Inyoites oweni*) for more accurate middle Smithian correlation in western USA.

-UAZ₅

Content: See Text-fig. 8A.

Characteristic species: *Arctoprionites resseri*, *Anasibirites multiformis*, *Anasibirites kingianus*, *Wasatchites perrini*, *Hemiprionites typus*.

Age: late Smithian. Correlative of the *Anasibirites* beds from Nevada (JENKS et al. 2010).

UAZ₅ correlates with UAZ S-13 (*Wasatchites distractus* beds, BRÜHWILER et al. 2011) from the NIM (Text-fig. 9). It is worth noting that a peculiar fauna was found above UAZ₅ at Palomino Ridge (Text-figs. 4, 5), whose characteristic species is *Pseudosageceras augustum*. BRAYARD et al. (2013) also described a fauna from strata located above UAZ₅ (Xenoceltitidae gen. indet. A beds). Unfortunately, each taxon from these beds is either restricted to Palomino Ridge or to the Mineral Mountains in Utah. It was therefore impossible to correlate the *P. augustum* beds from Palomino Ridge with the Xenoceltitidae gen. indet. A beds from Utah by means of the UA method. However, although very poorly preserved, the specimens described as Hedenstroemiidae gen. indet. A by BRAYARD et al. (2013) from the Xenoceltitidae gen. indet. A beds strongly invite comparison with *P. augustum*. Hypothesizing that these specimens are representative of *P. augustum* would lead to the creation of a sixth UAZ, representing the latest Smithian. This UAZ₆ (Text-fig. 8) would correlate with UAZ S-14 (*Glyptophiceras sinuatum* beds, BRÜHWILER et al. 2011) from the NIM (Text-fig. 9), characterized by its xenoceltiid fauna co-occurring with *P. augustum* (BRÜHWILER et al. 2010a, fig. 4). To corroborate the existence of a sixth UAZ representing the latest Smithian in western USA, undisputed representatives of *P. augustum* still need to be documented from Utah.

Systematic Palaeontology (JATTIOT & BUCHER)

Systematic descriptions mainly follow the classification established by TOZER (1981) and amended by BRAYARD et al (2013). The quantitative morphological range of each species is illustrated by plots provided at least four measureable specimens were available. Each set of measurements includes the classical geometric parameters of the ammonoid conch such as the shell diameter (D) and corresponding whorl height (H), whorl width (W) and umbilical diameter (U). To assess their variability within each species, these parameters are plotted as a

ratio of the size-related parameter D (H/D, W/D and U/D) in order to remove the influence of growth.

Abbreviations: non: material not forming part of the current species; p: pars; v.: video or vidimus; ?: questionable. Repository of specimens is abbreviated PIMUZ (Paläontologisches Institut und Museum der Universität Zürich, Switzerland).

Order Ammonoidea ZITTEL, 1884

Suborder Ceratitina HYATT, 1884

Superfamily Xenodiscaceae FRECH, 1902

Family Xenoceltitidae SPATH, 1930

Genus *Xenoceltites* SPATH, 1930

Type species: *Xenoceltites subevolutus* = *Xenodiscus* cf. *comptoni* (non DIENER) FREBOLD, 1930

Xenoceltites subevolutus SPATH, 1930

(Plate 1, Figs. P–AD)

1930 *Xenoceltites subevolutus* SPATH, p. 12.

1930 *Lecanites* cf. *ophioneus* – FREBOLD, p. 12, pl. 3, figs. 4, 4a, 5.

1930 *Xenodiscus* cf. *comptoni* – FREBOLD, p. 14, pl. 3, figs. 1–3.

? 1932 *Xenodiscus rotula* – SMITH, p. 45, pl. 79, figs. 5, 6.

1934 *Xenoceltites spitsbergensis* SPATH, p. 128, pl. 9, figs. 1, 2; pl. 11, figs. 5, 7, 8.

1934 *Xenoceltites gregoryi* SPATH, p. 129, pl. 5, fig. 3; pl. 6, figs. 4, 5; pl. 11, figs. 3, 4, 6.

1934 *Xenoceltites subevolutus* – SPATH, p. 130, pl. 2, fig. 2; pl. 8, fig. 2; pl. 9, fig. 4; pl. 11, fig. 2.

1961 *Xenoceltites subevolutus* – TOZER p. 53, pl. 16, fig 1.

1978 *Xenoceltites subevolutus* – ZAKHAROV, pl. 11, fig. 17.

1978 *Xenoceltites spitsbergensis* – WEITSCHAT & LEHMANN, p. 94, pl. 11, figs. 3b, 4, 5.

1978 *Xenoceltites subevolutus* – WEITSCHAT & LEHMANN, p. 95, pl. 11, figs. 1, 2, 3a.

1990 *Xenoceltites subevolutus* – DAGYS & ERMAKOVA, p. 23, pl. 5, fig. 4.

1994 *Xenoceltites subevolutus* – TOZER, p. 52, pl. 36, figs. 3–8.

? 2010 *Xenoceltites* sp. – STEPHEN et al., fig. 7d.

v 2013 *Xenoceltites* sp. indet. A – BRAYARD et al., p. 160, fig. 19 a–c.

v 2015 *Xenoceltites subevolutus* – PIAZZA, p. 48, pl. 1, figs. a–c.

Occurrence: *Xenoceltites subevolutus* co-occurs with *Anasibirites* in UAZ₅ (PLR24, PLR34 and PLR57) but also ranges up to the potential UAZ₆ (PLR32, PLR35 and PLR48). [n = 9]

Description: Moderately involute to evolute, compressed platycone with rounded venter, rounded ventral shoulders and slightly convex flanks, gently converging from ventral shoulders towards venter. Umbilicus wide, with moderately deep, oblique wall and rounded shoulders. Ornamentation highly variable, conforming to the Buckman's first law of covariation (WESTERMANN 1966). Involute and compressed specimens weakly ornamented, with constrictions only visible on venter; evolute and thicker specimens bearing conspicuous constrictions on venter that extend onto the flanks (e.g., Plate 1, Figs. T–V). Suture line not available in our material.

Measurements: See Text-fig. 10. Estimated maximal size: ~ 4 cm for our specimens.

Discussion: DAGYS & ERMAKOVA (1990) first treated *X. gregoryi* and *X. spitsbergensis* as junior synonyms of *X. subevolutus*. A few years later, in a written communication, WEITSCHAT (1994, to HB) stated ‘In my 1978 paper I distinguished two different species from

this horizon, *X. subevolutus* and *X. spitsbergensis* and put only *X. gregoryi* as a synonym. Today, it is clear for me that we have a fairly wide intraspecific variation of a single species (*X. subevolutus*)'. More recently, BRAYARD & BUCHER (2008) also stressed that all species of *Xenoceltites* morphologically overlap and display broad ranges of intraspecific variation. They nevertheless kept the species separated and erected a new species, namely *X. variocostatus*, based on its variocostate ribbing on the innermost whorls. However, *X. variocostatus*, whose whorl thickness also exceeds that of all other representatives of *Xenoceltites*, should be preferably assigned to a distinct genus. PIAZZA (2015) synonymized *X. gregoryi* and *X. spitsbergensis* with *X. subevolutus*, considering that the observed differences can be considered as minor and represent variable characters within *X. subevolutus*. Upon comparison of the type material of *Xenoceltites* species (FREBOLD 1930, SPATH 1934, BRAYARD & BUCHER 2008) and based on material from Nevada, China and Spitsbergen, we agree with the original interpretation of DAGYS & ERMAKOVA (1990). However, to firmly confirm this hypothesis, the biometry of large samples still needs to be investigated.

Genus *Palominoceras* n. gen.

Type species: *Palominoceras nevadanum* (SMITH, 1932)

Etymology: The genus name refers to Palomino Ridge locality.

Included species: Type species only.

Diagnosis: Xenoceltitid with a moderately deep umbilicus, abruptly rounded umbilical shoulders and a nearly smooth surface, except for occasional and extremely weak radial folds on upper flanks.

Discussion: *Palominoceras* n. gen. shares many features with the xenoceltitids (i.e., similar coiling, whorl shape, umbilicus and suture line), thus justifying its assignment to the family Xenoceltitidae.

Palominoceras n. gen. *nevadanum* (SMITH, 1932)

(Plate 2, Figs. A–AC)

1932 *Xenodiscus (Xenaspis) nevadanus* SMITH, p. 47, pl. 56, figs. 1–5.

Occurrence: Very abundant [n ~ 240], documented from the uppermost part of UAZ₄ (see Text-figs. 4, 5).

Description: Coiling with significant positive allometric growth of the umbilical diameter (Text-fig. 11). Flanks somewhat flattened. Rounded to subtabulate venter and abruptly rounded ventral shoulders. Umbilicus moderately deep with moderately high, perpendicular wall and abruptly rounded shoulders. Surface nearly smooth, except for very weak radial folds on upper flanks of some specimens. Suture line ceratitic, with a deep first lateral lobe, well-rounded saddles and a small umbilical saddle.

Measurements: See Text-fig. 11. Estimated maximal size: ~ 5 cm.

Discussion: This species was originally described by SMITH (1932) as *Xenodiscus (Xenaspis) nevadanus* (holotype figured on Plate 2, Figs. A–C) based on specimens from the Phelan Ranch locality (Text-fig. 3). However, as stated by SMITH (1932), this species “is not nearly related to any other species of American fauna”, thus justifying the erection of a new genus. Nevertheless, adult specimens of the contemporaneous species ?*Kashmirites cordilleranus* (see below) might be confused with adult specimens of *Palominoceras nevadanum*. Before the mature stage is reached (D<40 mm), specimens of *P. nevadanum* are more involute and show more marked umbilical shoulders than ?*K. cordilleranus* specimens, but the umbilicus of *P. nevadanum* becomes distinctively wider throughout ontogeny (Text-fig. 11). At the

mature stage, the coiling of *P. nevadanum* therefore closely resembles that of ?*K. cordilleranus*. However, mature specimens of ?*K. cordilleranus* differ by their conspicuous ornamentation, more rounded umbilical shoulders, and different whorl section. *P. nevadanum* differs from the late Smithian species *Xenoceltites subevolutus* SPATH, 1930 mainly by the absence of constrictions and its abruptly rounded umbilical shoulders.

Family Kashmiritidae SPATH, 1934

?*Kashmirites cordilleranus* (SMITH, 1932)

(Plate 1, Figs. A–O)

1932 *Xenodiscus cordilleranus* SMITH, p. 43, pl. 24, figs. 21–29.

? 1932 *Xenodiscus intermontanus* SMITH, p. 44, pl. 24, figs. 10–20.

p 1932 *Xenodiscus nivalis* – SMITH, p. 44, pl. 56, figs. 6–9 only.

? 1979 *Dieneroceras knechti* – NICHOLS & SILBERLING, pl. 1, figs. 22–26.

2010 ?*Kashmirites intermontanus* – STEPHEN et al., figs. 5e, f, h.

v 2013 *Xenoceltites cordilleranus* – BRAYARD et al., p. 159, fig. 17.

Occurrence: Uppermost part of UAZ₄ (PLR12, PLR13, PLR63, PLR71, PLR72 and PLR88).

[n = 10]

Description: Evolute, compressed platycone with a large intraspecific variation. Venter rounded or broadly arched with rounded shoulders forming rectangular to subquadratic whorl sections. Flanks almost parallel. Umbilicus wide, with moderately deep, steeply inclined wall and rounded shoulders. Ornamentation very poorly preserved on our specimens, varying from

regularly distant fold-like ribs on inner whorls to dense, rursiradiate and more variable strength ribs at maturity. Suture line ceratitic with broad saddles.

Measurements: See Text-fig. 12. Estimated maximal size: ~ 5 cm.

Discussion: BRAYARD et al. (2013) assigned *?Kashmirites cordilleranus* to the genus *Xenoceltites*. However, this species shares more similarities with the early Smithian genus *Kashmirites*, in particular by exhibiting a subquadratic whorl section with subparallel flanks, as well as ornamentation consisting of bullate and rectiradiate ribs. Since the genus *Kashmirites* is not known from the middle Smithian, the generic assignment of this species to *Kashmirites* is tentative only and remains to be confirmed.

Genus *Preflorianites* SPATH, 1930

Type species: *Danubites strongi* HYATT & SMITH, 1905

Preflorianites toulai (SMITH, 1932)

(Plate 1, Figs. AE–AK)

1932 *Xenodiscus toulai* SMITH, p. 45, pl. 25, figs. 1–3; pl. 53, figs. 9–12.

1932 *Proteusites rotundus* SMITH, p. 102, pl. 53, figs. 5–8.

1962 *Preflorianites toulai* – KUMMEL & STEELE, p. 669, pl. 100, figs. 18–20; pl. 102, fig. 5.

1995 *Preflorianites toulai* – SHEVYREV, p. 26, pl. 2, fig. 4.

Occurrence: Abundant [n ~ 70] throughout UAZ₄ (see Text-fig. 4).

Description: Evolute, with a compressed whorl section, but showing broad intraspecific variation. Venter broadly to narrowly arched with rounded shoulders forming near-rectangular to ovoid whorl sections. Flanks slightly convex. Large, shallow umbilicus with an oblique wall and rounded shoulders. Very regularly spaced, pronounced and radial ribs fading out towards the smooth venter. Faintly sinuous, fine growth lines barely perceptible. Suture line ceratitic, with deep lateral lobes, well-rounded saddles and a small umbilical saddle.

Measurements: See Text-figs. 13, 14. Estimated maximal size: ~ 6 cm.

Discussion: It has been commonly assumed that *P. toulai* differs from *P. radians* from South China (BRAYARD & BUCHER 2008) and Oman (BRÜHWILER et al. 2012a) only by its slightly more involute coiling and an apparently smaller mature size. Based on early Smithian specimens from Utah assigned to *P. toulai*, BRAYARD et al. (2013) hypothesized that *P. toulai* and *P. radians* may be conspecific. However, the *Preflorianites toulai* assignment of the early Smithian specimens from Utah should be re-assessed. Indeed, they are distinctively more evolute than the type specimens of *P. toulai* and instead show many similarities with the contemporaneous early Smithian genus *Kashmirites* (e.g., coiling and whorl shape). Measurement analyses (Text-fig. 14) show that *P. toulai* and *P. radians* are actually different, which contrasts with the preliminary analyses of BRAYARD et al. (2013, fig. 22). Indeed, *P. toulai* appears slightly more involute than *P. radians* (Text-fig. 14). Therefore, the two species are considered as valid.

Superfamily Meekocerataceae WAAGEN, 1895

Family Melagathiceratidae WAAGEN, 1895

Genus *Juvenites* SMITH, 1927

Type species: *Juvenites kraffti* SMITH, 1927

Juvenites thermarum (SMITH, 1927)

(Plate 3, Figs. A–AE)

1927 *Thermalites thermarum* SMITH, p. 24, pl. 21, figs. 11–20.

1932 *Prenkites depressus* SMITH, p. 110, pl. 31, figs. 16–18.

1932 *Thermalites thermarum* – SMITH, p. 111, pl. 21, figs. 11–20.

? 1962 *Juvenites thermarum* – KUMMEL & STEELE, p. 689, pl. 100, figs. 12, 13.

? 1973 *Arnautoceltites thermarum* – COLLIGNON, p. 17, pl. 4, fig. 10.

v 2007 *Paranannites* sp. indet. – KLUG et al., p. 1467, text-fig. 4A–E.

2010 *Juvenites septentrionalis* – STEPHEN et al., fig. 5k–l.

v 2012a *Juvenites* cf. *thermarum* – BRÜHWILER & BUCHER, p. 40, pl. 22, figs. 1–9.

v 2013 *Juvenites* cf. *thermarum* – BRAYARD et al., p. 165, fig. 24d–r.

Occurrence: Common [n = 15] in UAZ₄ (PLRA3, PLRA35, PLR12, PLR13, PLR27, PLR45, PLR61, PLR62 and PLR63).

Description: Globose shell with involute coiling. Venter rounded. Umbilicus relatively deep, with perpendicular wall and broadly rounded shoulders. Distant, prorsiradiate constrictions crossing the venter with varying strength. Suture line ceratitic and very simple with two broad, asymmetrical saddles.

Measurements: See Text-fig. 15. Estimated maximal size: ~ 4 cm.

Discussion: We follow here the species definition of SMITH (1932) and the rare measurements made available by KUMMEL & STEELE (1962) and BRAYARD et al. (2013) for the American species. *J. thermarum* differs from *J. septentrionalis* by its more involute coiling and more depressed whorl section (see BRAYARD et al. 2013, fig. 26). *J. spathi* (FREBOLD 1930) is distinguished by its distinct triangular whorl outline, its much deeper umbilicus with higher umbilical wall (crateriform umbilicus) and bluntly angular umbilical shoulders.

The holotype of *J. krafftii* SMITH, 1927 (plate 21, figs. 1–3) seems to display a crateriform umbilicus with bluntly angular umbilical shoulders, as well as a triangular venter. Thus, we hypothesize that *J. krafftii* and *J. spathi* may be conspecific. This supposition still needs confirmation by further biometric analysis of *J. krafftii*. The reader is referred to BRAYARD et al. (2013) for a thorough discussion of the taxonomy of *Juvenites* species.

Juvenites spathi (FREBOLD, 1930)

(Plate 3, Figs. AF–AW)

1930 *Prosphingites spathi* FREBOLD, p. 20, pl. 4, figs. 2, 3, 3a.

1934 *Prosphingites spathi* – SPATH, p. 195, pl. 13, figs. 1, 2.

p? 1959 *Prosphingites kwangsianus* CHAO, p. 296, pl. 28, figs. 17, 18.

p? 1959 *Prosphingites sinensis* CHAO, p. 297, pl. 27, figs. 14–17, text-fig. 40a.

? 1961 *Prosphingites spathi* – TOZER, p. 58, pl. 13, figs. 1, 2.

? 1982 *Prosphingites spathi* – KORCHINSKAYA, pl. 5, fig. 2.

? 1994 *Paranannites spathi* – TOZER, p. 77, pl. 36, figs. 1, 2.

v 2008 *Paranannites spathi* – BRAYARD & BUCHER, p. 63, pl. 35, figs. 10–19.

v 2010b *Paranannites spathi* – BRÜHWILER et al., p. 426, fig. 16 (1, 2).

v 2012a *Juvenites spathi* – BRÜHWILER & BUCHER, p. 38, pl. 22, figs. 12–17.

v 2012c *Juvenites* cf. *spathi* – BRÜHWILER et al., p. 161, figs. 37A–O.

? v 2013 *Juvenites* aff. *spathi* – BRAYARD et al., p. 166, fig. 27a-c.

Occurrence: Common [n = 15] in UAZ₄ (PLR9', PLR9, PLR110, PLRA10, PLR14, PLRA35, PLR27, PLR45, PLR61, PLR62 and PLR63).

Description: Globose and moderately evolute shell. Typical specimens exhibit a triangular whorl outline. Flanks gradually converging towards the venter from narrowly rounded umbilical shoulder. Umbilicus deep with high, perpendicular wall and bluntly angular umbilical shoulders. Ornamentation consists of prorsiradiate constrictions, becoming denser at maturity. Suture line ceratitic, with two main, broad saddles.

Measurements: See Text-fig. 16. Estimated maximal size: ~ 5 cm.

Discussion: *J. spathi* is mainly distinguished from other juvenitids by its triangular venter and its crateriform umbilicus. Some variants of *J. spathi* may however display an arched venter (see Plate 3, Figs. AH–AJ, but also KORCHINSKAYA 1982, TOZER 1994 and BRÜHWILER et al. 2010b, 2012a). Exceptionally preserved material from Timor (JATTIOT et al., ongoing work) also reveals that large-size specimens do not necessarily display a triangular whorl section, contrary to the preliminary statement of BRAYARD et al. (2013). Consequently, the marked crateriform umbilicus with bluntly angular umbilical shoulders is the most diagnostic trait of *J. spathi*.

Family Proptychitidae WAAGEN, 1895

Genus *Guodunites* BRAYARD & BUCHER, 2008

Type species: *Guodunites monneti* BRAYARD & BUCHER, 2008

Guodunites monneti BRAYARD & BUCHER, 2008

(Plate 4, Figs. A–K)

? 1968 *Owenites slavini* KUMMEL & ERBEN, p. 124, pl. 21, figs. 3–4.

v 2008 *Guodunites monneti* BRAYARD & BUCHER, p. 83, pl. 44, figs. 1–2.

v 2009b *Guodunites monneti* – BRAYARD et al., p. 473, pl. 1, figs. 1–14; text-fig. 3A–C.

v 2012a *Guodunites monneti* – BRÜHWILER & BUCHER, p. 19, pl. 7, figs. 1–5.

2014 *Guodunites monneti* – SHIGETA & NGUYEN, p. 91, fig. 63.

Occurrence: Uppermost part of UAZ₄ (PLR12, PLR14, PLR20, PLR45, PLR61, PLR63, PLR71, PLR72, PLR73 and PLR88). [n ~ 25]

Description: Shell moderately involute, compressed with convex flanks. Venter rounded without distinct shoulders. Umbilical wall gently sloping and without umbilical shoulder, forming a shallow, smooth umbilicus on inner whorls; umbilical seam markedly egressive in later growth stages. Striation and folds not preserved on our specimens. Growth lines strongly projected on lower flanks. Suture line subammonitic, with indentations almost reaching the tip of saddles.

Measurements: See Text-fig. 17. Estimated maximal size: ~ 30 cm (BRAYARD et al. 2009b).

Discussion: Surprisingly, *G. monneti* has apparently not been recorded from central and southern Utah (BRAYARD et al. 2013). As previously discussed by BRAYARD et al. (2009b), this genus is restricted to the late middle Smithian, and to date, its biogeographical distribution comprises Oman, South China, Nevada, Utah and California, thus indicating a

low paleolatitudinal distribution and the existence of long-distance faunal exchanges between opposite sides of the Panthalassa during the Early Triassic (BRAYARD et al. 2006, 2007b, 2009c, JENKS 2007, JENKS et al. 2010, BRAYARD et al. 2013).

Guodunites hooveri (HYATT & SMITH, 1905)

(Plate 4, Figs. L–V)

1905 *Aspidites hooveri* HYATT & SMITH, p. 153, pl. 17, figs. 1–12.

1932 *Clypeoceras hooveri* – SMITH, p. 63, pl. 17, figs. 1–12.

v 2009b *Guodunites hooveri* – BRAYARD et al., p. 476, pl. 2, figs. 1–30.

2010 ?*Clypeoceras hooveri* – STEPHEN et al., figs. 6e, f, i.

v 2013 *Guodunites hooveri* – BRAYARD et al., p. 170.

Occurrence: Uppermost part of UAZ₄ (PLR14, PLR27, PLR45, PLR61, PLR62, PLR63, PLR72 and PLR73). [n = 12]

Description: The reader is referred to BRAYARD et al. (2009b) for a thorough description. The main characteristics of this taxon are (a) involute, platycone shell with narrowly rounded venter, (b) slightly convex flanks with maximum thickness near mid-flank, (c) egressive coiling at submature stage, (d) deep funnel-like umbilicus and (e) projected lirae on outer shell (BRAYARD et al. 2013). Strigation or folds not visible on our specimens. Suture line subammonitic with finely crenulated saddles but too poorly preserved to be illustrated.

Measurements: See Text-fig. 18. Estimated maximal size: ~ 15 cm.

Discussion: *Guodunites hooveri* differs from *G. monneti* by its deeper umbilicus and more involute coiling.

Family Dieneroceratidae KUMMEL, 1952

Genus *Dieneroceras* SPATH, 1934

Type species: *Ophiceras dieneri* HYATT & SMITH, 1905

Dieneroceras dieneri (HYATT & SMITH, 1905)

(Plate 5, Figs. A–S)

1905 *Ophiceras dieneri* HYATT & SMITH, p. 118, pl. 8, figs. 16–29.

? 1905 *Xenaspis marcoui* HYATT & SMITH, p. 116, pl. 7, figs. 26–33.

1932 *Ophiceras dieneri* – SMITH, p. 48, pl. 8, figs. 16–29.

? 1932 *Xenodiscus (Xenaspis) marcoui* – SMITH, p. 47, pl. 7, figs. 26–33.

1955 *Ophiceras iuaiense* SAKAGAMI, p. 135, pl. 1, figs. 1–9.

1955 *Ophiceras* sp. – SAKAGAMI, p. 136, pl. 1, figs. 10–11.

? 1959 *Kariceltites indicus* JEANNET, p. XXX, pl. 7, figs. 10–12; pl. 8, fig. 15.

1960 *Dieneroceras iuaiense* – KUMMEL & SAKAGAMI, p. 4, pl. 1, figs. 3–5; pl. 2, figs. 7–9.

? 1961 *Dieneroceras dieneri* – KIPARISOVA, p. 47, pl. 9, fig. 2.

? 1961 *Dieneroceras chaoi* KIPARISOVA, p. 48, pl. 9, figs. 3–6.

? 1961 *Dieneroceras caucasicum* POPOV, p. 41, pl. 6, fig. 1.

? 1965 *Dieneroceras* cf. *dieneri* – KUENZI, p. 369, pl. 53, figs. 13–18, text-figs. 3, 4.

1968 *Dieneroceras dieneri* – NAKAZAWA & BANDO, p. 93, pl. 4, figs. 1–6.

1968 *Dieneroceras* aff. *chaoi* – NAKAZAWA & BANDO, p. 95, pl. 4, figs. 7, 8; pl. 5, fig. 1.

? 1973 *Dieneroceras knechti* – COLLIGNON, p. 131, pl. 1, figs. 2, 3.

? 1973 *Dieneroceras chaoi* – COLLIGNON, p. 132, pl. 1, figs. 6–8.

? 1995 *Dieneroceras caucasicum* – SHEVYREV, p. 25, pl. 1, figs. 3–5.

? 1995 *Dieneroceras magnum* SHEVYREV, p. 26, pl. 1, fig. 6.

2010 *Wyomingites arnoldi* – STEPHEN et al, fig. 5c, d.

v 2012a *Dieneroceras dieneri* – BRÜHWILER & BUCHER, p. 20, pl. 8, figs. 1–4; pl. 9, figs. 1–7; pl. 10, figs. 1–3.

v 2013 *Dieneroceras dieneri* – BRAYARD et al., p. 173, fig. 36a–s.

Occurrence: Rare [n = 2] within the lowermost part of UAZ₄ (PLR10); common [n ~ 20] within the uppermost part of UAZ₄ (PLR12, PLR13, PLR14, PLR27, PLR45, PLR61, PLR62, PLR63 and PLR71).

Description: Serpenticonic, laterally compressed shell with a subtabulate to tabulate venter and a large umbilicus. Broadly convex flanks with maximum thickness near umbilicus, imparting a slightly ovoid whorl section. Inner whorls slightly more rounded than outer whorls. Umbilical wall steeply inclined with rounded shoulders forming a shallow umbilicus. Surface smooth; spiral strigation described by HYATT & SMITH (1905) from type specimen not observed on our material. Suture line ceratitic and very simple, with two main large lateral saddles. Suture line goniatic at juvenile stages.

Measurements: See Text-fig. 19. Estimated maximal size: ~ 3.5 cm.

Discussion: *D. dieneri* is distinguished from *D. knechti* by its flatter venter. The reader is referred to BRAYARD et al. (2013) for further details.

Dieneroceras knechti (HYATT & SMITH, 1905)

(Plate 5, Figs. T-AA)

- 1905 *Lecanites knechti* HYATT & SMITH, p. 138, pl. 9, figs. 11–16.
- 1915 *Proavites knechti* – DIENER, p. 228.
- 1932 *Lecanites (Paralecanites) knechti* – SMITH, p. 41, 42, pl. 9, figs. 11–16; p. 28, figs. 1–7.
- 1934 "Lecanites" *knechti* – SPATH, p. 88, 93, 123, 134.
- 1962 *Dieneroceras knechti* – KUMMEL & STEELE, p. 662, pl. 99, figs. 14, 15.

Occurrence Rare [n = 5] in UAZ₄ (PLR87, PLR9, PLR14, PLRA34 and PLR45).

Description Serpenticonic, laterally compressed shell with rounded venter and broad umbilicus. Broadly convex flanks with maximum thickness near umbilicus, imparting a slightly ovoid whorl section. Inner whorls slightly more rounded than outer whorls. Umbilical wall steeply inclined with rounded shoulders forming a shallow umbilicus. Surface smooth. Simple ceratitic suture line with deep lateral lobe and two broad lateral saddles.

Measurements See Table 1. Estimated maximal size: ~ 4 cm.

Discussion See *Dieneroceras dieneri*.

Family Flemingitidae HYATT 1900

Genus *Anaflemingites* KUMMEL & STEELE, 1962

Type species: *Anaflemingites silberlingi* KUMMEL & STEELE, 1962

Anaflemingites cf. *silberlingi* KUMMEL & STEELE, 1962

(Plate 5, Figs. AB–AI)

1962 *Anaflemingites silberlingi* KUMMEL & STEELE, p. 667, pl. 102, fig. 10.

2010 *Anaflemingites silberlingi* – JENKS et al., p. 23, figs. 14, 16–18.

? v 2013 *Anaflemingites* aff. *silberlingi* – BRAYARD et al., p. 177, fig. 40.

Occurrence: Common [n ~ 30] in UAZ₄ (see Text-fig. 4).

Description: Moderately evolute and laterally compressed, discoidal shell with a well-rounded venter. Flanks slightly convex with maximum curvature near mid-flank, converging towards venter without distinct ventral shoulders. Umbilicus relatively shallow with gently sloping wall and rounded margin. No visible ornamentation on our specimens. Suture line ceratitic, with a deep and well-indented first lateral lobe.

Measurements: See Text-fig. 20. Estimated maximal size: ~ 15 cm.

Discussion: JENKS et al. (2010) provided a thorough revision of the genus, based on numerous specimens from Crittenden Springs, Nevada. Our specimens are roughly similar to the type species. However, most are small-sized and poorly preserved, thus preventing a firm assignment to *A. silberlingi*.

Family Arctoceratidae ARTHABER, 1911

Genus *Churkites* OKUNEVA, 1990

Type species: *Churkites egregius* ZHARNIKOVA & OKUNEVA in OKUNEVA 1990

Churkites noblei JENKS, 2007

(Plate 6, Figs. A–K)

2000 *Arctoceras* sp. – GARDNER & MAPES, pl. 2, fig. 1.

v 2007 *Churkites noblei* JENKS, p. 83, figs. 2, 4, 7–9.

v 2010 *Churkites noblei* – STEPHEN et al., figs. 5i, j.

v 2013 *Churkites noblei* – BRAYARD et al., p. 178, figs. 42, 43.

Occurrence: Common [n = 19] in the uppermost part of UAZ₄ (PLRA36, PLR13, PLR45, PLR61, PLR62, PLR72, PLR73 and PLR88).

Description: Very large sized Arctoceratid with narrowly rounded venter at juvenile stages, becoming acute or angular at maturity. Coiling moderately evolute with compressed and relatively high whorls but clearly egressive at maturity. Gently convex flanks forming slightly ovoid whorl section (see JENKS 2007 for a thorough description). Umbilical wall high and perpendicular with abruptly rounded shoulders on inner whorls, becoming less steep with more gently rounded shoulders on most large mature whorls. Ornamentation poorly preserved in our material but usually consisting of weak to strong tuberculations on umbilical shoulders becoming denser, more bullate and ridge-like on adult whorls. Ribs or folds not visible on our specimens. Well-preserved shells exhibit a faint strigation (see specimens from Crittenden Springs described by JENKS 2007). Suture line ceratitic, consisting of well denticulated ventral, first lateral and second lateral lobes, as well as short auxiliary series. Width of lobes gradually decreases towards umbilicus. First lateral saddle wide and well-rounded, second lateral saddle somewhat narrower, but still well-rounded.

Measurements: See Text-fig. 21. Estimated maximal size up to: ~ 40 cm.

Discussion: See Jenks (2007), BRAYARD et al. (2013) and SHIGETA & KUMAGAE (2015) for comprehensive discussions of the genus *Churkites*.

Genus Arctoceras HYATT, 1900

Type species: *Ceratites polaris* MOJSISOVICS, 1896

Arctoceras tuberculatum (SMITH, 1932)

(Plate 7, Figs. A–I)

1932 *Meekoceras tuberculatum* SMITH, p. 62, pl. 50, fig. 1–4.

1962 *Arctoceras tuberculatum* – KUMMEL & STEELE, p. 697, pl. 104, figs. 1–8.

1979 *Arctoceras tuberculatum* – NICHOLS & SILBERLING, pl. 1, figs. 5–9.

? 1994 *Arctoceras gigas* TOZER, p. 75, pl. 26, figs. 4–6.

2010 *Arctoceras tuberculatum* – JENKS et al., internal frontispiece.

v 2013 *Arctoceras tuberculatum* – BRAYARD et al., p. 180, fig. 45.

Occurrence: Common [n ~ 20], found in PLR94 (no UAZ assignment) and UAZ₄ (PLR87, PLRA4, PLR9, PLRA7, PLRA17, PLR10, PLR11, PLRA25 and PLR20).

Description: Large-sized Arctoceratid with moderately evolute and compressed shell. Venter varying from narrowly rounded to well-rounded on smaller specimens to well-rounded or broadly rounded on larger specimens. Flanks weakly convex, but whorl section maintaining its subquadratae outline. Umbilicus rather broad with a high, nearly perpendicular wall and narrowly rounded margins, becoming shallower with a less steep wall on some large, mature shells. Ornamentation consisting of conspicuous nodes on umbilical shoulders, often becoming approximated on adult whorls. Ribbing composed of straight and distant ribs connected with the umbilical nodes, slightly projected on ventral shoulders. Ribbing becoming denser at larger size. Fine striae described on specimens from Crittenden

Springs (KUMMEL & STEELE 1962, JENKS et al. 2010) barely perceptible on a single specimen from Palomino Ridge (Plate 7, Figs. G–I). Suture line ceratitic with broad lobes and an auxiliary series. Width of lobes gradually decreasing towards umbilicus.

Measurements: See Text-fig. 22. Estimated maximal size up to: ~ 25 cm.

Discussion: See BRAYARD et al. (2013) for a thorough discussion of the taxonomy of *Arctoceras* species. It can be somewhat difficult to distinguish *C. noblei* from *A. tuberculatum* on the basis of inner whorls only. However, the whorl section of most *A. tuberculatum* shells tends to be subquadrate with a more rounded, sometimes circular venter, with *C. noblei* being slightly more compressed (BRAYARD et al. 2013, fig. 47) with a more narrowly rounded venter.

Family Inyoitidae SPATH, 1934

Genus *Inyoites* HYATT & SMITH, 1905

Type species: *Inyoites oweni* HYATT & SMITH, 1905

Inyoites oweni HYATT & SMITH, 1905

(Plate 8, Figs. A–G)

1905 *Inyoites oweni* HYATT & SMITH, p. 134, pl. 6, figs. 1–16, pl. 69, figs. 1–9, pl. 78, figs. 1–8.

1932 *Inyoites oweni* – SMITH, p. 80, pl. 6, figs. 1–16, pl. 40, figs. 1–8, pl. 69, figs. 1–9.

1934 *Inyoites oweni* – SPATH, p. 138, fig. 37.

1968 *Inyoites spicini* ZAKHAROV, p. 151, pl. 30, fig. 2.

1973 *Inyoites oweni* – COLLIGNON, p. 12, pl. 1, fig. 9.

? 1995 *Inyoites oweni* – SHEVYREV, p. 12, pl. 1, fig. 9.

2010 *Inyoites oweni* – STEPHEN et al., figs. 5a, b.

v 2012a *Inyoites oweni* – BRÜHWILER & BUCHER, p. 34, pl. 21, figs. 1–6.

? v 2012a *Inyoites* sp. indet. – BRÜHWILER & BUCHER, p. 35, pl. 21, fig. 8.

v 2013 *Inyoites oweni* – BRAYARD et al., p. 185, fig. 49.

Occurrence: Documented from the uppermost part of UAZ₄ (PLRA36, PLR12, PLRA41, PLR27, PLR45, PLR62, PLR63 and PLR88). [n = 15]

Description: Moderately involute, lanceolate shell with convex flanks. Venter with high and acute keel. Ventral shoulders indistinct. Umbilicus shallow with moderately high wall, becoming distinctively steeper on later whorls, with narrowly rounded shoulders. Ornamentation consisting of rursiradiate wavy ribs, varying greatly in strength and width and fading away on outer half of the flanks. Outer shell bearing conspicuous radial lirae. Faint strigation visible on some specimens (Plate 8, Fig. G). Suture line not available in our material.

Measurements: See Text-fig. 23. Estimated maximal size: ~ 8 cm.

Discussion: *Inyoites krystyni* BRAYARD & BUCHER, 2008 from the *Owenites* beds, *Inyoites* horizon of Guangxi (South China) differs from the type species by its more evolute coiling, its larger maximum size (up to ~15 cm) and its weaker ornamentation. The reader is referred to BRAYARD et al. (2013) for a comprehensive discussion of *Inyoites*.

Inyoites sp. indet.

(Plate 8, Figs. H–N)

Occurrence: Occurs only in PLRA35 (UAZ₄). [n = 5]

Description: Evolute, laterally compressed shell with acute venter and small, delicate keel. Flanks parallel near umbilicus, rapidly becoming convergent towards venter. Umbilicus wide with rounded margins and oblique wall. Ornamentation consisting only of weak, radial folds at mid-flank. Suture line not available in our material.

Measurements: See Text-fig. 24. Estimated maximal size: ~ 4 cm.

Discussion: This species resembles *Inyoites beaverensis* BRAYARD et al., 2013 erected from the *Inyoites beaverensis* beds in Utah (UAZ₃, see Text-fig. 6B). However, our specimens appear more involute at a diameter of more than 30 mm (Text-fig. 24) and *I. beaverensis* is older (latest early Smithian). *Inyoites oweni* mainly differs from *Inyoites* sp. indet. by its much stronger ornamentation and more involute coiling. *Inyoites* sp. indet. could actually be considered as an intermediate morph between *I. oweni* and *I. beaverensis*. Nevertheless, due to the very poor preservation of our material and in the absence of sufficient specimens, we prefer to leave the species assignment open. *Subvishnuites welteri* SPATH, 1930 (see below) exhibits a rather similar coiling ratio, but does not bear a ventral keel. At first glance, *Inyoites* sp. indet. may also be considered as a morphologically ‘intermediate’ form between *Inyoites* and *Subvishnuites*.

Genus *Subvishnuites* SPATH, 1930

Type species: *Vishnuites* spec. WELTER, 1922 (= *Subvishnuites welteri* sp. nov. SPATH, 1930)

Subvishnuites welteri SPATH, 1930

(Plate 8, Figs. O–T)

1922 *Vishnuites* spec. – WELTER, p. 137, pl. 13, figs. 3–5.

1930 *Subvishnuites welteri* SPATH, p. 30, p. 90.

1934 *Subvishnuites welteri* – SPATH, p. 117, fig. 31.

1959 *Subvishnuites welteri* – KUMMEL, p. 443, fig. 7.

v 2008 *Subvishnuites stokesi* – BRAYARD & BUCHER, p. 60, pl. 29, figs. 8a–d.

v 2012a *Subvishnuites welteri* – BRÜHWILER & BUCHER, p. 36, pl. 21, figs. 9–13.

Occurrence: Occurs only in PLR12 (UAZ₄). [n = 2]

Description: Compressed, evolute shell. Convex flanks, subparallel on the inner half and strongly convergent towards the venter on the outer half. Venter narrowly rounded, almost acute. Umbilicus wide and shallow with low but steep wall and rounded shoulders. Surface apparently smooth. Suture line not available in our material.

Measurements: See Table 1. Estimated maximal size: ~ 4 cm for our specimens.

Discussion: *Subvishnuites stokesi* KUMMEL & STEELE, 1962 differs from the type species in being ribbed and by its deeper umbilicus (BRÜHWILER & BUCHER 2012a). The specimen from South China identified as *S. stokesi* by BRAYARD & BUCHER (2008) does not exhibit ribbing and has a shallow umbilicus, and is therefore here reassigned to *S. welteri*.

Family Lanceolitidae SPATH, 1934

Genus *Lanceolites* HYATT & SMITH, 1905

Type species: *Lanceolites compactus* HYATT & SMITH, 1905

Lanceolites compactus HYATT & SMITH, 1905

(Plate 9, Figs. A–M)

1905 *Lanceolites compactus* HYATT & SMITH, p. 113, pl. 4, figs. 4–10; pl. 5, figs. 7–9; pl. 78, figs. 9–11.

1932 *Lanceolites compactus* – SMITH, p. 90, pl. 4, figs. 4–10; pl. 5, figs. 7–9; pl. 21, figs. 21–23; pl. 28, figs. 17–20; pl. 40, figs. 9–11; pl. 60, fig. 10.

1962 *Lanceolites compactus* – KUMMEL & STEELE, p. 692, pl. 102, figs. 6–9.

? 1979 *Lanceolites compactus* – NICHOLS & SILBERLING, pl. 2, figs. 39–43.

1995 *Lanceolites compactus* – SHEVYREV, p. 39, pl. 2, figs. 1, 2.

v 2008 *Lanceolites compactus* – BRAYARD & BUCHER, p. 61, pl. 30, fig. 5, text-fig. 53.

v 2012a *Lanceolites compactus* – BRÜHWILER & BUCHER, p. 38, pl. 20, figs. 4–6.

v 2013 *Lanceolites compactus* – BRAYARD et al., p. 188, fig. 54.

Occurrence: Documented from the uppermost part of UAZ₄ (PLR12, PLR13, PLR27, PLRA43, PLR45, PLR72, PLR71 and PLR88). [n = 9]

Description: Occluded, discoidal shell with slightly convex flanks. Venter tabulate or slightly sulcate with angular shoulders. Maximum curvature of flanks on inner half. Ornamentation not present on our specimens but some previously described specimens exhibit weak folds. Illustrated suture line (Plate 9, Fig. E) highly weathered and representing a juvenile specimen. Suture line of mature specimens too poorly preserved to be illustrated but typical of the genus, i.e., subammonitic with broad and strongly indented lobes and lanceolate indentations.

Measurements: See Text-fig. 25. Estimated maximal size: ~ 10 cm.

Discussion: See BRAYARD et al. (2013) for a comprehensive discussion on the taxonomy of *Lanceolites* species. The species *L. bicarinatus* SMITH 1932, which supposedly differs from *L. compactus* by its narrower venter (BRAYARD et al. 2013), appears to be absent in our material. Conversely, *L. bicarinatus* is more abundant than *L. compactus* in Utah (BRAYARD et al. 2013).

Family Ussuridae SPATH, 1930

Genus *Parussuria* SPATH, 1934

Type species: *Ussuria compressa* HYATT & SMITH, 1905

Parussuria compressa (HYATT & SMITH, 1905)

(Plate 9, Figs. N–S)

1905 *Ussuria compressa* HYATT & SMITH, p. 89, pl. 3, figs. 6–11.

1932 *Sturia compressa* – SMITH, p. 93, pl. 3, figs. 6–11.

1934 *Parussuria compressa* – SPATH, p. 213, figs. 66c, d.

1962 *Parussuria compressa* – KUMMEL & STEELE, p. 690, pl. 99, fig. 23; pl. 102, fig. 11.

? 1968 *Parussuria semenovi* ZAKHAROV, p. 59, pl. 5, fig. 4.

1995 *Parussuria compressa* – SHEVYREV, p. 37, pl. 4, fig. 6, text-fig. 16.

v 2008 *Parussuria compressa* – BRAYARD & BUCHER, p. 56, pl. 12, fig. 17.

v 2012a *Parussuria compressa* – BRÜHWILER & BUCHER, p. 31, pl. 18, figs. 8–14.

v 2013 *Parussuria compressa* – BRAYARD et al., p. 191, fig. 57.

2014 *Parussuria compressa* – SHIGETA & NGUYEN, p. 112, figs. 81, 82.

Occurrence: Rare [n = 7] in the uppermost part of UAZ₄ (PLR12, PLR62 and PLR72).

Description: Involute, compressed oxycone with a typical narrowly rounded venter. Flanks slightly convex with maximum lateral curvature near umbilicus, gradually converging towards venter. Umbilicus nearly occluded, with moderately high, oblique wall and rounded shoulders. Ornamentation consisting only of very weak folds. Faint strigation and thin, radial growth lines visible when outer shell is preserved. Suture line typical of ussuriids with highly frilled lobes and saddles.

Measurements: See Text-fig. 26. Estimated maximal size: ~ 15 cm.

Discussion: *Metussuria waageni* HYATT & SMITH, 1905 mainly differs from *P. compressa* by its larger juvenile whorl section and its absence of strigation (BRAYARD et al. 2013).

Family Prionitidae HYATT, 1900

Genus *Wasatchites* MATHEWS, 1929

Type species: *Wasatchites perrini* MATHEWS, 1929

Wasatchites perrini MATHEWS, 1929

(Plate 10, Figs. A–L)

1929 *Wasatchites perrini* MATHEWS, p. 40, pl. 9, figs. 1–9.

1929 *Wasatchites meeki* MATHEWS, p. 41, pl. 7, figs. 1–3; pl. 8, figs. 11–14.

1929 *Wasatchites magnus* MATHEWS, p. 41, pl. 11, figs. 1, 2.

1929 *Wasatchites quadratus* MATHEWS, p. 42, pl. 7, figs. 23–25.

1929 *Kashmirites wasatchensis* MATHEWS, p. 37, pl. 6, figs. 26–28.

? 1929 *Kashmirites thornei* MATHEWS, p. 38, pl. 6, figs. 22–25.

? 1929 *Kashmirites gilberti* MATHEWS, p. 38, pl. 7, figs. 4–8.

1929 *Keyserlingites seerleyi* MATHEWS, p. 39, pl. 8, figs. 8–10.

1932 *Kashmirites meeki* – SMITH, p. 67, pl. 81, figs. 1, 2.

1932 *Kashmirites wasatchensis* – SMITH, p. 69, pl. 81, figs. 3–5.

1932 *Kashmirites perrini* – SMITH, p. 67, pl. 81, figs. 6–8.

1932 *Kashmirites seerleyi* – SMITH, p. 68, pl. 81, figs. 11, 12.

p 1961 *Wasatchites tardus* – TOZER, p. 71, pl. 19, figs. 1a-b (only).

1994 *Wasatchites perrini* – TOZER, p. 79, pl. 29, figs. 5a-c; pl. 35, figs. 2–4.

2010 *Wasatchites perrini* – STEPHEN et al., fig. 7c.

v 2013 *Wasatchites perrini* – BRAYARD et al., p. 191, figs. 13d, 59.

Occurrence: Common [n = 12] in UAZ₅ (PLR24, PLR60, PLR37, PLR59, PLR58 and PLR34).

Description: Moderately involute, somewhat compressed shell with convex flanks forming a trapezoidal whorl section. Venter ranging from tabulate on some inner whorls to subtabulate or slightly arched on mature whorls. Ventral shoulders bluntly angular. Umbilicus deep with a typical oblique wall and rounded shoulders. Ornamentation very conspicuous, consisting of projected ribs varying slightly in strength and width. Ribs typically alternating between strong and weak and may arise from umbilical tubercles, becoming larger and more bullate on mature whorls. Ribs usually well accentuated when crossing the venter. Intraspecific variation high, largely depending upon size at which transition between non-tuberculate to tuberculate stages occurs. Suture line ceratitic with rather deep lateral lobes and broad, rounded saddles, but poorly preserved on our specimens.

Measurements: See Text-fig. 27. Estimated maximal size: ~ 15 cm.

Discussion: *W. distractus* essentially differs from the type species by the more lateral position of its tubercles on the flank and its more radial and conspicuous ribs whose strength decreases at maturity. The reader is referred to BRAYARD et al. (2013) for a thorough discussion of the genus *Wasatchites*.

Genus Anasibirites MOJSISOVICS, 1896

Type species: *Sibirites kingianus* WAAGEN, 1895

Anasibirites kingianus (WAAGEN, 1895)

(Plate 11, Figs. A–F)

1895 *Sibirites kingianus* WAAGEN, p. 108, pl. 8, figs 1–2.

1895 *Sibirites chidruensis* WAAGEN, p. 109, pl. 8, figs 3–4.

1895 *Sibirites dichotomus* WAAGEN, p. 111, pl. 8, figs 5–6, 9.

1895 *Sibirites inaequicostatus* WAAGEN, p. 113, pl. 8, figs 7–8.

1895 *Sibirites ceratitoides* WAAGEN, p. 115, pl. 8, fig. 10.

1895 *Sibirites discoides* WAAGEN, p. 116, pl. 8, fig. 11.

1895 *Sibirites angulosus* WAAGEN, p. 117, pl. 8, figs 12–13.

1895 *Sibirites parvumbilicatus* WAAGEN, p. 119, pl. 9, figs 5–6.

1895 *Sibirites ibex* WAAGEN, p. 121, pl. 9, fig. 3.

1895 *Sibirites hircinus* WAAGEN, p. 123, pl. 9, fig. 4.

? 1905 *Sibirites noetlingi* HYATT & SMITH, p. 49, pl. 9, figs 1–3.

p ?1909 *Sibirites spiniger* KRAFFT & DIENER, p. 131, pl. 31, fig. 2 only.

p 1922 *Anasibirites multiformis* WELTER, p. 138, pl. 15, figs 9–27 ; pl. 16, figs 1–10, 14, 15 only.

- 1922 *Anasibirites robustus* WELTER, p. 144, pl. 17, figs 15–17.
- 1929 *Anasibirites kingianus* – MATHEWS, p. 8, pl. 7, figs 14–22.
- 1929 *Anasibirites madisoni* MATHEWS, p. 11, pl. 1, figs 23–26.
- 1929 *Anasibirites pseudoibex* MATHEWS, p. 21, pl. 3, figs 28–31; pl. 7, fig. 46.
- 1929 *Anasibirites mcclintocki* MATHEWS, p. 22, pl. 4, figs 1–6.
- 1929 *Anasibirites alternatus* MATHEWS, p. 23, pl. 4, figs 22–23.
- 1929 *Anasibirites romeri* MATHEWS, p. 23, pl. 4, figs 24–25.
- ? 1929 *Anasibirites hyatti* MATHEWS, p. 30, pl. 5, figs 6–11.
- ?1929 *Anasibirites mojsisovicsi* MATHEWS, p. 30, pl. 5, figs 1–3.
- ?1929 *Gurleyites chamberlini* MATHEWS, p. 44, pl. 11, figs 3–5.
- ?1929 *Gurleyites boutwelli* MATHEWS, p. 45, pl. 8, figs 1–3.
- ?1929 *Gurleyites milleri* MATHEWS, p. 45, pl. 9, figs 10–12.
- 1932 *Anasibirites multiformis* – SMITH, p. 74, pl. 79. fig. 18.
- ? 1932 *Anasibirites mojsisovicsi* – SMITH, p. 73, pl. 80, figs 1–2.
- ? 1932 *Anasibirites noetlingi* – SMITH, p. 74, pl. 9, figs 1–3.
- 1932 *Anasibirites tenuistriatus* – SMITH, p. 74, pl. 79, figs 9–10.
- 1932 *Anasibirites angulosus* – SMITH; p. 70, pl. 79, figs 13–15.
- 1964 *Anasibirites pacificus* – BANDO, p. 73, pl. 3, figs 5–7; pl. 5, figs 8, 11, 13–14; pl. 6, figs 8–9, 11.
- 1964 *Anasibirites ehimensis* BANDO, p. 74, pl. 3, figs 12a–c.
- 1964 *Anasibirites* sp. A – BANDO, p. 77, pl. 3, figs 8a–c.
- p 1968 *Anasibirites nevolini* ZAKHAROV, p. 131, pl. 25, fig. 5 only.
- 1968 *Anasibirites kingianus* – KUMMEL & ERBEN, p. 135, pl. 22, figs 12–17; pl. 23, figs 1–18.
- 1978 *Anasibirites kingianus* – GUEX, pl. 3, figs 2, 9; pl. 4, fig. 6.
- p 1978 *Anasibirites nevolini* – ZAKHAROV, pl. 11, figs 11–13 only.
- 1990 *Anasibirites ochotensis* – DAGYS & ERMAKOVA, p. 47, pl. 13, figs 2–5.

- 1994 *Anasibirites robustus* – TOZER, p. 78, pl. 28, fig. 2a–b.
- p ? 2007b *Anasibirites kingianus* – LUCAS et al., p. 104, fig. 3h–j only.
- v 2008 *Anasibirites nevolini* – BRAYARD & BUCHER, p. 57, pl. 28, fig. 7–9, text-fig. 49.
- v p 2012b *Anasibirites kingianus* – BRÜHWILER & BUCHER, p. 101, figs 84E–L, 84R–U only.
- v p 2012b *Anasibirites angulosus* – BRÜHWILER & BUCHER, p. 103, figs 84V–AA, 86A–U, 87A–D, K–M only.
- v 2012c *Anasibirites kingianus* – BRÜHWILER et al., p. 155, figs 31O, 32AA–BD.
- 2013 *Anasibirites nevolini* – ZAKHAROV et al., figs 6.1–6.2.
- v 2015 *Anasibirites kingianus* – JATTIOT et al., p. 29, figs 4, 6–9, 10A–M, 12, 15–18.

Occurrence: Rare [n = 7] in UAZ₅ (PLR24, PLR34, PLR57 and PLR37).

Description: JATTIOT et al. (2015) recently provided a thorough, revised description of this species. The main characteristics of this taxon are: 1) strong allometric growth characterized by quadratic early whorls and compressed mature whorls, 2) megastriae of highly variable magnitude on early whorls and 3) mature whorls without megastriae, but with growth lines and ribs (more pronounced on the venter) on some specimens. Suture line not available in our material.

Measurements: See Text-fig. 28. Estimated maximal size: ~ 10 cm (JATTIOT et al. 2015).

Discussion: *Anasibirites multiformis* is distinguished from *A. kingianus* by its nearly isometric growth characterized by compressed whorls and dense, regularly spaced, low magnitude megastriae from early whorls through maturity. See JATTIOT et al. (2015) for a thorough discussion of the taxonomy of *Anasibirites* species.

Anasibirites multiformis WELTER, 1922

(Plate 11, Figs. G-AA)

? 1895 *Sibirites tenuistriatus* – WAAGEN, p. 124, pl. 9, figs 1–2.

p. 1922 *Anasibirites multiformis* WELTER, p. 138, pl. 16, figs 9–13, 16–19; pl. 17, figs 1–3, 8–10 only.

1927 *Ophiceras multiplicatus* YEHARA, p. 162, pl. 14, figs 4, 4a.

1929 *Anasibirites salisburyi* MATHEWS, p. 9, pl. 1, figs 27–29; pl. 2, figs 1–2.

1929 *Anasibirites johannseni* MATHEWS, p. 12, pl. 1, figs 34, 36–37.

1929 *Anasibirites whitei* MATHEWS, p. 12, pl. 1, fig. 35; pl. 2, figs 15–16.

1929 *Anasibirites blackwelderi* MATHEWS, p. 13, pl. 2, figs 10–14.

1929 *Anasibirites fisheri* MATHEWS, p. 13, pl. 2, figs 3–9.

1929 *Anasibirites emmonsi* MATHEWS, p. 14, pl. 2, figs 20–26.

1929 *Anasibirites welleri* MATHEWS, p. 14, pl. 2, figs 17–19.

1929 *Anasibirites powelli* MATHEWS, p. 15, pl. 3, figs 1–5.

1929 *Anasibirites whitfieldi* MATHEWS, p. 16, pl. 3, figs 6–8.

1929 *Anasibirites crickmayi* MATHEWS, p. 16, pl. 3, figs 24–27.

1929 *Anasibirites veranus* MATHEWS, p. 17, pl. 3, figs 18–23.

1929 *Anasibirites perrini* MATHEWS, p. 18, pl. 3, figs 34–36.

1929 *Anasibirites ketchumi* MATHEWS, p. 18, pl. 3, figs 12–17.

1929 *Anasibirites weaveri* MATHEWS, p. 19, pl. 3, figs 10–11, 32–33.

1929 *Anasibirites wardi* MATHEWS, p. 19, pl. 2, figs 27–29.

1929 *Anasibirites clarki* MATHEWS, p. 25, pl. 4, figs 26–28.

1929 *Anasibirites bretzi* MATHEWS, p. 25, pl. 4, figs 14–18; pl. 7, fig. 13.

1929 *Anasibirites vanbuskirki* MATHEWS, p. 26, pl. 4, figs 36–38.

1929 *Anasibirites rollini* MATHEWS, p. 27, pl. 1, figs 30–33; pl. 4, figs 10–13.

- 1929 *Anasibirites gibsoni* MATHEWS, p. 29, pl. 5, figs 4–5.
- 1932 *Anasibirites hircinus* – SMITH, p. 72, pl. 79, figs 11–12.
- 1932 *Anasibirites emmonsi* – SMITH, p. 71, pl. 79, figs 22–24.
- ? 1932 *Anasibirites desertorum* SMITH, p. 71, pl. 51, figs 7–10; pl. 56, figs 19–20.
- 1964 *Anasibirites onoi* – BANDO, p. 72, pl. 3, figs 13a–b, 14a–b, 15a–d, 16; pl. 5, fig. 7.
- ?1964 *Anasibirites intermedius* BANDO, p. 75, pl. 5, figs 9a–b.
- 1964 *Anasibirites multiplicatus* – BANDO, p. 76, pl. 3, figs 4a–b, 9a–b, 11a–b, 13a–b, 17; pl. 5, figs 10, 15.
- ? 1964 *Anasibirites* sp. B – BANDO, p. 77, pl. 3, figs 1–2.
- ? 1964 *Anasibirites* sp. C – BANDO, p. 78, pl. 5, fig. 12.
- p 1978 *Anasibirites nevolini* – ZHAKAROV, pl. 11, figs 9–10 only.
- 1981 *Meekoceras* sp – DEAN, pl. 1, fig. 5.
- 1994 *Anasibirites crickmayi* – TOZER, p. 78, pl. 28, fig. 1a–b.
- 2007 *Anasibirites kingianus* – LUCAS et al., p. 104, figs 3d–g; figs 4a–b, e–h, j–l.
- v 2008 *Anasibirites multiformis* – BRAYARD & BUCHER, p. 56, pl. 28, figs 1–6, text-figs. 48–49.
- v p 2008 *Hemiprionites* cf. *butleri* – BRAYARD & BUCHER, p. 58, pl. 29, fig. 5 only.
- 2010 *Anasibirites kingianus* – STEPHEN et al., fig. 7a–b.
- v 2012a *Anasibirites multiformis* – BRÜHWILER & BUCHER, p. 33, pl. 19, figs 1–6.
- v p 2013 *Anasibirites kingianus* – BRAYARD et al., p. 195, fig. 62a–g, j–k only.
- v 2013 *Anasibirites multiformis* – BRAYARD et al., p. 195, fig. 64a–g.
- 2013 *Anasibirites simanenkoi* ZAKHAROV et al., p. 603, figs 6.3 –6.8.
- v 2015 *Anasibirites multiformis* – JATTIOT et al., p. 30, figs. 10N–S, 21–23.

Occurrence: Very abundant [n ~ 120] in UAZ₅ (PLR24, PLR30, PLR37, PLR58, PLR34 and PLR57).

Description: Growth isometric, maintaining a moderately involute shell throughout development. Venter tabulate to subtabulate, with angular shoulders on inner whorls and subtabulate on mature whorls, with bluntly angular shoulders. Umbilicus relatively shallow with oblique wall and rounded shoulders. Flanks sub-parallel and flat on inner whorls. Sculpture typically consisting of dense, thin megastriae persisting through maturity. Strong ribbing unusual and restricted to the thickest whorled, extreme evolute variants (e.g., Plate 11, Figs. X–Z). Suture line ceratitic with rather deep lateral lobes and broad and rounded saddles.

Measurements: See Text-fig. 29. Estimated maximal size: ~ 10 cm.

Discussion: See *Anasibirites kingianus*. The reader should refer to JATTIOT et al. (2015) for a revision and extended discussion of this species. One specimen of *H. cf. butleri* from China (BRAYARD & BUCHER, pl. 29, fig. 5) shows identical megastriae and therefore belongs to the species *A. multiformis*.

Genus *Hemiprionites* SPATH, 1929

Type species: *Goniodiscus typus* WAAGEN, 1895

Hemiprionites typus (WAAGEN, 1895)

(Plate 12, Figs. A–M; Plate 13, Figs. A–X)

1895 *Goniodiscus typus* WAAGEN, p. 128, pl. 9, figs. 7–10.

1929 *Goniodiscus typus* – MATHEWS, p. 31, pl. 5, figs. 12–21.

1929 *Goniodiscus americanus* MATHEWS, p. 32, pl. 5, figs. 22–27.

1929 *Goniodiscus shumardi* MATHEWS, p. 33, pl. 6, figs. 11–14.

1929 *Goniodiscus utahensis* MATHEWS, p. 33, pl. 6, figs. 29–31.

1929 *Goniodiscus ornatus* MATHEWS, p. 34, pl. 6, figs. 6–10.

1929 *Goniodiscus slocomi* MATHEWS, p. 34, pl. 6, figs. 15–17.

1929 *Goniodiscus butleri* MATHEWS, p. 35, pl. 6, figs. 18–21.

1932 *Anasibirites typus* – SMITH, p. 76, pl. 80, figs. 6–8.

1932 *Anasibirites utahensis* – SMITH, p. 77, pl. 80, figs. 9, 10.

1932 *Anasibirites ornatus* – SMITH, p. 75, pl. 80, figs. 11, 12.

1934 *Hemiprionites typus* – SPATH, p. 331, figs. 114a–c.

v p 2008 *Hemiprionites cf. butleri* – BRAYARD & BUCHER, p. 58, pl. 29, figs. 1, 4, 7 only.

v 2012b *Hemiprionites typus* – BRÜHWILER & BUCHER, p. 103, figs. 89A–AH.

v 2013 *Hemiprionites cf. typus* – BRAYARD et al., p. 197, fig. 66.

Occurrence: Very abundant [n ~ 130] in UAZ₅ (PLR24, PLR30, PLR34, PLR36, PLR37, PLR57, PLR58 and PLR59).

Description: Involute, compressed shell with deeply embracing whorls and slightly egressive coiling. Flanks convex and convergent with or without an *Ambites*-like depression (minute depression on outer edge of flank) immediately below ventral shoulders. Depression near ventral shoulders sometimes only present in early ontogeny, then fading away on outer whorl (e.g., Plate 13, Figs. A–C). Maximum whorl width near mid-flank. Venter tabulate to weakly sulcate in rare instances or even bicarinate when the depression near the ventral shoulders is marked. Ventral area ornamented with spiral lines on well-preserved specimens. Ventral shoulders angular, or less abrupt on specimens without depression. Umbilical shoulders broadly rounded forming a deep umbilicus with inclined wall. Ornamentation visible on very well preserved specimens consisting of very low radial folds occasionally giving rise to crenulated ventral shoulders. Flexuous growth lines parallel to folds. Suture line (Plate 13, Fig.

R) ceratitic with strongly tapered first and second lateral saddles, but suture line highly variable.

Measurements: See Text-fig. 30. Estimated maximal size: ~ 10 cm.

Discussion: *H. typus* was originally described (WAAGEN 1895) as exhibiting a typical depression near the ventral shoulders, and other workers have subsequently referred to this feature (e.g., MATHEWS 1929, BRÜHWILER & BUCHER 2012b, BRAYARD et al. 2013). However, our material from Palomino Ridge as well as extensive material from Timor (JATTIOT et al., ongoing work) demonstrate that specimens of *H. typus* do not always exhibit such a depression. With regard to standard shell parameters, specimens with or without the depression are identical (Text-fig. 30).

According to BRAYARD & BUCHER (2008) and BRAYARD et al. (2013), all species erected by MATHEWS (1929) can be grouped as variants of the type species, with the exception of *Hemiprionites butleri* and *H. walcotti*. *Hemiprionites roberti* from Crittenden Springs (JENKS et al. 2010) and *H. klugi* from South China (BRAYARD & BUCHER 2008) and the Salt Range (BRÜHWILER et al. 2012b) mainly differ from the type species by their involute coiling and funnel-like umbilicus. *Hemiprionites butleri* from northern Utah (MATHEWS 1929) and South China (BRAYARD & BUCHER 2008) was mainly distinguished from the type species on the basis of its marked sulcate, bicarinate venter (see MATHEWS's 1929 descriptions and discussion in BRAYARD & BUCHER 2008 and BRÜHWILER et al. 2012a)

However, the material from Palomino Ridge shows that the morphology of the ventral shoulders in *H. typus* results from the strength of the depression near the ventral shoulders: specimens without a depression exhibit bluntly angular shoulders (Plate 12, Figs. A–M) whereas specimens with a depression exhibit narrower angular shoulders (e.g., Plate 13, Figs. O–Q); specimens with a marked depression display developed keels (Plate 13, Figs. G–I, U–

V). We thus consider here that the presence of a bicarinate venter is not a robust diagnostic character to discriminate between *Hemiprionites* species. Therefore, *H. butleri* does not significantly differ from *H. typus* and is synonymized with this species.

Hemiprionites walcotti (MATHEWS, 1929)

(Plate 14, Figs. A–Y)

p 1922 *Anasibirites multiformis* WELTER, p. 17, figs. 4–7, 11–14.

1929 *Goniodiscus walcotti* MATHEWS, p. 32, pl. 6, figs. 1–5.

1934 *Hemiprionites timorensis* SPATH, p. 331.

v p 2008 *Hemiprionites* cf. *butleri* – BRAYARD & BUCHER, p. 58, pl. 29, figs. 2, 3, 6 only.

v 2008 *Hemiprionites klugi* BRAYARD & BUCHER, p. 59, pl. 30, figs. 1–4.

v p 2012a *Hemiprionites* cf. *butleri* – BRÜHWILER & BUCHER, p. 33, pl. 19, fig. 10 only.

v p 2012b *Anasibirites angulosus* – BRÜHWILER & BUCHER, p. 103, figs. 87H–J, N–P only.

v 2012b *Hemiprionites klugi* – BRÜHWILER & BUCHER, p. 103, figs. 87Q–AB.

Occurrence: Common [n ~ 25] in UAZ₅ (PLR24, PLR37, PLR58, PLR34, PLR57 and

PLR55).

Description: Coiling involute throughout juvenile stages, becoming slightly egressive at maturity. Compressed shell with tabulate venter (thinner than *H. typus*), angular or bluntly angular ventral shoulders and convex flanks with maximum curvature at mid-flank. Very low keels associated with very angular ventral shoulders in a few specimens only. Umbilicus deep with steeply inclined wall, very narrow at juvenile stages and becoming slightly more open at mature stages. Umbilical shoulders broadly rounded. Very low radial folds occurring in a few

variants. Flexuous growth lines parallel to folds when present. Suture line ceratitic, with tapered first and second lateral saddles. Paratype of the species exhibiting a broad and rounded second lateral saddle (MATHEWS 1929, pl. 6, fig. 5), thus illustrating highly variable detailed patterns of the suture line.

Measurements: See Text-fig. 30. Estimated maximal size: ~ 7 cm.

Discussion: According to MATHEWS (1929), *H. walcotti* is characterized by its ‘compressed, wedge-shaped form; its narrow, smooth venter; its indistinct keels; and its very narrow, deep umbilicus’.

Based on our material from Palomino Ridge, we confirm that *H. walcotti* differs from *H. typus* by its more involute coiling, its greater whorl height (Text-fig. 30) and its narrower venter. Furthermore, a depression is not visible near the ventral shoulders. Juvenile specimens of both *H. walcotti* and *H. typus* are sometimes barely distinguishable, especially when dealing with involute juvenile specimens of *H. typus* that lack the depression near the ventral shoulders.

According to BRAYARD & BUCHER (2008), *H. klugi* is similar to *H. walcotti*, but the lack of measurements prevented them from comparing the two species. After a careful examination of the type material of *H. klugi*, we were unable to detect any differences in our *H. walcotti* specimens. With regard to classical measurement parameters, the holotype of *H. klugi* is identical to *H. walcotti* specimens from Nevada (Text-fig. 30). According to BRAYARD & BUCHER (2008), *H. klugi* also shows a peculiar suture line. However, the intra- and interspecific variability of the suture line in *Hemiprionites* is very high. Hence, we here synonymize *H. klugi* with *H. walcotti*.

Specimens of *H. cf. butleri* from South China (BRAYARD & BUCHER 2008) are here reassigned to *H. typus* and *H. walcotti*. One specimen of *H. cf. butleri* from Oman (BRÜHWILER et al. 2012a), of middle Smithian origin, is tentatively placed within *H. roberti* JENKS et al. 2010, also of middle Smithian origin. The second specimen of *H. cf. butleri* from Oman (BRÜHWILER et al. 2012a) is placed within *H. walcotti*.

Genus *Arctopriionites* (FREBOLD, 1930)

Type species: *Goniodiscus nodosus* FREBOLD, 1930

Arctopriionites resseri (MATHEWS, 1929)

(Plate 12, Figs. N–X)

1929 *Kashmirites resseri* MATTHEWS, p. 38, pl. 8, figs. 4–7.

1932 *Kashmirites resseri* – SMITH, p. 67, pl. 81, figs. 9, 10.

1961 *Arctopriionites* sp. indet – TOZER, pl. 20, fig. 1.

1962 *Arctopriionites* sp. indet. – KUMMEL & STEELE, p. 699, pl. 101, fig. 2.

1994 *Arctopriionites williamsi* TOZER, p. 83, pl. 34, figs. 1–4.

v 2013 *Arctopriionites resseri* – BRAYARD et al., p. 198, fig. 67.

Occurrence: Documented from UAZ₅ (PLR24, PLR30, PLR34, PLR37 and PLR58). [n = 9]

Description: Involute, compressed shell with slightly egressive coiling. Flanks slightly convex and whorl section trapezoidal. Depression near ventral shoulders visible on immature whorls. Venter tabulate with angular shoulders, but sulcate or even bicarinate if in association with a marked depression near ventral shoulders (e.g., Plate 12, Figs. P–R). Venter becoming flat with bluntly angular shoulders on mature whorls. Umbilical shoulders broadly rounded,

with a deep umbilicus and inclined wall. Ornamentation consisting of slightly projected, angular and elongated bullae near umbilical margin. Bullae fading away near mid-flank. Weak folds occasionally persisting, inducing a crenulation on ventral shoulders. Folds generally not crossing the venter. Suture line ceratitic with broad rounded saddles and deep first lateral lobe.

Measurements: See Text-fig. 31. Estimated maximal size: ~ 12 cm.

Discussion: See BRAYARD et al. (2013) for a comprehensive discussion of the taxon *Arctopriionites resseri*. The genus *Hemiprionites* mainly differs by the absence of umbilical bullae.

Genus *Meekoceras* HYATT, 1879

Type species: *Meekoceras gracilitatis* WHITE, 1879

Meekoceras gracilitatis WHITE, 1879

(Plate 15, Figs. A–U)

1879 *Meekoceras gracilitatis* WHITE, p. 114.

1880 *Meekoceras gracilitatis* – WHITE, p. 115, pl. 31, fig. 2.

1902 *Meekoceras gracilitatis* – FRECH, p. 631, fig. 2.

p 1904 *Meekoceras gracilitatis* – SMITH, p. 370, pl. 42, only fig. 1; pl. 43, figs. 3, 4.

1905 *Meekoceras gracilitatis* – HYATT & SMITH, p. 143, pl. 12, figs. 1–13; pl. 13, figs. 1–18; pl. 14, figs. 1–8; pl. 70, figs. 4–7.

p 1932 *Meekoceras gracilitatis* – SMITH, p. 57, pl. 12, figs. 1–13; pl. 13, figs. 1–18; pl. 14, figs. 1–8; pl. 36, figs. 19–28; pl. 37, figs. 1–7; pl. 38, figs. 2, 3 and 5, 6 only; pl. 70, figs. 4–7.

1961 *Meekoceras gracilitatis* – TOZER, p. 65, pl. 15, fig. 6; pl. 17, figs. 1–3; pl. 18, figs. 4–6.

1962 *Meekoceras gracilitatis* – KUMMEL & STEELE, p. 693, pl. 103, figs. 1–6.

1968 *Meekoceras gracilitatis* – KUMMEL & ERBEN, p. 129, pl. 20, figs. 1–3, 8–13.

1979 *Meekoceras gracilitatis* – NICHOLS & SILBERLING, p. B3, pl. 1, figs. 1–4.

1990 *Meekoceras gracilitatis* – DAGYS & ERMAKOVA, p. 35, pl. 6, fig. 5; pl. 7, fig. 1; pl. 8, figs. 1, 2.

? 1994 *Meekoceras gracilitatis* – TOZER, p. 70, pl. 21, fig. 2.

v 2013 *Meekoceras gracilitatis* – BRAYARD et al., p. 200, fig. 68.

Occurrence: Very abundant [n ~ 120] in UAZ₄ (see Text-figs. 4, 5). This species is not abundant in Utah sections studied by BRAYARD et al. (2013), but it is documented from UAZ₂ to UAZ₄ in this area.

Description: Involute coiling and compressed shell. Distinct egressive coiling, evolution increasing with larger diameter (Text-fig. 32). Flanks slightly convex forming a trapezoidal whorl section. Venter sulcate (true bicarinate venter) with very angular shoulders. Umbilicus with inclined wall and broadly rounded shoulders forming a moderately deep umbilicus. No folds visible on our specimens. Suture line ceratitic with fairly low saddles.

Measurements: See Text-fig. 32. Estimated maximal size: ~ 20 cm.

Discussion: The reader is referred to BRAYARD et al. (2013).

Meekoceras olivieri BRAYARD et al., 2013

(Plate 16, Figs. A–D)

2013 *Meekoceras olivieri* BRAYARD et al., p. 204, fig. 71.

Occurrence: Occurs only in PLR95 (UAZ₁). [n = 2]

Description: Compressed shell with a moderately involute coiling, similar to *M. gracilitatis*. Venter at small and medium sizes tabulate with marked rounded shoulders. Venter becoming arched at larger size and ventral shoulders becoming indistinct. Suture line not available in our material.

Measurements: Not available. Estimated maximal size: ~ 15 cm (BRAYARD et al. 2013).

Discussion: *M. olivieri* differs from the type species by its arched venter at large sizes, which contrasts with the typical sulcate venter of *M. gracilitatis*. At small sizes, these two species are almost indistinguishable. Even though our specimens are poorly preserved, their typical arched venter at larger sizes permit an assignment to *M. olivieri*. This species represents the oldest occurrence of *Meekoceras* in Nevada and Utah.

Prionitidae indet. 1

(Plate 16, Figs. E–H)

? v 2013 *Anasibirites* cf. *angulosus* – BRAYARD et al., p. 195, fig. 65.

Occurrence: Documented from UAZ₅ (PLR24, PLR59 and PLR34). [n = 8]

Description: Compressed shell with slightly convex flanks. Tabulate venter with angular shoulders. Umbilicus with an oblique wall and rounded shoulders, conforming to that of prionitids. Ornamentation consisting of spaced, sinuous, mostly concave, projected ribs crossing the venter. Sometimes ribs thicken forming elongate umbilical tubercles. Ribs may also form tubercles on ventral shoulders. Suture line not available in our material.

Measurements: Not available.

Discussion: Our material may represent a new taxon, perhaps at the genus level. Unfortunately, the fragmentary preservation and scarcity of the material preclude the establishment of an adequate diagnosis. Specimens from Utah assigned to “*Anasibirites* cf. *angulosus*” (BRAYARD et al. 2013) resemble our material, but they do not display obvious tubercles on the ventral shoulders. Additional material is needed in order to definitely attribute specimens described by BRAYARD et al. (2013) to Prionitidae indet. 1.

Prionitidae indet. 2

(Plate 16, Figs. I–L)

Occurrence: Found only in PLR38 and PLR60, which belong to a single horizon.

Association with *W. perrini* indicates that both localities belong to UAZ₅. [n = 10]

Description: Slightly involute, thick shell with somewhat convex flanks. Venter very broadly rounded with rounded shoulders. Moderately deep umbilicus typical of prionitids, i.e., with an oblique wall and rounded shoulders. Ornamentation consisting of shallow, distant, prorsiradiate and sinuous constriction-like furrows on flanks. Suture line not available in our material.

Measurements: See Table 1.

Discussion: This form may possibly represent a new genus. Its shell geometry is somewhat reminiscent of that of *Wasatchites*, but it lacks the diagnostic ornamentation of that genus. Unfortunately, the poor preservation and scarcity of the material hinder further discussion. No other ammonoids were found in association with Prionitidae indet. 2, except for a very incomplete and poorly preserved specimen of *Wasatchites perrini*.

Family Paranannitidae SPATH, 1930

Genus *Paranannites* HYATT & SMITH, 1905

Type species: *Paranannites aspenensis* HYATT & SMITH, 1905

Paranannites aspenensis HYATT & SMITH, 1905

(Plate 17, Figs. A–C)

1905 *Paranannites aspenensis* HYATT & SMITH, p. 81, pl. 8, figs. 1–15; pl. 73, figs. 1–30.

1932 *Paranannites aspenensis* – SMITH, p. 98, pl. 8, figs. 1–15; pl. 73, figs. 1–30.

1934 *Paranannites aspenensis* – SPATH, p. 190, pl. 14, figs. 6a–c, text-fig. 57a, h.

1957 *Paranannites aspenensis* – KUMMEL in ARKELL et al., p. L138, figs. 172–7a–c.

1959 *Paranannites* cf. *aspenensis* – CHAO, p. 284, pl. 24, figs. 1–7, 11, 12.

? 1959 *Paranannites ptychoides* CHAO, p. 284, pl. 24, figs. 8–10, text-fig. 37a.

1962 *Paranannites aspenensis* – KUMMEL & STEELE, p. 676, pl. 100, figs. 14–17.

? 1966 *Paranannites aspenensis* – HADA, p. 112, pl. 4, figs. 5a–b.

Occurrence: Extremely rare [n = 1], in PLR110 (UAZ₄).

Description: Involute, compressed paranannitid with rounded, nearly indistinct ventral shoulders and tightly rounded umbilical shoulders; parallel flanks near umbilicus gradually converging towards the arched venter. Umbilicus with high, perpendicular wall. No ornamentation visible on our specimen. Suture line not available in our material.

Measurements: See Text-fig. 33. Estimated maximal size: ~ 4 cm.

Discussion: Our unique specimen is very similar to the holotype (HYATT & SMITH 1905, pl. 73, figs. 1–2). *Paranannites baudi* from Oman (BRÜHWILER et al. 2012a) and *P. ovum* from China (BRAYARD & BUCHER 2008) display a more depressed whorl section.

Parannanites cf. baudi BRÜHWILER & BUCHER, 2012a
(Plate 17, Figs. D–J)

2012a *Paranannites baudi* BRÜHWILER & BUCHER, p. 41, pl. 23, fig. 1–10.

Occurrence: Extremely rare [n = 2], documented only from PLR9 (UAZ₄).

Description: Very involute shell with rounded venter. Subglobose outline on inner whorls, becoming slightly compressed on outer whorls. Flanks convex and converging, with maximum thickness at umbilical margin. Umbilicus small and very deep with a vertical wall and narrowly rounded to subangular umbilical shoulders. Ornamentation consists of very fine prorsiradiate plications that cross the venter. Suture line simple and ceratitic with only one lateral lobe.

Measurements: See Text-fig. 34. Estimated maximal size: ~ 5 cm.

Discussion: The overall morphology as well as measurements are very similar to typical specimens of *P. baudi* (BRÜHWILER & BUCHER 2012a). However, this taxon is older (early Smithian, *Rohillites omanensis* fauna). *Paranannites baudi* is very similar to *P. ovum* BRAYARD & BUCHER, 2008, which is however, more evolute at all growth stages and displays egressive coiling at maturity. *Paranannites ovum* also exhibits a suture line with more elements than the type species of *Paranannites*.

Genus *Owenites* HYATT & SMITH, 1905

Type species: *Owenites koeneni* HYATT & SMITH, 1905

Owenites koeneni HYATT & SMITH, 1905

(Plate 17, Figs. K–AD)

1905 *Owenites koeneni* HYATT & SMITH, p. 83, pl. 10, figs. 1–22.

1915 *Owenites koeneni* – DIENER, p. 214.

1932 *Owenites koeneni* – SMITH, p. 100, pl. 10, figs. 1–22.

1932 *Owenites egrediens* – SMITH, p. 100, pl. 52, figs. 6–8.

1932 *Owenites zitteli* SMITH, p. 101, pl. 52, figs. 1–5.

1934 *Owenites koeneni* – SPATH, p. 185, fig. 57.

1947 *Owenites* aff. *egrediens* – KIPARISOVA, p. 139, pl. 32, figs. 1–3.

1955 *Kingites shizimizui* SAKAGAMI, p. 138, pl. 2, figs. 2a–c.

1957 *Owenites koeneni* – KUMMEL in ARKELL et al., p. L138, figs. 171–8a–b.

1959 *Owenites costatus* CHAO, p. 249, pl. 22, figs. 10–18, 22, 23, text-fig. 26c.

1959 *Owenites pakungensis* CHAO, p. 248, pl. 21, figs. 6–8.

- 1959 *Owenites pakungensis* var. *compressus* CHAO, p. 248, pl. 21, figs. 4, 5.
- 1959 *Pseudowenites oxynotus* CHAO, p. 252, pl. 23, figs. 1–16, text-figs. 27a–d.
- 1959 *Owenites shimizui* – KUMMEL, p. 430.
- 1959 *Owenites cf. koeneni* – KUMMEL, p. 441, figs. 2–4.
- 1960 *Owenites shimizui* – KUMMEL & SAKAGAMI, p. 6, pl. 2, figs. 5, 6.
- 1962 *Owenites koeneni* – KUMMEL & STEELE, p. 674, pl. 101, figs. 3–7.
- 1962 *Owenites koeneni* – POPOV, p. 44, pl. 6, fig. 6.
- 1965 *Owenites koeneni* – KUENZI, p. 374, pl. 53, figs. 1–6, text-figs. 3d, 6.
- 1966 *Owenites koeneni* – HADA, p. 112, pl. 4, figs. 2–4.
- 1968 *Owenites koeneni* – KUMMEL & ERBEN, p. 121, figs. 12; pl. 19, figs. 10–15.
- 1968 *Owenites carinatus* SHEVYREV, p. 189, pl. 16, fig. 1.
- 1968 *Owenites koeneni* – ZAKHAROV, p. 94, pl. 18, figs. 1–3.
- 1973 *Owenites koeneni* – COLLIGNON, p. 139, pl. 4, figs. 2, 3.
- 1979 *Owenites koeneni* – NICHOLS & SILBERLING, pl. 1, figs. 17, 18.
- 1981 *Owenites koeneni* – BANDO, p. 158, pl. 17, fig. 7.
- 1984 *Owenites carinatus* – VU KHUC, p. 81, pl. 6, figs. 1–4, text-fig. H16.
- 1984 *Pseudowenites oxynotus* – VU KHUC, p. 82, pl. 7, figs. 3, 4.
- 1990 *Owenites koeneni* – SHEVYREV, p. 118, pl. 1, fig. 5.
- 1995 *Owenites koeneni* – SHEVYREV, p. 51, pl. 5, figs. 1–3.
- ? 2004 *Owenites pakungensis* – TONG et al., p. 199, pl. 2, figs. 9–10, text-fig. 7.
- v 2008 *Owenites koeneni* – BRAYARD & BUCHER, p. 67, pl. 36, figs. 1–8, fig. 58.
- v 2010b *Owenites koeneni* – BRÜHWILER et al., p. 426, fig. 15(9).
- v 2012a *Owenites koeneni* – BRÜHWILER & BUCHER, p. 43, pl. 25, figs. 1–6.
- v 2013 *Owenites koeneni* – BRAYARD et al., p. 204, fig. 74.
- 2014 *Owenites koeneni* – SHIGETA & NGUYEN, p. 126, figs. 89–96.

Occurrence: Common [n = 15] within the uppermost part of UAZ₄ (PLRA36, PLRA39, PLR14, PLR12, PLR13, PLR61, PLR62, PLR71, PLR72 and PLR88).

Description: Very involute, somewhat compressed shell with an inflated, lenticular whorl section and a typical, subangular to angular venter that may resemble a keel on some specimens. Very narrow and shallow umbilicus, occluded on some rare specimens (e.g., Plate 17, Figs. P–R). Umbilical shoulders narrowly rounded and very low umbilical wall. Whorl height and umbilical diameter of *O. koeneni* display significant allometric growth (BRAYARD & BUCHER 2008). Egressive coiling at maturity. Surface generally smooth, with occasional weak, forward projected constrictions and folds. Suture line ceratic with several divided umbilical lobes; indentations of lobes not preserved.

Measurements: See Text-fig. 35. Estimated maximal size: ~ 8 cm (BRÜHWILER & BUCHER 2012a).

Owenites carpenteri SMITH, 1932

(Plate 17, Figs. AE–AF)

1932 *Owenites carpenteri* SMITH, p. 100, pl. 54, figs. 31–34.

1966 *Owenites carpenteri* – HADA, p. 112, pl. 4, figs. 1a–e.

1968 *Owenites costatus* – KUMMEL & ERBEN, p. 122, fig. 12l.

1973 *Owenites carpenteri* – COLLIGNON, p. 139, pl. 4, figs. 5, 6.

v 2008 *Owenites carpenteri* – BRAYARD & BUCHER, p. 70, pl. 43, figs. 15, 16.

v 2010b *Owenites carpenteri* – BRÜHWILER et al., p. 426, fig. 16(7, 8).

v 2012a *Owenites carpenteri* – BRÜHWILER & BUCHER, p. 44, pl. 25, figs. 7, 8.

v 2013 *Owenites carpenteri* – BRAYARD et al., p. 208, fig. 75.

Occurrence A single specimen, from the uppermost part of UAZ₄ (PLR61). This species is also relatively rare in Utah (BRAYARD et al., 2013).

Description Small, very involute, with a slightly inflated, lenticular whorl section. Venter narrowly rounded. Flanks convex, umbilicus occluded. Maximum thickness near the umbilicus. Surface generally smooth, but may display weak, forward projected constrictions and folds. Suture line not available in our material.

Measurements See Text-fig. 36. Estimated maximal size: ~ 3.5 cm.

Discussion According to BRAYARD et al. (2013), *Owenites carpenteri* can be distinguished from the type species by its occluded umbilicus and its narrowly curved venter.

Family Galfettitidae BRÜHWILER & BUCHER 2012a

?*Galfettites* sp. indet.

(Plate 18, Figs. P–AE)

v 2012a ?*Galfettites* sp. indet.; BRÜHWILER & BUCHER, p. 29, pl. 16, fig. 2.

Occurrence: Common [n ~ 20] within the uppermost part of UAZ₄ (PLR14, PLR45, PLR61, PLR71 and PLR27).

Description: Involute and compressed shell with subparallel, slightly convex flanks. Venter tabulate with angular ventral shoulders. Umbilicus with high, vertical wall and angular

shoulders. Suture line ceratitic with slightly asymmetrical second lateral saddle; indentations of lobes very poorly preserved.

Measurements: See Text-fig. 37. Estimated maximal size: ~ 5 cm.

Discussion: This species is more involute than all known species of *Galfittites*. The single specimen from Oman described as ?*Galfittites* sp. indet. (BRÜHWILER et al. 2012a, plate 16, fig. 2) very likely belongs to the same species. Although our additional Nevada material may possibly justify the erection of a new species, an open nomenclature is here preferred in the absence of sufficient material.

Superfamily Sagecerataceae HYATT, 1884

Family Hedenstroemiidae WAAGEN, 1895

Genus *Hedenstroemia* WAAGEN, 1895

Type species: *Ceratites hedenstroemi* KEYSERLING, 1845

Hedenstroemia kossmati HYATT & SMITH, 1905

(Plate 18, Figs. I–L)

1905 *Hedenstroemia kossmati* HYATT & SMITH, p. 101, pl. 67, figs. 3–7; pl. 84, figs. 1–10.

1932 *Hedenstroemia kossmati* – SMITH, p. 78, pl. 28, figs. 11–16; pl. 41, figs. 1–10; pl. 67, figs. 3–7.

1932 *Hedenstroemia hyatti* SMITH, p. 78, pl. 27, figs. 13–18.

2010 Proptychitid gen. et sp. indet. – STEPHEN et al., fig. 4g–i.

v 2013 *Hedenstroemia kossmati* – BRAYARD et al., p. 210, fig. 79.

Occurrence: Rare in UAZ₄ (PLR9', PLRA6, PLRA25, PLR27, PLR71 and PLR72). [n = 6]

Description: Very involute, compressed shell presenting a sulcate venter at all growth stages. Flanks convex, with maximum thickness at mid-flank. Umbilicus very narrow with broadly rounded shoulders forming a deep funnel. Surface smooth. Complex ceratitic suture line, typical of hedenstromiids with an adventitious element and a well-developed auxiliary series bending towards the umbilicus.

Measurements: See Table 1. Estimated maximal size: ~ 20 cm (BRAYARD et al. 2013).

Discussion: The reader is referred to BRAYARD et al. (2013) for a thorough discussion of *H. kossmati*.

Genus *Pseudosageceras* DIENER, 1895

Type species: *Pseudosageceras* sp. indet. DIENER, 1895

Pseudosageceras multilobatum NOETLING, 1905

(Plate 19, Figs. A–I)

1905 *Pseudosageceras multilobatum* NOETLING, pl. 25, fig. 1, pl. 26, fig. 3.

1905 *Pseudosageceras intermontanum* HYATT & SMITH, p. 99, pl. 4, figs. 1–3; pl. 5, figs. 1–6; pl. 63, figs. 1, 2.

1909 *Pseudosageceras multilobatum* – KRAFFT & DIENER, p. 145, pl. 21, fig. 5.

1911 *Pseudosageceras drinense* ARTHABER, p. 201, pl. 17, figs. 6, 7.

1913 *Pseudosageceras multilobatum* – WANNER, p. 181, pl. 7, fig. 4.

1922 *Pseudosageceras multilobatum* – WELTER, p. 94, fig. 3.

- 1929 *Pseudosageceras intermontanum* – MATHEWS, p. 3, pl. 1, figs. 18–22.
- 1932 *Pseudosageceras multilobatum* – SMITH, p. 87–89, pl. 4, figs. 1–3; pl. 5, figs. 1–6; pl. 25, figs. 7–16; pl. 60, fig. 32; pl. 63, figs. 1–6.
- 1934 *Pseudosageceras multilobatum* – COLLIGNON, p. 56–58, pl. 11, fig. 2.
- 1934 *Pseudosageceras multilobatum* – SPATH, p. 54, fig. 6a.
- 1947 *Pseudosageceras multilobatum* – KIPARISOVA, p. 127, pl. 25, figs. 3, 4.
- 1947 *Pseudosageceras multilobatum* var. *giganteum* – KIPARISOVA, p. 127, pl. 26, figs. 2–5.
- 1948 *Pseudosageceras* cf. *clavisellatum* – RENZ & RENZ, p. 90, pl. 16, fig. 3.
- 1948 *Pseudosageceras drinense* – RENZ & RENZ, p. 92, pl. 16, fig. 6.
- 1948 *Pseudosageceras intermontanum* – RENZ & RENZ, p. 90, pl. 16, figs. 4, 7.
- 1959 *Pseudosageceras multilobatum* – CHAO, p. 183, pl. 1, figs. 9, 12.
- 1959 *Pseudosageceras tsotengense* CHAO, p. 184, pl. 1, figs. 7, 8, text-fig. 5b.
- 1959 *Pseudosageceras curvatum* CHAO, p. 185, pl. 1, figs. 13, 14, text-fig. 5a.
- ? 1959 *Pseudosageceras multilobatum* var. nov. – JEANNET, p. 30, pl. 6, fig. 1.
- 1961 *Pseudosageceras schamarensis* – KIPARISOVA, p. 31, pl. 7, fig. 3.
- 1961 *Pseudosageceras multilobatum* var. *gigantea* – POPOV, p. 13, pl. 2, figs. 1, 2.
- ? 1966 *Pseudosageceras multilobatum* – HADA, p. 112, pl. 4, fig. 6.
- ? 1968 *Pseudosageceras multilobatum* – KUMMEL & ERBEN, p. 112, pl. 19, fig. 9.
- 1968 *Pseudosageceras multilobatum* – SHEVYREV, p. 791, pl. 1, figs. 1, 2.
- ? 1973 *Pseudosageceras multilobatum* – COLLIGNON, p. 5, pl. 1, fig. 1.
- 1978 *Pseudosageceras multilobatum* – WEITSCHAT & LEHMANN, p. 95, pl. 10, figs. 2ab.
- 1984 *Pseudosageceras multilobatum* – VU KHUC, p. 26, pl. 1, fig. 1.
- 1994 *Pseudosageceras multilobatum* – TOZER, p. 83, pl. 18, figs. 1a, b; p. 384, fig. 17.
- v 2008 *Pseudosageceras multilobatum* – BRAYARD & BUCHER, p. 70, pl. 37, figs. 1–5.
- 2010 *Pseudosageceras multilobatum* – STEPHEN et al., figs. 6c, d, h.
- v 2010b *Pseudosageceras multilobatum* – BRÜHWILER et al., p. 429, fig. 16(14).

v 2012a *Pseudosageceras multilobatum* – BRÜHWILER & BUCHER, p. 47, pl. 26, fig. 4.

v 2012b *Pseudosageceras multilobatum* – BRÜHWILER & BUCHER, p. 109, figs. 95A–N.

2013 *Pseudosageceras multilobatum* – BRAYARD et al., p. 208, fig. 77.

2014 *Pseudosageceras multilobatum* – SHIGETA & NGUYEN, p. 137, figs. 98, 99.

Occurrence: Long-ranging, cosmopolitan species, found only in the uppermost part of UAZ₄ at Palomino Ridge (PLRA34, PLR12, PLR45, PLR62, PLR63, PLR71 and PLR72). [n = 8]

Description: Extremely involute compressed oxyconic shell with an occluded umbilicus.

Venter extremely narrow, bicarinate or very rarely acute. Flanks weakly convex, convergent from umbilicus to venter. Surface smooth without ornamentation. Suture line ceratitic, complex and composed of many adventitious elements with characteristic trifid lateral lobe. Other lobes are bifid.

Measurements: See Text-fig. 38. Estimated maximal size: ~ 15 cm.

Discussion: Some rare specimens (e.g., Plate 19, Figs. A–C) appear to exhibit an acute venter instead of an extremely narrow, bicarinate venter. Species easily recognizable by its compressed and involute oxyconic shell, as well as its typical suture line architecture.

Pseudosageceras augustum (BRAYARD & BUCHER, 2008)

(Plate 19, Figs. J–N)

v 2008 *Hedenstroemia augusta* BRAYARD & BUCHER, p. 72, pl. 39, figs 1–11, text-fig. 63.

2010 *Pseudosageceras augustum* – JENKS et al., p. 35, fig. 24.

v 2010b *Pseudosageceras augustum* – BRÜHWILER et al., p. 429, fig. 16(10–11).

v 2012c *Pseudosageceras augustum* – BRÜHWILER et al., p. 171, fig. 41Z–AI.

Occurrence: Documented from the potential UAZ₆ (PLR32 and PLR35). [n = 4]

Description: Extremely involute, compressed oxyconic shell. Slight change in slope between lower and upper flanks. Maximum thickness near mid-flank. Venter very narrow and weakly bicarinate. Umbilicus occluded. Surface smooth except for strongly biconcave growth lines. Suture line ceratitic with several adventitious lobes and long auxiliary series.

Measurements: Not available.

Discussion: Although the longitudinal line at about mid-flank described for this species by BRAYARD & BUCHER (2008) and BRÜHWILER et al. (2012c) is not visible on our specimens, the other shell characteristics of our material, such as the slight change of slope at mid-flank, are in perfect agreement with the diagnosis of *Pseudosageceras augustum* (BRAYARD & BUCHER 2008).

?*Pseudosageceras bullatum* n. sp.

(Plate 19, Figs. O–U)

Etymology: After the typical bullae of this species.

Holotype: PIMUZ 32101 (Plate 19, Figs. R–T), loc. PLR47, Palomino Ridge.

Occurrence: Documented from the potential UAZ₆ (PLR47 and PLR48). [n = 2]

Diagnosis: Very small, extremely involute hedenstroemiid with characteristic regularly spaced bullae placed at mid-flank.

Description: Extremely involute, compressed shell with a tabulate venter. Ventral shoulders bluntly angular. Flanks slightly convex. Umbilicus very narrow with broadly rounded shoulders forming a rather deep funnel. Surface almost smooth, with exception of regularly spaced bullae placed at mid-flank. Although only known from small size specimens, suture line invites comparisons with that of typical representatives of the genus *Pseudosageceras*, with a trifid lateral lobe and a long auxiliary series.

Measurements: See Table 1. Estimated maximal size: ~ 2 cm.

Discussion: This species is very similar to *P. augustum*, but it differs by the presence of characteristic regularly spaced bullae located at mid-flank.

Family Aspenitidae SPATH, 1934

Genus *Aspenites* HYATT & SMITH, 1905

Type species: *Aspenites acutus* HYATT & SMITH, 1905

Aspenites acutus HYATT & SMITH, 1905

(Plate 18, Figs. A–H)

1905 *Aspenites acutus* HYATT & SMITH, 1905, p. 96, pl. 2, figs. 9–13; pl. 3, figs. 1–5.

? 1909 *Hedenstroemia acuta* KRAFFT & DIENER, p. 157, pl. 9, fig. 2.

1922 *Aspenites acutus* – WELTER, p. 98, fig. 7.

1922 *Aspenites laevis* WELTER, p. 99, pl. 1, figs. 4, 5.

1932 *Aspenites acutus* – SMITH, p. 86, pl. 2, figs. 9–13, pl. 3, figs. 1–5, pl. 30, figs. 1–26, pl. 60, figs. 4–6.

1932 *Aspenites laevis* – SMITH, p. 86, pl. 28, figs. 28–33.

- 1932 *Aspenites obtusus* SMITH, p. 86, pl. 31, figs. 8–10.
- 1934 *Aspenites acutus* – SPATH, p. 229, fig. 76.
- ? 1934 *Parahedenstroemia acuta* – SPATH, p. 221, fig. 70.
- 1957 *Aspenites acutus* – KUMMEL, p. L142, fig. 173a–c.
- 1959 *Aspenites acutus* – CHAO, p. 269, pl. 35, figs. 12–18, 23, text-fig. 34a.
- 1959 *Aspenites laevis* – CHAO, p. 270, pl. 35, figs. 9–11, text-fig. 34b.
- 1962 *Aspenites acutus* – KUMMEL & STEELE, p. 692, pl. 99, figs. 16–17.
- 1962 *Hemiaspenites obtusus* – KUMMEL & STEELE, p. 666, pl. 99, fig. 18.
- . 1962 *Pseudosageceras multilobatum* – KUMMEL & STEELE, p. 701, pl. 102, figs. 1, 2.
- 1979 *Aspenites cf. acutus* – NICHOLS & SILBERLING, pl. 1, figs. 10–11.
- 1979 *Aspenites acutus* – NICHOLS & SILBERLING, pl. 1, figs. 12–14.
- v 2008 *Aspenites acutus* – BRAYARD & BUCHER, p. 77, pl. 42, figs. 1–9.
- 2010 *Aspenites acutus* – STEPHEN et al., fig. 4f.
- v 2010b *Aspenites acutus* – BRÜHWILER et al., p. 429, fig. 16(12, 13).
- v 2012a *Aspenites acutus* – BRÜHWILER & BUCHER, p. 48, pl. 26, figs. 1, 2.
- v 2012c *Aspenites acutus* – BRÜHWILER et al., p. 164, figs. 41A–M.
- v 2013 *Aspenites acutus* – BRAYARD et al., p. 212, fig. 81.
- 2014 *Aspenites acutus* – SHIGETA & NGUYEN, p. 136, fig. 97.

Occurrence: Documented from UAZ₄ (PLR87, PLRA34, PLR14, PLRA35, PLR12 and PLR71). [n = 11]

Description: Extremely involute, very compressed oxyconic shell with an occluded umbilicus. Maximum curvature at mid-flank. Venter with a characteristic acute keel. Flanks slightly convex. Umbilical region slightly depressed. Surface nearly smooth except for fine

radial folds and falcoid growth lines. Suture line ceratitic with two adventitious saddles and a long auxiliary series.

Measurements: See Text-fig. 39. Estimated maximal size: ~ 8 cm.

Discussion: The reader is referred to BRAYARD & BUCHER (2008) and BRAYARD et al. (2013) for in-depth systematic review and discussion of this species. *Aspenites acutus* mainly differs from other aspenitid taxa (e.g., *Pseudaspenites layeriformis*) by its occluded umbilicus. This species is distributed throughout the paleotropical latitudes (e.g., South China, Oman, Tibet, Timor).

Superfamily Otocerataceae HYATT, 1900

Family Anderssonoceratidae RUZHENCEV, 1959

Genus *Proharpoceras* CHAO, 1950

Type species: *Proharpoceras carinatitabulatum* CHAO, 1950

Proharpoceras carinatitabulatum CHAO, 1950

(Plate 18, Figs. M–O)

1950 *Proharpoceras carinatitabulatus* CHAO, p. 8, pl. 1, fig. 8a–b.

1950 *Tuyangites marginalis* CHAO, p. 9, pl. 1, fig. 9.

1959 *Proharpoceras carinatitabulatum* – CHAO, p. 324, pl. 43, figs. 1–7.

1959 *Tuyangites marginalis* – CHAO, p. 327, pl. 43, figs. 17–18.

1968 *Proharpoceras carinatitabulatum* – ZAKHAROV, p. 147, pl. 29, fig. 6.

v 2007a *Proharpoceras carinatitabulatum* – BRAYARD et al., p. 178, fig. 3a–s, v–z.

v 2008 *Proharpoceras carinatitabulatum* – BRAYARD & BUCHER, p. 80, pl. 38, figs. 5–9.

v 2012a *Proharpoceras carinatitabulatum* – BRÜHWILER & BUCHER, p. 14, pl. 1, fig. 1.

Occurrence: A single fragmentary specimen from the uppermost part of UAZ₄ (PLR63).

Description: Moderately evolute shell with a quadratic whorl section and flat, parallel flanks. Venter tabulate with a raised median keel and angular shoulders. Suture line too poorly preserved to be illustrated.

Measurements: Not available.

Discussion: Well preserved specimens from South China show that the venter of this species is actually tricarinate (BRAYARD & BUCHER 2008). This is the first record of *Proharpoceras* from western USA and it considerably enlarges its known paleogeographic distribution, which is restricted to the paleotropical belt (BRAYARD et al. 2007a). It also well exemplifies that many Early Triassic taxa crossed the wide Panthalassa Ocean, indicating significant faunal exchanges at that time (BRAYARD et al. 2007b, 2009c, JENKS et al. 2010, BRAYARD et al. 2013, BRAYARD & BUCHER 2015, SHIGETA & KUMAGAE 2015)

Superfamily and family INCERTAE SEDIS

Gen. et sp. indet.

(Plate 6, Figs. L, M)

Occurrence: A single fragmentary, poorly-preserved specimen from UAZ₄ (PLRA10).

Description: Shell probably moderately evolute with depressed, convex flanks. Maximum whorl width above mid-flank. Venter broadly rounded with indistinct shoulders. Ribbing typically plicate, probably becoming approximate towards aperture. Strength of ribbing accentuated on venter. Suture line not available in our material.

Discussion: Plicate ribbing is thus far unknown among Smithian ammonoids, with the notable exception of a possible globose representative of Acrochordiceratidae in the middle Smithian of the Salt Range (BRÜHWILER & BUCHER 2012b, fig. 93A–D). The specimen from Palomino Ridge differs from the Salt Range material by its smaller size and more evolute shell shape.

Measurements: Not available.

Acknowledgements

We deeply acknowledge the long-term support of the Claraz Fund for fieldwork research in northeastern Nevada, as well as the support of the Swiss SNF (project 200020-160055 to H.B.) and to the French ANR-13-JS06-0001-01 AFTER project (to A.B.). Rosie Roth is thanked for her photographic skills, as well as Thomas Brühwiler for his help with mechanical preparation. The Palomino Ridge localities mentioned in this report are located on US public land under the stewardship of the Bureau of Land Management (BLM) of the US Department of the Interior. Their management and access to these lands is much appreciated.

References

ANGIOLINI, L. & BUCHER, H. (1999): Taxonomy and quantitative biochronology of Guadalupian brachiopods from the Khuff Formation, Southeastern Oman. – *Geobios* **32** (5): 665–699.

ARTHABER, G. (1911): Die Trias von Albanien. – *Beitr. Paläontol. und Geol. Österreich-Ungarns und des Orients* **24**: 169–288.

BANDO, Y. (1964): The Triassic Stratigraphy and Ammonite Fauna of Japan. – *The Sci. Rep. Tohoku Univ., Sendai, Japan, Second Ser. (Geol.)* **36**: 1–137.

BANDO, Y. (1981): Lower Triassic ammonoids from Guryul Ravine and the spur three kilometers north of Barus. – In: NAKAZAWA, K. & KAPOOR, H.M. (ed.): The Upper Permian and Lower Triassic fossils of Kashmir. – *Paleontol. Indica* **46**: 135–178.

BRAYARD, A. & BUCHER, H. (2008): Smithian (Early Triassic) ammonoid faunas from northwestern Guangxi (South China): taxonomy and biochronology. – *Fossils and Strata* **55**: 1–179.

BRAYARD, A. & BUCHER, H. (2015): Permian-Triassic Extinctions and Rediversifications. – In: KLUG, C., KORN, D., DE BAETS, K., KRUTA, I. and MAPES, R.H. (ed.). *Ammonoid Paleobiology: From macroevolution to paleogeography*. – *Topics in Geobiology* **44**: 465–473.

BRAYARD, A., BUCHER, H., ESCARGUEL, G., FLUTEAU, F., BOURQUIN, S. & GALFETTI, T. (2006): The Early Triassic ammonoid recovery: Paleoclimatic significance of diversity gradients. – *Palaeogeogr., Palaeoclimatol., Palaeoecol.* **239**: 374–395.

BRAYARD, A., BUCHER, H., BRÜHWILER, T., GALFETTI, T., GOUDEMAND, N., GUODUN, K., ESCARGUEL, G. & JENKS, J. (2007a): *Proharpoceras* Chao: a new ammonoid lineage surviving the end-Permian mass extinction. – Lethaia **40**: 175–181.

BRAYARD, A., ESCARGUEL, G. & BUCHER, H. (2007b): The biogeography of Early Triassic ammonoid faunas: Clusters, gradients, and networks. – Geobios **40**: 749–765.

BRAYARD, A., ESCARGUEL, G., BUCHER, H., MONNET, C., BRÜHWILER, T., GOUDEMAND, N., GALFETTI, T. & GUEX, J. (2009a): Good Genes and Good Luck: Ammonoid Diversity and the End-Permian Mass Extinction. – Science **325**: 1118–1121.

BRAYARD, A., BRÜHWILER, T., BUCHER, H. & JENKS, J. (2009b): *Guodunites*, a low-palaeolatitude and trans-Panthalassic Smithian (Early Triassic) ammonoid genus. – Palaeontol. **52**: 471–481.

BRAYARD, A., ESCARGUEL, G., BUCHER, H. & BRÜHWILER, T. (2009c): Smithian and Spathian (Early Triassic) ammonoid assemblages from terranes: Paleoceanographic and paleogeographic implications. – J. Asian Earth Sci. **36**: 420–433.

BRAYARD, A., VENNIN, E., OLIVIER, N., BYLUND, K.G., JENKS, J.F., STEPHEN, D.A., BUCHER, H., HOFMANN, R., GOUDEMAND, N. & ESCARGUEL, G. (2011): Transient metazoan reefs in the aftermath of the end-Permian mass extinction. – Nat. Geosci. **4**: 693–697.

BRAYARD, A., BYLUND, K.G., JENKS, J.F., STEPHEN, D.A., OLIVIER, N., ESCARGUEL, G., FARA, E. & VENNIN, E. (2013): Smithian ammonoid faunas from Utah: implications for Early

Triassic biostratigraphy, correlation and basinal paleogeography. – Swiss J. Palaeontol. **132** (2): 141–219.

BROSSE, M., BUCHER, H. & GOUDEMAND N. (2016): Quantitative biochronology of the Permian-Triassic boundary in South China based on conodont unitary associations. – Earth-Sci. Rev. (accepted).

BRÜHWILER, T. & BUCHER, H. (2012a): Systematic Palaeontology. – In: BRÜHWILER, T., BUCHER, H., GOUDEMAND, N. & GALFETTI, T. (2012a): Smithian (Early Triassic) ammonoids faunas from Exotic Blocks from Oman: taxonomy and biochronology. – Palaeontographica Abt. A **296**: 13–107.

BRÜHWILER, T. & BUCHER, H. (2012b): Systematic Palaeontology. – In: BRÜHWILER, T., BUCHER, H., WARE, D., HERMANN, E., HOCHULI, P.A., ROOHI, G., REHMAN K. & YASEEN A. (2012b): Smithian (Early Triassic) ammonoids from the Salt Range. – Spec. Pap. Palaeontol. **88**: 22–111.

BRÜHWILER, T., BUCHER, H., BRAYARD, A. & GOUDEMAND, N. (2010a): High-resolution biochronology and diversity dynamics of the Early Triassic ammonoid recovery: the Smithian faunas of the Northern Indian Margin. – Palaeogeogr., Palaeoclimatol., Palaeoecol. **297**: 491–501.

BRÜHWILER, T., BUCHER, H. & GOUDEMAND, N. (2010b): Smithian (Early Triassic) ammonoids from Tulong, South Tibet. – Geobios **43**: 403–431.

BRÜHWILER, T., BUCHER, H., ROOHI, G., YASEEN, A. & REHMAN, K. (2011): A new early Smithian ammonoid fauna from the Salt Range (Pakistan). – Swiss J. Palaeontol. **130** (2): 187–201.

BRÜHWILER, T., BUCHER, H., GOUDMAND, N. & GALFETTI, T. (2012a): Smithian (Early Triassic) ammonoids faunas from Exotic Blocks from Oman: taxonomy and biochronology. – Palaeontographica Abt. A **296**: 3–107.

BRÜHWILER, T., BUCHER, H., WARE, D., HERMANN, E., HOCHULI, P.A., ROOHI, G., REHMAN, K. & YASEEN, A. (2012b): Smithian (Early Triassic) ammonoids from the Salt Range. – Spec. Pap. Palaeontol. **88**: 1–114.

BRÜHWILER, T., BUCHER, H. & KRYSTYN, L. (2012c): Middle and late Smithian (Early Triassic) ammonoids from Spiti, India. – Spec. Pap. Palaeontol. **88**: 115–174.

BURGESS, S.D., BOWRING, S. & SHEN, S-Z. (2014): High-precision timeline for Earth's most severe extinction. – Proc. Nat. Acad. Sci. **111** (9): 3316–3321.

CHAO, K. (1950): Some new ammonite genera of Lower Triassic from western Kwangsi. – Palaeontol. Nov. **5**: 1–11.

CHAO, K. (1959): Lower Triassic ammonoids from Western Kwangsi, China. – Palaeontol. Sinica B **9**: 355 pp.

COLLIGNON, M. (1933–1934): Paléontologie de Madagascar XX – Les céphalopodes du Trias inférieur. – Ann. Paléontol. **12-13**: 151–162 & 1–43.

COLLIGNON, M. (1973): Ammonites du Trias inférieur et moyen d'Afghanistan. – Ann. Paléontol. (Invertébrés) **59**: 127–163.

DAGYS, A.S. & ERMAKOVA, S.P. (1990): Early Olenekian ammonoids of Siberia. – Nauka, Moscow: 112 pp.

DEAN, J.S. (1981): Carbonate petrology and depositional environments of the Sinbad Limestone Member of the Moenkopi Formation in the Teasdale Dome Area, Wayne and Garfield Counties, Utah. – Brigham Young Univ. Geol. Stud. **28**: 19–51.

DIENER, C. (1895): Triadische Cephalopodenfaunen der ostsibirischen Küstenprovinz. – Mém. Comité Géol. St. Petersburg **14**: 1–59.

DIENER, C. (1915): Fossilium Catalogus I, Animalia. Part 8, Cephalopoda Triadica. – W. Junk, Berlin.

EHIRO, M., HASEGAWA, H. & MISAKI, A. (2005): Permian ammonoids *Prostacheoceras* and *Perrinites* from the Southern Kitakami Massif, Northeast Japan. – J. Paleontol. **79**: 1222–1228.

FREBOLD, H. (1930): Die Altersstellung des Fischhorizontes, des Grippianniveaus und des unteren Saurierhorizontes in Spitzbergen. – Skrifter om Svalbard og Ishavet **28**: 1–36.

FRECH, F. (1902): Die Dyas: Lethaea Geognostica, Theil I. – Lethaea Palaeozoica **2**: 579–788.

GALFETTI, T., BUCHER, H., OVTCHAROVA, M., SCHALTEGGER, U., BRAYARD, A., BRÜHWILER, T., GOUDMAND, N., WEISSERT, H., HOCHULI, P.A., CORDEY, F. & GUODUN, K. (2007): Timing of the Early Triassic carbon cycle perturbations inferred from new U–Pb ages and ammonoid biochronozones. *Earth and Planet. Sci. Lett.* **258** (3): 593–604.

GARDNER, G.E., & MAPES, R.H. (2000): The relationships of color patterns and habitat for Lower Triassic ammonoids from Crittenden Springs, Elko County, Nevada. – *Rev. Paléobiol.* **8**: 109–122.

GUEX, J. (1978): Le Trias inférieur des Salt Ranges (Pakistan): problèmes biochronologiques. – *Eclogae Geologicae Helvetiae* **71**: 105–141.

GUEX, J. (1991): Biochronological Correlations. – Springer: 252 pp.

GUEX, J., HUNGERBÜHLER, A., JENKS, J., O'DOGHERTY, L., ATUDOREI, V., TAYLOR, D.G., BUCHER, H. & BARTOLINI, A. (2010): Spathian (Lower Triassic) ammonoids from western USA (Idaho, California, Utah and Nevada). – *Mém. Géol. Lausanne* **49**: 1–81.

GUEX, J., GALSTER, F. & HAMMER, Ø. (2015): Discrete Biochronological Time Scales. – Springer: 160 pp.

HADA, S. (1966): Discovery of Early Triassic ammonoids from Gua Musang, Kelantan, Malaya. – *J. Geosci. Osaka Univ.* **9**: 111–121.

HERMANN, E., HOCHULI, P.A., BUCHER, H., BRÜHWILER, T., HAUTMANN, M., WARE, D. & ROOHI, G. (2011): Terrestrial ecosystems on North Gondwana in the aftermath of the end-Permian mass extinction. – *Gondwana Res.* **20** (2): 630–637.

HYATT, A. (1879): In: WHITE, C.A. (1879): Paleontological papers no. 9: fossils from the Jura-Trias of south-eastern Idaho. – *U.S. Geol. and Geogr. Surv. Territ. Bull.* **5**: 105–117.

HYATT, A. (1884): Genera of fossil cephalopods. – *Proc. Boston Soc. Nat. Hist.* **22**: 253–338.

HYATT, A. (1900): Cephalopoda. – In: ZITTEL, K.A.v. (ed.): *Textbook of paleontology* **1**, 1st English ed., Eastman, London.

HYATT, A. & SMITH, J.P. (1905): The Triassic cephalopod genera of America. – *U.S. Geol. Surv., prof. pap* **40**: 1–394.

JATTIOT, R., BUCHER, H., BRAYARD, A., MONNET, C., JENKS, J.F. & HAUTMANN, M. (2015): Revision of the genus *Anasibirites* Mojsisovics (Ammonoidea): an iconic and cosmopolitan taxon of the late Smithian (Early Triassic) extinction. – *Pap. Palaeontol.* **2** (1): 155–188.

JEANNET, A. (1959): Ammonites Permiennes et faunes Triassiques de l'Himalaya Central (Expédition Suisse A. Heim et A. Gansser, 1936). – *Palaeontol. Indica* **34**: 1–190.

JENKS, J. (2007): Smithian (Early Triassic) ammonoid biostratigraphy at Crittenden Springs, Elko County, Nevada and a new ammonoid from the *Meekoceras gracilitatis* Zone. – *New Mexico Mus. Nat. Hist. and Sci. Bull.* **40**: 81–90.

JENKS, J.F., BRAYARD, A., BRÜHWILER, T. & BUCHER, H. (2010): New Smithian (Early Triassic) ammonoids from Crittenden Springs, Elko County, Nevada: Implications for taxonomy, biostratigraphy and biogeography. – New Mexico Mus. Nat. Hist. and Sci. Bull. **48**: 1–41.

JENKS, J.F., GUEX, J., HUNGERBÜHLER, A., TAYLOR, D.G. & BUCHER, H. (2013): Ammonoid biostratigraphy of the Early Spathian *Columbites parisianus* Zone (Early Triassic) at Bear Lake Hot Springs, Idaho. – New Mexico Mus. Nat. Hist. and Sci. Bull. **61**: 268–283.

KEYSERLING, A. (1845): Beschreibung einiger von Dr. A. Th. v. Middendorff mitgebrachten Ceratiten des arctischen Sibiriens. – Bull. Acad. Imp. Sci. St. Pétersbourg **5**: 161–174.

KHUC, V. (1984): Triassic ammonoids in Vietnam. – Geoinf. and Geodata Inst. Hanoi: 134 pp.

KIPARISOVA, L.D. (1947): Triassic sediments of the USSR. Atlas of the guide forms of the fossil faunas of the USSR. – All Union Sci. Geol. Res. Inst. (VSEGEI) **7**: 5–51; Leningrad.

KIPARISOVA, L.D. (1961): Palaeontological fundamentals for the stratigraphy of Triassic deposits of the Primor'ye region, I, Cephalopod Mollusca. – Transact. All Union Sci. Res. Geol. Inst. (VSEGEI) **48**.

KLUG, C., BRÜHWILER, T., KORN, D., SCHWEIGERT, G., BRAYARD, A. & TILSTEY, J. (2007): Ammonoid shell structures of primary organic composition. – Palaeontology **50**: 1463–1478.

KORCHINSKAYA, M.V. (1982): Explanatory note on the biostratigraphic scheme of the Mesozoic (Trias) of Spitsbergen. – USSR Minist. Geol., PGO Sevmorgeologiya: 40–99.

KRAFFT, A.v. & DIENER, C. (1909): Lower Triassic Cephalopoda from Spiti, Malla Johar, and Byans. – Palaeontol. Indica, **15** (6): 1–186.

KUENZI, W.D. (1965): Early Triassic (Scythian) ammonoids from northeastern Washington. – J. Paleontol. **39**: 365–378.

KUMMEL, B. (1952): A classification of the Triassic ammonoids. – J. Paleontol. **26**: 847–853.

KUMMEL, B. (1957): Systematic descriptions, L138-L139, L142-L143. - In: ARKELL, W.J., FURNISH, W.M., KUMMEL, B., MILLER, A.K., MOORE, R.C., SCHINDEWOLF, O., SYLVESTER-BRADLEY, P.C. & WRIGHT, C.W. (ed.): Cephalopoda Ammonoidea. Treatise on Invertebrate Paleontology (MOORE, R.C. ed.): Part L, Mollusca **4**: 490 pp., Geol. Soc. Amer., Boulder, Colorado, and Univ. Kansas Press, Lawrence, Kansas.

KUMMEL, B. (1959): Lower Triassic ammonoids from Western Southland, New Zealand. – New Zealand J. Geol. and Geophys. **2**: 429–447.

KUMMEL, B. & SAKAGAMI, S. (1960): Mid-Scythian ammonites from Iwai Formation, Japan. – Breviora **126**: 1–11.

KUMMEL, B. & STEELE, G. (1962): Ammonites from the *Meekoceras gracilitatus* Zone at Crittenden Spring, Elko County, Nevada. – J. Paleontol. **36**: 638–703.

KUMMEL, B. & ERBEN, H.K. (1968): Lower and Middle Triassic cephalopods from Afghanistan. – *Palaeontographica Abt. A* **129**: 95–148.

LUCAS, S.G., KRAINER, K., & MILNER, A.R. (2007a): The type section and age of the Timpowep Member and stratigraphic nomenclature of the Triassic Moenkopi Group in Southwestern Utah. – *New Mexico Mus. Nat. Hist. and Sci. Bull.* **40**: 109–117.

LUCAS, S.G., GOODSPED, T.H., & ESTEP, J.W. (2007b): Ammonoid biostratigraphy of the Lower Triassic Sinbad Formation, East-Central Utah. – *New Mexico Mus. Nat. Hist. and Sci. Bull.* **40**: 103–108.

MATHEWS, A.A.L. (1929): The Lower Triassic cephalopod fauna of the Fort Douglas area, Utah. – *Walker Mus. Mem.* **1**: 1–46.

MOJSISOVICS, E.v. (1896): Beiträge zur Kenntnis der obertriadischen Cephalopoden-Faunen des Himalaya. – *Denkschr. Akad. Wissensch. Wien* **63**: 573–701.

MONNET, C. & BUCHER, H. (2002): Cenomanian (early Late Cretaceous) ammonoid faunas of Western Europe. Part I: biochronology (unitary associations) and diachronism of datums. – *Eclogae Geologicae Helvetiae* **95** (1): 57–74.

MONNET, C., KLUG, C., GOUDEMAND, N., DE BAETS, K. & BUCHER, H. (2011): Quantitative biochronology of Devonian ammonoids from Morocco and proposals for a refined unitary association method. – *Lethaia* **44** (4): 469–489.

MONNET, C., BUCHER, H., BRAYARD, A. & JENKS, J.F. (2013): *Globacrochordiceras* gen. nov.(Acrochordiceratidae, late Early Triassic) and its significance for stress-induced evolutionary jumps in ammonoid lineages (cephalopods). – Fossil Record **16** (2): 197–215.

MONNET, C., BRAYARD, A. & BUCHER, H. (2015): Ammonoids and quantitative biochronology—a unitary association perspective. – In: KLUG, C., KORN, D., DE BAETS, K., KRUTA, I. and MAPES, R.H. (ed.). Ammonoid Paleobiology: From macroevolution to paleogeography. – Topics in Geobiology **44**: 277–298.

NAKAZAWA, K. & BANDO, Y. (1968): Lower and Middle Triassic Ammonites from Portuguese Timor (Palaeontological Study of Portuguese Timor, 4). – Mem. Fac. Sci. Kyoto Univ., Ser. Geol. and Mineral. **34**: 83–114.

NICHOLS, K.M. & SILBERLING, N.J. (1979): Early Triassic (Smithian) ammonites of Paleoequatorial affinity from the Chulitna terrane, south central Alaska. – U.S. Geol. Surv., prof. pap. **1121**: 1–5.

NOETLING, F. (1905): Die asiatische Trias. – In: FRECH, F. (ed.): Lethaea geognostica: Handbuch der Erdgeschichte mit Abbildungen der für die Formationen bezeichnendsten Versteinerungen: 107–221; Schweizerbart, Stuttgart.

OKUNEVA, T.M. (1990): Triassic biostratigraphy of southern regions of the East USSR without the Primorye territory. – In: ZAKHAROV Y.D., BELYAEVA G.V. & NIKITINA A.P. (ed.): New data on Palaeozoic and Mesozoic biostratigraphy of the south Far East. – Vladivostok: Far Eastern Branch of the USSR Academy of Sciences 125–136.

ORCHARD, M.J. (2007): Conodont diversity and evolution through the latest Permian and Early Triassic upheavals. – *Palaeogeogr., Palaeoclimatol., Palaeoecol.* **252** (1): 93–117.

OVTCHAROVA, M., BUCHER, H., SCHALTEGGER, U., GALFETTI, T., BRAYARD, A. & GUEX, J. (2006): New Early to Middle Triassic U–Pb ages from South China: Calibration with ammonoid biochronozones and implications for the timing of the Triassic biotic recovery. – *Earth and Planet. Sci. Lett.* **243** (3): 463–475.

OVTCHAROVA, M., GOUDEMAND, N., HAMMER, Ø., GUODUN, K., CORDEY, F., GALFETTI, T., SCHALTEGGER, U. & BUCHER, H. (2015): Developing a strategy for accurate definition of a geological boundary through radio-isotopic and biochronological dating: the Early-Middle Triassic boundary (South China). – *Earth-Sci. Rev.* **146**: 65–76.

PIAZZA, V. (2015): Late Smithian (Early Triassic) ammonoids from the uppermost Lusitaniadalen Member (Vikinghøgda Formation), Svalbard. – Msc Thesis, University of Oslo: 135 pp.

POPOV, Y. (1961): Triassic ammonoids of northeastern USSR. – *Transact. Sci. Res. Inst. Geol. Arctic (NIIGA)* **79**: 1–179.

POPOV, Y. (1962): Some Early Triassic ammonoids of northern Caucasia. – *Transact. Acad. Sci. USSR* **127**: 176–184.

RAUP, D.M. & SEPkoski, J.J. (1982): Mass Extinctions in the Marine Fossil Record. – *Science* **215**: 1501–1503.

RENZ, C. & RENZ, O. (1948): Eine untertriadische Ammonitenfauna von der griechischen Insel Chios. – Schweiz. Paläontol. Abh. **66**: 1–98.

RICOU, L.E. (1994): Tethys reconstructed—plates, continental fragments and their boundaries since 260 Ma from Central-America to South-Eastern Asia. – Geodinamica Acta **7**: 169–218.

RUZHENCEV, V.E. (1959): Classification of the superfamily Otocerataceae. – Paleontol. Zh. **2**: 56–67.

SAKAGAMI, S. (1955): Lower Triassic ammonites from Iwai, Orguno-Mura, Nishitamagun, Kwanto massif, Japan. – Sci. Rep. Tokyo Kyoiku Diagaku C **30**: 131–140.

SAVARY, J. & GUEX, J. (1991): BioGraph: un nouveau programme de construction des corrélations biochronologiques basées sur les associations unitaires. – Bull. Soc. Vaudoise Sci. Nat. **80** (3): 317–340.

SAVARY, J. & GUEX, J. (1999): Discrete biochronological scales and unitary associations: description of the BioGraph computer program (No. 34). – Mém. Géol. Lausanne 1015–3578.

SHEVYREV, A.A. (1968). Triassic ammonoidea from the southern part of the USSR. – Transact. Palaeontol. Inst., Nauka, Moscow **119**: 272 pp.

SHEVYREV, A.A. (1990): Ammonoids and chronostratigraphy of the Triassic. – Trudy Paleontol. Inst., Akad. Nauk SSR **241**: 1–179.

SHEVYREV, A.A. (1995): Triassic ammonites of northwestern Caucasus. – Trudy Paleontol. Inst. Akad. Nauk SSR **264**: 1–174.

SHIGETA, Y. & ZAKHAROV, Y. (2009): Systematic paleontology: cephalopods. – In: SHIGETA, Y., ZAKHAROV, Y., MAEDA, H. & POPOV, A.M. (ed.): The Lower Triassic system in the Abrek Bay area, South Primorye, Russia. – Nat. Mus. Nat. and Sci. Monogr. **38**: 44–140; Tokyo.

SHIGETA, Y. & NGUYEN, H.D. (2014): Systematic paleontology: cephalopods. – In: SHIGETA, Y., KOMATSU, T., MAEKAWA, T. & DANG, H.T. (ed.): Olenekian (Early Triassic) stratigraphy and fossil assemblages in northeastern Vietnam. – Nat. Mus. Nat. and Sci. Monogr. **45**: 65–167; Tokyo.

SHIGETA, Y., & KUMAGAE, T. (2015). *Churkites*, a Trans-Panthalassic Early Triassic Ammonoid Genus from South Primorye, Russian Far East. – Paleontol. Res. **19** (3): 219–236.

SHIGETA, Y., MAEDA, H. & ZAKHAROV, Y. (2009): Biostratigraphy: ammonoid succession. – In: SHIGETA, Y., ZAKHAROV, Y., MAEDA, H. & POPOV, A.M. (ed.): The Lower Triassic system in the Abrek Bay area, South Primorye, Russia. – Nat. Mus. Nat. and Sci. Monogr. **38**: 24–27; Tokyo.

SILBERLING, N.J. & TOZER, E.T. (1968): Biostratigraphic classification of the marine Triassic in North America. – Geol. Soc. Amer. Spec. Pap. **110**: 1–63.

SMITH, J.P. (1904): The comparative stratigraphy of the marine Trias of Western America. – Proc. Calif. Acad. Sci. ser. **3**: 323–430.

SMITH, J.P. (1927): Upper Triassic marine invertebrate faunas of North America. – U.S. Geol. Surv., prof. pap. **141**: 262 pp.

SMITH, J.P. (1932): Lower Triassic ammonoids of North America. – U.S. Geol. Surv., prof. pap. **167**: 1–199.

SPATH, L.F. (1929): Corrections of cephalopod nomenclature. – The Naturalist: 269–271.

SPATH, L.F. (1930): The Eotriassic invertebrate fauna of East Greenland. – Meddelelser om Grøland **83**: 1–90.

SPATH, L.F. (1934): Part 4: The Ammonoidea of the Trias, Catalogue of the Fossil Cephalopoda in the British Museum (Natural History). – Trustees Brit. Mus. London: 521 pp.

STEPHEN, D.A., BYLUND, K.G., BYBEE, P.J. & REAM, W.J. (2010): Ammonoid beds in the Lower Triassic Thaynes Formation of western Utah, USA. – In: TANABE, K., SHIGETA, Y., SASAKI, T. & HIRANO, H. (ed.). – Cephalopods—present and past 243–252; Tokyo.

TONG, J.N., ZAKHAROV, Y.D. & WU, S.B. (2004): Early Triassic ammonoid succession in Chaohu, Anhui Province. – Acta Palaeontol. Sinica **43**: 192–204.

TOZER, E.T. (1961): Triassic stratigraphy and faunas, Queen Elizabeth Islands, arctic archipelago. – Geol. Surv. Canada Mem. **316**: 1–116.

TOZER, E.T. (1982): Marine Triassic Faunas of North-America: Their Significance for Assessing Plate and Terrane Movements. – Geol. Runds. **71**: 1077–1104.

TOZER, E.T. (1994): Canadian Triassic ammonoid faunas. – Geol. Surv. Canada Bull.: 663 pp.

WAAGEN, W. (1895): Salt-Range fossils. Vol 2: Fossils from the Ceratite Formation. – Palaeontol. Indica **13**: 1–323.

WANNER, J. (1913): Geologie von Westtimor. – Geol. Runds. **4** (2): 136–150.

WARE, D., BUCHER, H., BRAYARD, A., SCHNEEBELI-HERMANN, E. & BRÜHWILER, T. (2015): High-resolution biochronology and diversity dynamics of the Early Triassic ammonoid recovery: The Dienerian faunas of the Northern Indian Margin. – Palaeogeogr., Palaeoclimatol., Palaeoecol. **440**: 363–373.

WEITSCHAT, W. & LEHMANN, U. (1978): Biostratigraphy of the uppermost part of the Smithian stage (Lower Triassic) at the Botneheia, W-Spitsbergen. – Mitt. Geol.-Palaeontol. Inst. Univ. Hamburg **48**: 85–100.

WELTER, O.A. (1922): Die ammoniten der Unteren Trias von Timor. – Paläontol. Timor **11**: 83–160.

WESTERMANN, G.E.G. (1966): Covariation and taxonomy of the Jurassic ammonite *Sonninia adicra* (Waagen). – N. Jb. Geol. Paläontol., Abh. **124**: 289–312.

WHITE, C.A. (1879): Paleontological papers no. 9: fossils from the Jura-Trias of south-eastern Idaho. – U.S. Geol. and Geograph. Surv. Territ. Bull. **5**: 105–117.

WHITE, C.A. (1880): Contributions to invertebrate paleontology, no. 5: Triassic fossils of south-eastern Idaho. – U.S. Geol. Surv. Territ., 12th Ann. Rep. **1**: 105–118.

YEHARA, S. (1927): The Lower Triassic cephalopod and bivalve fauna of Shikoku. – Jpn. J. Geol. and Geogr. **5** (4): 135–172.

ZAKHAROV, Y.D. (1968): Lower Triassic biostratigraphy and ammonoids of South Primorye (in Russian, original title translated). – Nauka Moskva: 175 pp.

ZAKHAROV, Y.D. (1978): Lower Triassic Ammonoids of East USSR. – Nauka, Moskva (in Russian): 224 pp.

ZAKHAROV, Y.D. & ABNAVI, N.M. (2013): The ammonoid recovery after the end-Permian mass extinction: evidence from the Iran-Transcaucasia area, Siberia, Primorye, and Kazakhstan. – Acta Palaeont. Pol. **58**: 127–147.

ZAKHAROV, Y.D. & POPOV, A.M. (2014): Recovery of Brachiopod and Ammonoid Faunas Following the End-Permian Crisis: Additional Evidence from the Lower Triassic of the Russian Far East and Kazakhstan. – J. Earth Sci. **25** (1): 1–44.

ZAKHAROV, Y.D., SHIGETA, Y., POPOV, A.M., BURYI, G.I., OLEINIKOV, A.V., DORUKHOVSKAYA, E.A. & MIKHALIK, T.M. (2002). Triassic ammonoid succession in South

Primorye: 1. Lower Olenekian *Hedenstroemia bosphorensis* and *Anasibirites nevolini* Zones.

– Albertiana. **27:** 42–64.

ZAKHAROV, Y.D., BONDARENKO, L.G., SMYSHLYAEVA, O.P. & POPOV, A.M. (2013): Late Smithian (Early Triassic) ammonoids from the *Anasibirites nevolini* Zone of South Primorye, Russian Far East. – New Mexico Mus. Nat. Hist. and Sci. Bull. **61:** 597–612.

ZITTEL, K.A.v. (1884): Handbuch der Palaeontologie. Cephalopoda. – 239–522; Munich.

List of the described ammonoids

Xenoceltites subevolutus SPATH, 1930

Palominoceras n. gen. *nevadanum* (SMITH, 1932)

?*Kashmirites cordilleranus* (SMITH, 1932)

Preflorianites toulai (SMITH, 1932)

Juvenites thermarum (SMITH, 1927)

Juvenites spathi (FREBOLD, 1930)

Guodunites monneti BRAYARD & BUCHER, 2008

Guodunites hooveri (HYATT & SMITH, 1905)

Dieneroceras dieneri (HYATT & SMITH, 1905)

Dieneroceras knechti (HYATT & SMITH, 1905)

Anaflemingites cf. *silberlingi* KUMMEL & STEELE, 1962

Churkites noblei JENKS, 2007

Arctoceras tuberculatum (SMITH, 1932)

Inyoites oweni HYATT & SMITH, 1905

Inyoites sp. indet.

Subvishnuites welteri SPATH, 1930

Lanceolites compactus HYATT & SMITH, 1905
Parussuria compressa (HYATT & SMITH, 1905)
Wasatchites perrini MATHEWS, 1929
Anasibirites kingianus (WAAGEN, 1895)
Anasibirites multiformis WELTER, 1922
Hemiprionites typus (WAAGEN, 1895)
Hemiprionites walcotti (MATHEWS, 1929)
Arctopriionites resseri (MATHEWS, 1929)
Meekoceras gracilitatis WHITE, 1879
Meekoceras olivieri BRAYARD et al., 2013
Prionitidae indet. 1
Prionitidae indet. 2
Paranannites aspenensis HYATT & SMITH, 1905
Parannanites cf. baudi BRÜHWILER & BUCHER, 2012a
Owenites koeneni HYATT & SMITH, 1905
Owenites carpenteri SMITH, 1932
?*Galfettites* sp. indet.
Hedenstroemia kossmati HYATT & SMITH, 1905
Pseudosageceras multilobatum NOETLING, 1905
Pseudosageceras augustum (BRAYARD & BUCHER, 2008)
?*Pseudosageceras bullatum* n. sp.
Aspenites acutus HYATT & SMITH, 1905
Proharpoceras carinatitabulatum CHAO, 1950
Gen. et sp. indet.

Explanation of the plates

Scale bars are 10 mm unless otherwise indicated.

PLATE 1

Figs. A–C. *?Kashmirites cordilleranus* (SMITH, 1932). PIMUZ 32118. UAZ₄, loc. PLR12, Palomino Ridge, middle Smithian.

Figs. D–F. *?Kashmirites cordilleranus* (SMITH, 1932). PIMUZ 31928. UAZ₄, loc. PLR12, Palomino Ridge, middle Smithian.

Figs. G–H. *?Kashmirites cordilleranus* (SMITH, 1932). PIMUZ 31929, X2. UAZ₄, loc. PLR71, Palomino Ridge, middle Smithian.

Figs. I–J. *?Kashmirites cordilleranus* (SMITH, 1932). PIMUZ 31930. UAZ₄, loc. PLR13, Palomino Ridge, middle Smithian.

Figs. K–L. *?Kashmirites cordilleranus* (SMITH, 1932). PIMUZ 31931. UAZ₄, loc. PLR88, Palomino Ridge, middle Smithian.

Figs. M–N. *?Kashmirites cordilleranus* (SMITH, 1932). PIMUZ 31932. UAZ₄, loc. PLR88, Palomino Ridge, middle Smithian.

Fig. O. *?Kashmirites cordilleranus* (SMITH, 1932). Suture line of PIMUZ 31928 with scale bar representing 5 mm, at H = 8.3 mm. UAZ₄, loc. PLR12, Palomino Ridge, middle Smithian.

Fig. P. *Xenoceltites subevolutus* SPATH, 1930. PIMUZ 31933. UAZ₅, loc. PLR32, Palomino Ridge, late Smithian.

Figs. Q–S. *Xenoceltites subevolutus* SPATH, 1930. PIMUZ 31934. UAZ₅, loc. PLR32, Palomino Ridge, late Smithian.

Figs. T–V. *Xenoceltites subevolutus* SPATH, 1930, evolute morphotype. PIMUZ 31935. UAZ₅, loc. PLR24, Palomino Ridge, late Smithian.

Figs. W–Y. *Xenoceltites subevolutus* SPATH, 1930. PIMUZ 32115. UAZ₅, loc. PLR35, Palomino Ridge, late Smithian.

Figs. Z–AB. *Xenoceltites subevolutus* SPATH, 1930. PIMUZ 31936. UAZ₅, loc. PLR32,

Palomino Ridge, late Smithian.

Figs. AC–AD. *Xenoceltites subevolutus* SPATH, 1930. PIMUZ 31937. UAZ₅, loc. PLR57,

Palomino Ridge, late Smithian.

Figs. AE–AG. *Preflorianites toulai* (SMITH, 1932). PIMUZ 31938. UAZ₄, loc. PLR11,

Palomino Ridge, middle Smithian.

Figs. AH–AJ. *Preflorianites toulai* (SMITH, 1932). PIMUZ 31939. UAZ₄, loc. PLR11,

Palomino Ridge, middle Smithian.

Fig. AK. *Preflorianites toulai* (SMITH, 1932). Suture line of PIMUZ 31938 with scale bar representing 5 mm, at H = 12.2 mm. UAZ₄, loc. PLR11, Palomino Ridge, middle Smithian.

PLATE 2

Fig. A. *Palominoceras* n. gen. *nevadanum* (SMITH, 1932). Holotype, Phelan Ranch, Nevada, middle Smithian.

Figs. B–C. *Palominoceras* n. gen. *nevadanum* (SMITH, 1932). Holotype as figured in Smith (1932, pl. 56, figs. 1, 2), Phelan Ranch, Nevada, middle Smithian.

Fig. D. *Palominoceras* n. gen. *nevadanum* (SMITH, 1932). PIMUZ 31940. UAZ₄, loc. PLR71, Palomino Ridge, middle Smithian.

Fig. E. *Palominoceras* n. gen. *nevadanum* (SMITH, 1932). PIMUZ 31941. UAZ₄, loc. PLR12, Palomino Ridge, middle Smithian.

Fig. F. *Palominoceras* n. gen. *nevadanum* (SMITH, 1932). PIMUZ 31942. UAZ₄, loc. PLR71, Palomino Ridge, middle Smithian.

Fig. G. *Palominoceras* n. gen. *nevadanum* (SMITH, 1932). PIMUZ 31943. UAZ₄, loc. PLR71, Palomino Ridge, middle Smithian.

Fig. H. *Palominoceras* n. gen. *nevadanum* (SMITH, 1932). Suture line of PIMUZ 32120 with scale bar representing 5 mm, at H = 9.5 mm. UAZ₄, loc. PLR12, Palomino Ridge, middle Smithian.

Figs. I–K. *Palominoceras* n. gen. *nevadanum* (SMITH, 1932). PIMUZ 31944. UAZ₄, loc. PLR71, Palomino Ridge, middle Smithian.

Fig. L. *Palominoceras* n. gen. *nevadanum* (SMITH, 1932). PIMUZ 31945. UAZ₄, loc. PLR71, Palomino Ridge, middle Smithian.

Fig. M. *Palominoceras* n. gen. *nevadanum* (SMITH, 1932). PIMUZ 31946. UAZ₄, loc. PLR71, Palomino Ridge, middle Smithian.

Fig. N. *Palominoceras* n. gen. *nevadanum* (SMITH, 1932). PIMUZ 31947. UAZ₄, loc. PLR72, Palomino Ridge, middle Smithian.

Fig. O. *Palominoceras* n. gen. *nevadanum* (SMITH, 1932). PIMUZ 31948. UAZ₄, loc. PLR72, Palomino Ridge, middle Smithian.

Fig. P. *Palominoceras* n. gen. *nevadanum* (SMITH, 1932). PIMUZ 31949. UAZ₄, loc. PLR12, Palomino Ridge, middle Smithian.

Fig. Q. *Palominoceras* n. gen. *nevadanum* (SMITH, 1932). PIMUZ 31950. UAZ₄, loc. PLR71, Palomino Ridge, middle Smithian.

Fig. R. *Palominoceras* n. gen. *nevadanum* (SMITH, 1932). PIMUZ 31951. UAZ₄, loc. PLR71, Palomino Ridge, middle Smithian.

Fig. S. *Palominoceras* n. gen. *nevadanum* (SMITH, 1932). PIMUZ 31952. UAZ₄, loc. PLR12, Palomino Ridge, middle Smithian.

Fig. T. *Palominoceras* n. gen. *nevadanum* (SMITH, 1932). Suture line of PIMUZ 32121 with scale bar representing 5 mm, at H = 6.1 mm. UAZ₄, loc. PLR72, Palomino Ridge, middle Smithian.

Fig. U. *Palominoceras* n. gen. *nevadanum* (SMITH, 1932). PIMUZ 31953. UAZ₄, loc. PLR71, Palomino Ridge, middle Smithian.

Fig. V. *Palominoceras* n. gen. *nevadanum* (SMITH, 1932). PIMUZ 31954. UAZ₄, loc. PLR12, Palomino Ridge, middle Smithian.

Figs. W–Y. *Palominoceras* n. gen. *nevadanum* (SMITH, 1932). PIMUZ 31955. UAZ₄, loc. PLR71, Palomino Ridge, middle Smithian.

Fig. Z. *Palominoceras* n. gen. *nevadanum* (SMITH, 1932). PIMUZ 31956. UAZ₄, loc. PLR72, Palomino Ridge, middle Smithian.

Figs. AA–AB. *Palominoceras* n. gen. *nevadanum* (SMITH, 1932). PIMUZ 31957. UAZ₄, loc. PLR73, Palomino Ridge, middle Smithian.

Fig. AC. *Palominoceras* n. gen. *nevadanum* (SMITH, 1932). PIMUZ 31958. UAZ₄, loc. PLR71, Palomino Ridge, middle Smithian.

PLATE 3

Figs. A–C. *Juvenites thermarum* (SMITH, 1927). PIMUZ 31959. UAZ₄, loc. PLR45, Palomino Ridge, middle Smithian.

Figs. D–E. *Juvenites thermarum* (SMITH, 1927). PIMUZ 31960. UAZ₄, loc. PLR45, Palomino Ridge, middle Smithian.

Figs. F–I. *Juvenites thermarum* (SMITH, 1927). PIMUZ 31961. UAZ₄, loc. PLR45, Palomino Ridge, middle Smithian.

Figs. J–L. *Juvenites thermarum* (SMITH, 1927). PIMUZ 31962. UAZ₄, loc. PLR45, Palomino Ridge, middle Smithian.

Figs. M–O. *Juvenites thermarum* (SMITH, 1927). PIMUZ 31963. UAZ₄, loc. PLR61, Palomino Ridge, middle Smithian.

Fig. P. *Juvenites thermarum* (SMITH, 1927). Suture line of PIMUZ 31963 with scale bar representing 5 mm, at H = 5 mm. UAZ₄, loc. PLR61, Palomino Ridge, middle Smithian.

Figs. Q–T. *Juvenites thermarum* (SMITH, 1927). PIMUZ 31964. UAZ₄, loc. PLR45, Palomino Ridge, middle Smithian.

Figs. U–X. *Juvenites thermarum* (SMITH, 1927). PIMUZ 31965. UAZ₄, loc. PLR61, Palomino Ridge, middle Smithian.

Figs. Y–AB. *Juvenites thermarum* (SMITH, 1927). PIMUZ 31966. UAZ₄, loc. PLR45, Palomino Ridge, middle Smithian.

Figs. AC–AE. *Juvenites thermarum* (SMITH, 1927). PIMUZ 31967. UAZ₄, loc. PLR63, Palomino Ridge, middle Smithian.

Figs. AF–AG. *Juvenites spathi* (FREBOLD, 1930). PIMUZ 31968. UAZ₄, loc. PLR9', Palomino Ridge, middle Smithian.

Figs. AH–AJ. *Juvenites spathi* (FREBOLD, 1930). PIMUZ 31969. UAZ₄, loc. PLR27, Palomino Ridge, middle Smithian.

Figs. AK–AL. *Juvenites spathi* (FREBOLD, 1930). PIMUZ 31970. UAZ₄, loc. PLR45, Palomino Ridge, middle Smithian.

Fig. AM. *Juvenites spathi* (FREBOLD, 1930). Suture line of PIMUZ 31973 with scale bar representing 5 mm, at H = 5.3 mm. UAZ₄, loc. PLR63, Palomino Ridge, middle Smithian.

Fig. AN. *Juvenites spathi* (FREBOLD, 1930). PIMUZ 31971. UAZ₄, loc. PLR61, Palomino Ridge, middle Smithian.

Figs. AO–AQ. *Juvenites spathi* (FREBOLD, 1930). PIMUZ 31972. UAZ₄, loc. PLR45, Palomino Ridge, middle Smithian.

Figs. AR–AT. *Juvenites spathi* (FREBOLD, 1930). PIMUZ 31973. UAZ₄, loc. PLR63, Palomino Ridge, middle Smithian.

Figs. AU–AW. *Juvenites spathi* (FREBOLD, 1930). PIMUZ 31974. UAZ₄, loc. PLR62, Palomino Ridge, middle Smithian.

PLATE 4

Figs. A–B. *Guodunites monneti* BRAYARD & BUCHER, 2008. PIMUZ 31975, X0.75. UAZ₄, loc. PLR72, Palomino Ridge, middle Smithian.

Figs. C–D. *Guodunites monneti* BRAYARD & BUCHER, 2008. PIMUZ 31976, X0.5. UAZ₄, loc. PLR73, Palomino Ridge, middle Smithian.

Figs. E–G. *Guodunites monneti* BRAYARD & BUCHER, 2008. PIMUZ 31977. UAZ₄, loc.

PLR72, Palomino Ridge, middle Smithian.

Fig. H. *Guodunites monneti* BRAYARD & BUCHER, 2008. Suture line of PIMUZ 31977 with scale bar representing 5 mm, at H = 18 mm. UAZ₄, loc. PLR72, Palomino Ridge, middle Smithian.

Fig. I. *Guodunites monneti* BRAYARD & BUCHER, 2008. PIMUZ 31978. UAZ₄, loc. PLR73, Palomino Ridge, middle Smithian.

Figs. J–K. *Guodunites monneti* BRAYARD & BUCHER, 2008. PIMUZ 31979. UAZ₄, loc. PLR71, Palomino Ridge, middle Smithian.

Figs. L–N. *Guodunites hooveri* (HYATT & SMITH, 1905). PIMUZ 31980. UAZ₄, loc. PLR73, Palomino Ridge, middle Smithian.

Figs. O–P. *Guodunites hooveri* (HYATT & SMITH, 1905). PIMUZ 31981. UAZ₄, loc. PLR61, Palomino Ridge, middle Smithian.

Figs. Q–S. *Guodunites hooveri* (HYATT & SMITH, 1905). PIMUZ 31982. UAZ₄, loc. PLR27, Palomino Ridge, middle Smithian.

Figs. T–V. *Guodunites hooveri* (HYATT & SMITH, 1905). PIMUZ 31983, X0.75. UAZ₄, loc. PLR72, Palomino Ridge, middle Smithian.

PLATE 5

Figs. A–C. *Dieneroceras dieneri* (HYATT & SMITH, 1905). PIMUZ 31984, X2. UAZ₄, loc. PLR27, Palomino Ridge, middle Smithian.

Fig. D. *Dieneroceras dieneri* (HYATT & SMITH, 1905). PIMUZ 31985. UAZ₄, loc. PLR45, Palomino Ridge, middle Smithian.

Figs. E–G. *Dieneroceras dieneri* (HYATT & SMITH, 1905). PIMUZ 31986. UAZ₄, loc. PLR61, Palomino Ridge, middle Smithian.

Figs. H–J. *Dieneroceras dieneri* (HYATT & SMITH, 1905). PIMUZ 31987. UAZ₄, loc. PLR71, Palomino Ridge, middle Smithian.

Figs. K–L. *Dieneroceras dieneri* (HYATT & SMITH, 1905). PIMUZ 31988. UAZ₄, loc. PLR45, Palomino Ridge, middle Smithian.

Figs. M–O. *Dieneroceras dieneri* (HYATT & SMITH, 1905). PIMUZ 31989. UAZ₄, loc. PLR45, Palomino Ridge, middle Smithian.

Fig. P. *Dieneroceras dieneri* (HYATT & SMITH, 1905). Suture line of PIMUZ 31986 with scale bar representing 5 mm, at H = 4.2 mm. UAZ₄, loc. PLR61, Palomino Ridge, middle Smithian.

Figs. Q–S. *Dieneroceras dieneri* (HYATT & SMITH, 1905). PIMUZ 31990. UAZ₄, loc. PLR12, Palomino Ridge, middle Smithian.

Figs. T–V. *Dieneroceras knechti* (HYATT & SMITH, 1905). PIMUZ 31991. UAZ₄, loc. PLR45, Palomino Ridge, middle Smithian.

Fig. W. *Dieneroceras knechti* (HYATT & SMITH, 1905). Suture line of PIMUZ 31993 with scale bar representing 5 mm, at H = 8.6 mm. UAZ₄, loc. PLRA34, Palomino Ridge, middle Smithian.

Figs. X–Y. *Dieneroceras knechti* (HYATT & SMITH, 1905). PIMUZ 31992. UAZ₄, loc. PLR9, Palomino Ridge, middle Smithian.

Figs. Z–AA. *Dieneroceras knechti* (HYATT & SMITH, 1905). PIMUZ 31993. UAZ₄, loc. PLRA34, Palomino Ridge, middle Smithian.

Figs. AB–AD. *Anaflemingites* cf. *silberlingi* KUMMEL & STEELE 1962. PIMUZ 31994. UAZ₄, loc. PLR9, Palomino Ridge, middle Smithian.

Fig. AE. *Anaflemingites* cf. *silberlingi* KUMMEL & STEELE 1962. Suture line of PIMUZ 31994 with scale bar representing 5 mm, at H = 12 mm. UAZ₄, loc. PLR9, Palomino Ridge, middle Smithian.

Figs. AF–AH. *Anaflemingites* cf. *silberlingi* KUMMEL & STEELE 1962. PIMUZ 31995. UAZ₄, loc. PLR14, Palomino Ridge, middle Smithian.

Fig. AI. *Anaflemingites* cf. *silberlingi* KUMMEL & STEELE 1962. PIMUZ 31996. UAZ₄, loc. PLR87, Palomino Ridge, middle Smithian.

PLATE 6

Figs. A–C. *Churkites noblei* JENKS, 2007. PIMUZ 31997. UAZ₄, loc. PLR72, Palomino Ridge, middle Smithian.

Figs. D–E. *Churkites noblei* JENKS, 2007. PIMUZ 31998. UAZ₄, loc. PLR72, Palomino Ridge, middle Smithian.

Fig. F. *Churkites noblei* JENKS, 2007. Suture line of PIMUZ 32001 with scale bar representing 5 mm, at H = 22.5 mm. UAZ₄, loc. PLR88, Palomino Ridge, middle Smithian.

Figs. G–H. *Churkites noblei* JENKS, 2007. PIMUZ 31999, X0.75. UAZ₄, loc. PLR88, Palomino Ridge, middle Smithian.

Figs. I–K. *Churkites noblei* JENKS, 2007. PIMUZ 32000. UAZ₄, loc. PLR72, Palomino Ridge, middle Smithian.

Figs. L–M. Gen. et sp. indet. PIMUZ 32002. UAZ₄, loc. PLRA10, Palomino Ridge, middle Smithian.

PLATE 7

Figs. A–B. *Arctoceras tuberculatum* (SMITH, 1932). PIMUZ 32003, X0.5. UAZ₄, loc. PLR94, Palomino Ridge, middle Smithian.

Figs. C–E. *Arctoceras tuberculatum* (SMITH, 1932). PIMUZ 32004, X0.5. UAZ₄, loc. PLR9', Palomino Ridge, middle Smithian.

Fig. F. *Arctoceras tuberculatum* (SMITH, 1932). Suture line of PIMUZ 32005 with scale bar representing 5 mm, H unavailable. UAZ₄, loc. PLR11, Palomino Ridge, middle Smithian.

Figs. G–I. *Arctoceras tuberculatum* (SMITH, 1932). PIMUZ 32006. UAZ₄, loc. PLR87, Palomino Ridge, middle Smithian.

PLATE 8

Fig. A. *Inyoites oweni* HYATT & SMITH, 1905. PIMUZ 32007. UAZ₄, loc. PLR45, Palomino Ridge, middle Smithian.

Figs. B–D. *Inyoites oweni* HYATT & SMITH, 1905. PIMUZ 32008. UAZ₄, loc. PLR45, Palomino Ridge, middle Smithian.

Figs. E–F. *Inyoites oweni* HYATT & SMITH, 1905. PIMUZ 32009. UAZ₄, loc. PLR63, Palomino Ridge, middle Smithian.

Fig. G. *Inyoites oweni* HYATT & SMITH, 1905. PIMUZ 32010. UAZ₄, loc. PLR88, Palomino Ridge, middle Smithian.

Figs. H–I. *Inyoites* sp. indet. PIMUZ 32011, X2. UAZ₄, loc. PLRA35, Palomino Ridge, middle Smithian.

Figs. J–K. *Inyoites* sp. indet. PIMUZ 32012, X2. UAZ₄, loc. PLRA35, Palomino Ridge, middle Smithian.

Figs. L–N. *Inyoites* sp. indet. PIMUZ 32013. UAZ₄, loc. PLRA35, Palomino Ridge, middle Smithian.

Figs. O–Q. *Subvishnuites welteri* SPATH, 1930. PIMUZ 32014. UAZ₄, loc. PLR12, Palomino Ridge, middle Smithian.

Figs. R–T. *Subvishnuites welteri* SPATH, 1930. PIMUZ 32015. UAZ₄, loc. PLR12, Palomino Ridge, middle Smithian.

PLATE 9

Figs. A–B. *Lanceolites compactus* HYATT & SMITH, 1905. PIMUZ 32016. UAZ₄, loc. PLR12, Palomino Ridge, middle Smithian.

Figs. C–D. *Lanceolites compactus* HYATT & SMITH, 1905. PIMUZ 32017, X0.75. UAZ₄, loc. PLR88, Palomino Ridge, middle Smithian.

Fig. E. *Lanceolites compactus* HYATT & SMITH, 1905. Suture line of PIMUZ 32018 with scale bar representing 5 mm, at H = 8 mm. UAZ₄, loc. PLR71, Palomino Ridge, middle Smithian.

Figs. F–G. *Lanceolites compactus* HYATT & SMITH, 1905. PIMUZ 32018. UAZ₄, loc. PLR71, Palomino Ridge, middle Smithian.

Figs. H–J. *Lanceolites compactus* HYATT & SMITH, 1905. PIMUZ 32019. UAZ₄, loc. PLR72, Palomino Ridge, middle Smithian.

Figs. K–M. *Lanceolites compactus* HYATT & SMITH, 1905. PIMUZ 32020. UAZ₄, loc. PLR13, Palomino Ridge, middle Smithian.

Figs. N–P. *Parussuria compressa* (HYATT & SMITH, 1905). PIMUZ 32021. UAZ₄, loc. PLR72, Palomino Ridge, middle Smithian.

Figs. Q–R. *Parussuria compressa* (HYATT & SMITH, 1905). PIMUZ 32022. UAZ₄, loc. PLR72, Palomino Ridge, middle Smithian.

Fig. S. *Parussuria compressa* (HYATT & SMITH, 1905). Suture line of PIMUZ 32023 with scale bar representing 5 mm, at H = 10.5 mm. UAZ₄, loc. PLR62, Palomino Ridge, middle Smithian.

PLATE 10

Figs. A–C. *Wasatchites perrini* MATHEWS, 1929. PIMUZ 32024. UAZ₅, loc. PLR24, Palomino Ridge, late Smithian.

Figs. D–F. *Wasatchites perrini* MATHEWS, 1929. PIMUZ 32025. UAZ₅, loc. PLR24,

Palomino Ridge, late Smithian.

Fig. G. *Wasatchites perrini* MATHEWS, 1929. PIMUZ 32026. UAZ₅, loc. PLR24, Palomino

Ridge, late Smithian.

Figs. H–I. *Wasatchites perrini* MATHEWS, 1929. PIMUZ 32027. UAZ₅, loc. PLR58,

Palomino Ridge, late Smithian.

Figs. J–L. *Wasatchites perrini* MATHEWS, 1929. PIMUZ 32028. UAZ₅, loc. PLR34,

Palomino Ridge, late Smithian.

PLATE 11

Figs. A–C. *Anasibirites kingianus* (WAAGEN, 1895). PIMUZ 32029. UAZ₅, loc. PLR34,

Palomino Ridge, late Smithian.

Figs. D–F. *Anasibirites kingianus* (WAAGEN, 1895). PIMUZ 32030. UAZ₅, loc. PLR37,

Palomino Ridge, late Smithian.

Figs. G–I. *Anasibirites multiformis* WELTER, 1922. PIMUZ 32031. UAZ₅, loc. PLR30,

Palomino Ridge, late Smithian.

Figs. J–K. *Anasibirites multiformis* WELTER, 1922. PIMUZ 32032. UAZ₅, loc. PLR34,

Palomino Ridge, late Smithian.

Figs. L–N. *Anasibirites multiformis* WELTER, 1922. PIMUZ 32033. UAZ₅, loc. PLR34,

Palomino Ridge, late Smithian.

Figs. O–P. *Anasibirites multiformis* WELTER, 1922. PIMUZ 32034, X0.75. UAZ₅, loc.

PLR34, Palomino Ridge, late Smithian.

Figs. Q–R. *Anasibirites multiformis* WELTER, 1922. PIMUZ 32035. UAZ₅, loc. PLR34,

Palomino Ridge, late Smithian.

Figs. S–T. *Anasibirites multiformis* WELTER, 1922. PIMUZ 32036. UAZ₅, loc. PLR57,

Palomino Ridge, late Smithian.

Figs. U–W. *Anasibirites multiformis* WELTER, 1922. PIMUZ 32037. UAZ₅, loc. PLR57, Palomino Ridge, late Smithian.

Figs. X–Z. *Anasibirites multiformis* WELTER, 1922. PIMUZ 32038. UAZ₅, loc. PLR57, Palomino Ridge, late Smithian.

Fig. AA. *Anasibirites multiformis* WELTER, 1922. Suture line of PIMUZ 32039 with scale bar representing 5 mm, at H = 16.1 mm. UAZ₅, loc. PLR34, Palomino Ridge, late Smithian.

PLATE 12

Figs. A–B. *Hemiprionites typus* (WAAGEN, 1895) without depression near venter. PIMUZ 32040, X0.75. UAZ₅, loc. PLR24, Palomino Ridge, late Smithian.

Figs. C–D. *Hemiprionites typus* (WAAGEN, 1895) without depression near venter. PIMUZ 32041, X0.75. UAZ₅, loc. PLR34, Palomino Ridge, late Smithian.

Fig. E. *Hemiprionites typus* (WAAGEN, 1895) without depression near venter. PIMUZ 32042. UAZ₅, loc. PLR30, Palomino Ridge, late Smithian.

Figs. F–H. *Hemiprionites typus* (WAAGEN, 1895) without depression near venter. PIMUZ 32043, X0.75. UAZ₅, loc. PLR34, Palomino Ridge, late Smithian.

Figs. I–J. *Hemiprionites typus* (WAAGEN, 1895) without depression near venter. PIMUZ 32044. UAZ₅, loc. PLR37, Palomino Ridge, late Smithian.

Figs. K–M. *Hemiprionites typus* (WAAGEN, 1895) without depression near venter. PIMUZ 32045. UAZ₅, loc. PLR57, Palomino Ridge, late Smithian.

Figs. N–O. *Arctopriionites resseri* (MATHEWS, 1929). PIMUZ 32046. UAZ₅, loc. PLR37, Palomino Ridge, late Smithian.

Figs. P–R. *Arctopriionites resseri* (MATHEWS, 1929). PIMUZ 32047. UAZ₅, loc. PLR30, Palomino Ridge, late Smithian.

Figs. S–U. *Arctopriionites resseri* (MATHEWS, 1929). PIMUZ 32048. UAZ₅, loc. PLR58, Palomino Ridge, late Smithian.

Fig. V. *Arctopriionites resseri* (MATHEWS, 1929). PIMUZ 32049. UAZ₅, loc. PLR37, Palomino Ridge, late Smithian.

Fig. W. *Arctopriionites resseri* (MATHEWS, 1929). Suture line of PIMUZ 32050 with scale bar representing 5 mm, at H = 14.4 mm. UAZ₅, loc. PLR24, Palomino Ridge, late Smithian.

Fig. X. *Arctopriionites resseri* (MATHEWS, 1929). PIMUZ 32051, X0.75. UAZ₅, loc. PLR34, Palomino Ridge, late Smithian.

PLATE 13

Figs. A–C. *Hemiprionites typus* (WAAGEN, 1895) with depression near venter. PIMUZ 32052. UAZ₅, loc. PLR30, Palomino Ridge, late Smithian.

Figs. D–F. *Hemiprionites typus* (WAAGEN, 1895) with depression near venter. PIMUZ 32053. UAZ₅, loc. PLR30, Palomino Ridge, late Smithian.

Figs. G–I. *Hemiprionites typus* (WAAGEN, 1895) with depression near venter. PIMUZ 32054. UAZ₅, loc. PLR30, Palomino Ridge, late Smithian. Arrow indicates a developed keel.

Figs. J–K. *Hemiprionites typus* (WAAGEN, 1895) with depression near venter. PIMUZ 32055. UAZ₅, loc. PLR30, Palomino Ridge, late Smithian.

Figs. L–N. *Hemiprionites typus* (WAAGEN, 1895) with depression near venter. PIMUZ 32056. UAZ₅, loc. PLR30, Palomino Ridge, late Smithian.

Figs. O–Q. *Hemiprionites typus* (WAAGEN, 1895) with depression near venter. PIMUZ 32116, X0.5. UAZ₅, loc. PLR30, Palomino Ridge, late Smithian.

Fig. R. *Hemiprionites typus* (WAAGEN, 1895). Suture line of PIMUZ 32117 with scale bar representing 5 mm, at H = 15.5 mm. UAZ₅, loc. PLR34, Palomino Ridge, late Smithian.

Figs. S–T. *Hemiprionites typus* (WAAGEN, 1895) with depression near venter. PIMUZ 32057, X0.5. UAZ₅, loc. PLR34, Palomino Ridge, late Smithian.

Figs. U–V. *Hemiprionites typus* (WAAGEN, 1895) with depression near venter. PIMUZ 32058. UAZ₅, loc. PLR37, Palomino Ridge, late Smithian. Arrow indicates a developed keel.

Figs. W–X. *Hemiprionites typus* (WAAGEN, 1895) with depression near venter. PIMUZ 32059, X0.75. UAZ₅, loc. PLR37, Palomino Ridge, late Smithian.

PLATE 14

Figs. A–C. *Hemiprionites walcotti* (MATHEWS, 1929). PIMUZ 32060. UAZ₅, loc. PLR24, Palomino Ridge, late Smithian.

Figs. D–F. *Hemiprionites walcotti* (MATHEWS, 1929). PIMUZ 32061. UAZ₅, loc. PLR34, Palomino Ridge, late Smithian.

Figs. G–I. *Hemiprionites walcotti* (MATHEWS, 1929). PIMUZ 32062. UAZ₅, loc. PLR34, Palomino Ridge, late Smithian.

Figs. J–K. *Hemiprionites walcotti* (MATHEWS, 1929). PIMUZ 32063. UAZ₅, loc. PLR55, Palomino Ridge, late Smithian.

Figs. L–M. *Hemiprionites walcotti* (MATHEWS, 1929). PIMUZ 32064. UAZ₅, loc. PLR34, Palomino Ridge, late Smithian.

Fig. N. *Hemiprionites walcotti* (MATHEWS, 1929). PIMUZ 32065, X0.75. UAZ₅, loc. PLR34, Palomino Ridge, late Smithian.

Figs. O–Q. *Hemiprionites walcotti* (MATHEWS, 1929). PIMUZ 32066. UAZ₅, loc. PLR58, Palomino Ridge, late Smithian.

Fig. R. *Hemiprionites walcotti* (MATHEWS, 1929). Suture line of PIMUZ 32067 with scale bar representing 5 mm, at H = 15.6 mm. UAZ₅, loc. PLR58, Palomino Ridge, late Smithian.

Figs. S–T. *Hemiprionites walcotti* (MATHEWS, 1929). PIMUZ 32068, X0.75. UAZ₅, loc. PLR34, Palomino Ridge, late Smithian.

Figs. U–W. *Hemiprionites walcotti* (MATHEWS, 1929). PIMUZ 32069. UAZ₅, loc. PLR57, Palomino Ridge, late Smithian.

Figs. X–Y. *Hemiprionites walcotti* (MATHEWS, 1929). PIMUZ 32070. UAZ₅, loc. PLR58, Palomino Ridge, late Smithian.

PLATE 15

Figs. A–D. *Meekoceras gracilitatis* WHITE, 1879. PIMUZ 32071, X0.5. UAZ₄, loc. PLR87, Palomino Ridge, middle Smithian.

Figs. E–F. *Meekoceras gracilitatis* WHITE, 1879. PIMUZ 32072, X0.5. UAZ₄, loc. PLR11, Palomino Ridge, middle Smithian.

Figs. G–I. *Meekoceras gracilitatis* WHITE, 1879. PIMUZ 32073, X0.5. UAZ₄, loc. PLR87, Palomino Ridge, middle Smithian.

Figs. J–L. *Meekoceras gracilitatis* WHITE, 1879. PIMUZ 32074, X0.5. UAZ₄, loc. PLR87, Palomino Ridge, middle Smithian.

Fig. M. *Meekoceras gracilitatis* WHITE, 1879. Suture line of PIMUZ 32075 with scale bar representing 5 mm, at H = 32.7 mm. UAZ₄, loc. PLR87, Palomino Ridge, middle Smithian.

Figs. N–P. *Meekoceras gracilitatis* WHITE, 1879. PIMUZ 32075, X0.5. UAZ₄, loc. PLR87, Palomino Ridge, middle Smithian.

Figs. Q–S. *Meekoceras gracilitatis* WHITE, 1879. PIMUZ 32076, X0.5. UAZ₄, loc. PLR87, Palomino Ridge, middle Smithian.

Figs. T–U. *Meekoceras gracilitatis* WHITE, 1879. PIMUZ 32077, X0.5. UAZ₄, loc. PLR72, Palomino Ridge, middle Smithian.

PLATE 16

Figs. A–B. *Meekoceras olivieri* BRAYARD et al., 2013. PIMUZ 32078, X0.75. UAZ₁, loc. PLR95, Palomino Ridge, early Smithian.

Figs. C–D. *Meekoceras olivieri* BRAYARD et al., 2013. PIMUZ 32079. UAZ₁, loc. PLR95, Palomino Ridge, early Smithian.

Figs. E–F. Prionitidae indet. 1. PIMUZ 32080. UAZ₅, loc. PLR34, Palomino Ridge, late Smithian.

Figs. G–H. Prionitidae indet. 1. PIMUZ 32081. UAZ₅, loc. PLR34, Palomino Ridge, late Smithian.

Figs. I–J. Prionitidae indet. 2. PIMUZ 32082. UAZ₅, loc. PLR38, Palomino Ridge, late Smithian.

Figs. K–L. Prionitidae indet. 2. PIMUZ 32083. UAZ₅, loc. PLR38, Palomino Ridge, late Smithian.

PLATE 17

Figs. A–C. *Paranannites aspenensis* HYATT & SMITH, 1905. PIMUZ 32084. UAZ₄, loc. PLR110, Palomino Ridge, middle Smithian.

Figs. D–F. *Paranannites* cf. *baudi* BRÜHWILER & BUCHER, 2012a. PIMUZ 32085. UAZ₄, loc. PLR9, Palomino Ridge, middle Smithian.

Fig. G. *Paranannites* cf. *baudi* BRÜHWILER & BUCHER, 2012a. Suture line of PIMUZ 32086 with scale bar representing 5 mm, at H = 8.5 mm. UAZ₄, loc. PLR9, Palomino Ridge, middle Smithian.

Figs. H–J. *Paranannites* cf. *baudi* BRÜHWILER & BUCHER, 2012a. PIMUZ 32086. UAZ₄, loc. PLR9, Palomino Ridge, middle Smithian.

Fig. K. *Owenites koeneni* HYATT & SMITH, 1905. PIMUZ 32087. UAZ₄, loc. PLR12, Palomino Ridge, middle Smithian.

Figs. L–O. *Owenites koeneni* HYATT & SMITH, 1905. PIMUZ 32088. UAZ₄, loc. PLR71, Palomino Ridge, middle Smithian.

Figs. P–R. *Owenites koeneni* HYATT & SMITH, 1905. PIMUZ 32089. UAZ₄, loc. PLR13, Palomino Ridge, middle Smithian.

Figs. S–U. *Owenites koeneni* HYATT & SMITH, 1905. PIMUZ 32090. UAZ₄, loc. PLR12, Palomino Ridge, middle Smithian.

Fig. V. *Owenites koeneni* HYATT & SMITH, 1905. Suture line of PIMUZ 32088 with scale bar representing 5 mm, at H = 9.2 mm. UAZ₄, loc. PLR71, Palomino Ridge, middle Smithian.

Figs. W–Z. *Owenites koeneni* HYATT & SMITH, 1905. PIMUZ 32091. UAZ₄, loc. PLR71, Palomino Ridge, middle Smithian.

Figs. AA–AD. *Owenites koeneni* HYATT & SMITH, 1905. PIMUZ 32092. UAZ₄, loc. PLR71, Palomino Ridge, middle Smithian.

Figs. AE–AF. *Owenites carpenteri* SMITH, 1932. PIMUZ 32093, X2. UAZ₄, loc. PLR61, Palomino Ridge, middle Smithian.

PLATE 18

Fig. A. *Aspenites acutus* HYATT & SMITH, 1905. PIMUZ 32102. UAZ₄, loc. PLR12, Palomino Ridge, middle Smithian.

Fig. B. *Aspenites acutus* HYATT & SMITH, 1905. PIMUZ 32103. UAZ₄, loc. PLR71, Palomino Ridge, middle Smithian.

Fig. C. *Aspenites acutus* HYATT & SMITH, 1905. Suture line of PIMUZ 32104 with scale bar representing 5 mm, at H = 21.6 mm. UAZ₄, loc. PLR87, Palomino Ridge, middle Smithian.

Figs. D–F. *Aspenites acutus* HYATT & SMITH, 1905. PIMUZ 32105. UAZ₄, loc. PLR87, Palomino Ridge, middle Smithian.

Figs. G–H. *Aspenites acutus* HYATT & SMITH, 1905. PIMUZ 32104. UAZ₄, loc. PLR87, Palomino Ridge, middle Smithian.

Figs. I–K. *Hedenstroemia kossmati* HYATT & SMITH, 1905. PIMUZ 32106. UAZ₄, loc. PLR9', Palomino Ridge, middle Smithian.

Fig. L. *Hedenstroemia kossmati* HYATT & SMITH, 1905. Suture line of PIMUZ 32107 with scale bar representing 5 mm, at H = 52.7 mm. UAZ₄, loc. PLR72, Palomino Ridge, middle Smithian.

Figs. M–O. *Proharpoceras carinatitabulatum* CHAO, 1950. PIMUZ 32108, X2. UAZ₄, loc.

PLR63, Palomino Ridge, middle Smithian.

Figs. P–R. ?*Galfettites* sp. indet. PIMUZ 32109. UAZ₄, loc. PLR27, Palomino Ridge, middle Smithian.

Fig. S. ?*Galfettites* sp. indet. PIMUZ 32110. UAZ₄, loc. PLR45, Palomino Ridge, middle Smithian.

Figs. T–U. ?*Galfettites* sp. indet. PIMUZ 32111. UAZ₄, loc. PLR45, Palomino Ridge, middle Smithian.

Figs. V–X. ?*Galfettites* sp. indet. PIMUZ 32112. UAZ₄, loc. PLR45, Palomino Ridge, middle Smithian.

Figs. Y–AA. ?*Galfettites* sp. indet. PIMUZ 32113. UAZ₄, loc. PLR45, Palomino Ridge, middle Smithian.

Figs. AB–AD. ?*Galfettites* sp. indet. PIMUZ 32114. UAZ₄, loc. PLR45, Palomino Ridge, middle Smithian.

Fig. AE. ?*Galfettites* sp. indet. Suture line of PIMUZ 32109 with scale bar representing 5 mm, at H = 7.5 mm. UAZ₄, loc. PLR27, Palomino Ridge, middle Smithian.

PLATE 19

Figs. A–C. *Pseudosageceras multilobatum* NOETLING, 1905. PIMUZ 32094. UAZ₄, loc.

PLR72, Palomino Ridge, middle Smithian.

Figs. D–E. *Pseudosageceras multilobatum* NOETLING, 1905. PIMUZ 32095. UAZ₄, loc. PLR12, Palomino Ridge, middle Smithian.

Fig. F. *Pseudosageceras multilobatum* NOETLING, 1905. Suture line of PIMUZ 32094 with scale bar representing 5 mm, at H = 31.6 mm. UAZ₄, loc. PLR72, Palomino Ridge, middle Smithian.

Figs. G–H. *Pseudosageceras multilobatum* NOETLING, 1905. PIMUZ 32096. UAZ₄, loc.

PLR71, Palomino Ridge, middle Smithian.

Fig. I. *Pseudosageceras multilobatum* NOETLING, 1905. PIMUZ 32097. UAZ₄, loc. PLR12,

Palomino Ridge, middle Smithian.

Figs. J–K. *Pseudosageceras augustum* (BRAYARD & BUCHER, 2008). PIMUZ 32098.

Potential UAZ₆, loc. PLR32, Palomino Ridge, late Smithian.

Fig. L. *Pseudosageceras augustum* (BRAYARD & BUCHER, 2008). Suture line of PIMUZ

32098 with scale bar representing 5 mm, at H = 10.4 mm. Potential UAZ₆, loc. PLR32,

Palomino Ridge, late Smithian.

Figs. M–N. *Pseudosageceras augustum* (BRAYARD & BUCHER, 2008). PIMUZ 32099.

Potential UAZ₆, loc. PLR35, Palomino Ridge, late Smithian.

Figs. O–Q. ?*Pseudosageceras bullatum* n. sp., paratype. PIMUZ 32100, X1.5. Potential

UAZ₆, loc. PLR48, Palomino Ridge, late Smithian. Arrows indicate location of bullae.

Figs. R–T. ?*Pseudosageceras bullatum* n. sp., holotype. PIMUZ 32101, X2. Potential UAZ₆,

loc. PLR47, Palomino Ridge, late Smithian. Arrow indicates location of a bullae.

Fig. U. ?*Pseudosageceras bullatum* n. sp. Suture line of PIMUZ 32101 with scale bar representing 5 mm, at H = 6 mm. Potential UAZ₆, loc. PLR47, Palomino Ridge, late Smithian.

Figure captions

TABLE 1. Measurements of some Smithian ammonoids from Palomino ridge.

Text-fig 1. Early Triassic subdivision calibrated with published radiometric ages

(OVTCHAROVA et al. 2006; GALFETTI et al. 2007; BURGESS et al. 2014). $\delta\text{C}^{13}_{\text{carb}}$ curves and

anoxic/euxinic events from GALFETTI et al. (2007). A: *Anasibirites*, X: *Xenoceltites*, ea.: early, mi.: middle, l.: late.

Text-fig 2. Early Triassic location of the western USA basin (black star). White stars indicate some other basins from which Smithian ammonoids have been documented.

Text-fig 3. A, Generalized map showing location of Palomino Ridge locality. B, Aerial view (Google Earth, map data: Landsat) of Palomino Ridge locality with location and designation of sampled sections.

Text-fig 4. Distribution of ammonoid taxa in Palomino Ridge, ‘Section 1’.

Text-fig 5. Distribution of ammonoid taxa in Palomino Ridge, ‘Section 2’; and biostratigraphical correlation between ‘Section 2’ and the uppermost part of ‘Section 1’.

Text-fig 6. A, Sequence of unitary associations (UAs) resulting from the biochronological analyses; 6 unitary associations, 0 cliques in cycle, 0 Z4 circuits, 0 S3 circuits. B, Sequence of unitary association zones (UAZs) resulting from the biochronological analyses.

Text-fig 7. Lateral reproducibility of the 5 UAZs. Dark squares represent unequivocal identification of single UAZ, white squares represent unidentified UAZ assignment with ranges of uncertainty.

Text-fig 8. A, Synthetic range chart for western USA basin showing the distribution of Smithian ammonoid species. Species marked by an asterisk (*) were omitted in the data set for the construction of the UAs (see text). They are dated and reincorporated into the range

chart at the end of the processing. B, Synthetic range chart for western USA basin showing the distribution of Smithian ammonoid genera. White squares indicate virtual occurrences. Genera marked by an asterisk (*) are endemic of a locality.

Text-fig 9. UAZs of the Smithian of the western USA basin and correlation with zonation of the northern Indian Margin (NIM). Modified after BRÜHWILER et al. 2011.

Text-fig 10. Scatter diagrams of H, W and U, and H/D, W/D, and U/D for *Xenoceltites subevolutus* (open symbols indicate specimens from Palomino Ridge, UAZ₅ and UAZ₆ [n = 7]; grey symbols indicate specimens from Spitsbergen; data from PIAZZA 2015 [n = 2]).

Text-fig 11. Scatter diagrams of H, W and U, and H/D, W/D, and U/D for *?Kashmirites cordilleranus* from Palomino Ridge, UAZ₄ [n = 6] and from Utah, UAZ₄ (data from BRAYARD et al. 2013) [n = 14]; and *Palominoceras* n. gen. *nevadanum* from Palomino Ridge, UAZ₄ [n = 125].

Text-fig 12. Scatter diagrams of H, W and U, and H/D, W/D, and U/D for *?Kashmirites cordilleranus* (open symbols indicate specimens from Palomino Ridge, UAZ₄ [n = 6]; grey symbols indicate specimens from Utah, UAZ₄; data from BRAYARD et al. 2013 [n = 14]).

Text-fig 13. Scatter diagrams of H, W and U, and H/D, W/D, and U/D for *Preflorianites toulai* (open symbols indicate specimens from Palomino Ridge, UAZ₄ [n = 3]; grey symbols indicate specimens from Nevada [n = 12] and Caucasus [n = 2]; data respectively from KUMMEL & STEELE 1962 and SHEVYREV 1995).

Text-fig 14. Box plots of H/D, W/D, and U/D for *Preflorianites toulai* from Nevada (this work, KUMMEL & STEELE 1962) and the Caucasus (SHEVYREV 1995) and *Preflorianites radians* from Primorye, South China and Oman (ZAKHAROV 1968, BRAYARD & BUCHER 2008 and BRÜHWILER et al. 2012a, respectively).

Text-fig 15. Scatter diagrams of H, W and U, and H/D, W/D, and U/D for *Juvenites thermarum* from Palomino Ridge (open symbols, UAZ₄ [n = 10]) and *Juvenites* cf. *thermarum* from Utah and Oman (grey symbols; data from BRAYARD et al. 2013, UAZ₄ [n = 9] and BRÜHWILER et al. 2012a [n = 20]).

Text-fig 16. Scatter diagrams of H, W and U, and H/D, W/D, and U/D for *Juvenites spathi* (open symbols indicate specimens from Palomino Ridge, UAZ₄ [n = 6]; grey symbols indicate specimens from South China and Oman [n = 82]; data respectively from BRAYARD & BUCHER 2008 and BRÜHWILER et al. 2012a).

Text-fig 17. Scatter diagrams of H, W and U, and H/D, W/D, and U/D for *Guodunites monneti* (open symbols indicate specimens from Palomino Ridge, UAZ₄ [n = 7]; grey symbols indicate specimens from South China [n = 1] and Oman [n = 3]; data from BRAYARD et al. 2009b).

Text-fig 18. Scatter diagrams of H, W and U, and H/D, W/D, and U/D for *Guodunites hooveri* (open symbols indicate specimens from Palomino Ridge, UAZ₄ [n = 4]; grey symbols indicate specimens from Utah, UAZ₄ [n = 56]; data from BRAYARD et al. 2013).

Text-fig 19. Scatter diagrams of H, W and U, and H/D, W/D, and U/D for *Dieneroceras dieneri* (open symbols indicate specimens from Palomino Ridge, UAZ₄ [n = 12]; grey symbols indicate specimens from Utah, UAZ₄ [n = 23]; data from BRAYARD et al. 2013).

Text-fig 20. Scatter diagrams of H, W and U, and H/D, W/D, and U/D for *Anaflemingites cf. silberlingi* from Palomino Ridge (open symbols, UAZ₄ [n = 3]) and *Anaflemingites silberlingi* from Nevada (grey symbols; data from JENKS et al. 2010 [n = 20]).

Text-fig 21. Scatter diagrams of H, W and U, and H/D, W/D, and U/D for *Churkites noblei* (open symbols indicate specimens from Palomino Ridge, UAZ₄ [n = 13]; grey symbols indicate specimens from Utah, UAZ₄ and Crittenden Springs, Nevada [n = 14]; data respectively from BRAYARD et al. 2013 and JENKS 2007).

Text-fig 22. Scatter diagrams of H, W and U, and H/D, W/D, and U/D for *Arctoceras tuberculatum* (open symbols indicate specimens from Palomino Ridge, UAZ₄ [n = 1]; grey symbols indicate specimens from Utah, UAZ₄ [n = 1] and Crittenden Springs, Nevada [n = 12]; data respectively from BRAYARD et al. 2013 and KUMMEL & STEELE 1962).

Text-fig 23. Scatter diagrams of H, W and U, and H/D, W/D, and U/D for *Inyoites oweni* (open symbols indicate specimens from Palomino Ridge, UAZ₄ [n = 3]; grey symbols indicate specimens from Utah, UAZ₄ [n = 46]; data from BRAYARD et al. 2013).

Text-fig 24. Scatter diagrams of H, W and U, and H/D, W/D, and U/D for *Inyoites* sp. indet. from Palomino Ridge (open symbols, UAZ₄ [n = 3]) and *Inyoites beaverensis* from Utah, UAZ₃ (grey symbols, [n = 16]; data from BRAYARD et al. 2013).

Text-fig 25. Scatter diagrams of H, W and U, and H/D, W/D, and U/D for *Lanceolites compactus* (open symbols indicate specimens from Palomino Ridge, UAZ₄ [n = 6]; grey symbols indicate specimens from Utah, UAZ₄ [n = 3], the Caucasus, Oman, and China [n = 8]; data respectively from BRAYARD et al. 2013, SHEVYREV 1995, BRÜHWILER et al. 2012a, BRAYARD & BUCHER 2008).

Text-fig 26. Scatter diagrams of H, W and U, and H/D, W/D, and U/D for *Parussuria compressa* (open symbols indicate specimens from Palomino Ridge, UAZ₄ [n = 3]; grey symbols indicate specimens from Utah, UAZ₄ [n = 2], South China, California, Primorye, Oman, and the Caucasus [n = 22]; data respectively from BRAYARD et al. 2013, BRAYARD & BUCHER 2008, KUMMEL & STEELE 1962, ZAKHAROV 1968, BRÜHWILER et al. 2012a, SHEVYREV 1995).

Text-fig 27. Scatter diagrams of H, W and U, and H/D, W/D, and U/D for *Wasatchites perrini* (open symbols indicate specimens from Palomino Ridge, UAZ₅ [n = 4]; grey symbols indicate specimens from Utah, UAZ₅ [n = 2]; data from BRAYARD et al. 2013).

Text-fig 28. Scatter diagrams of H, W and U, and H/D, W/D, and U/D for *Anasibirites kingianus* from Palomino Ridge, UAZ₅ [n = 6].

Text-fig 29. Scatter diagrams of H, W and U, and H/D, W/D, and U/D for *Anasibirites multiformis* (open symbols indicate specimens from Palomino Ridge, UAZ₅ [n = 52]; grey symbols indicate specimens from Timor [n = 52]; data from JATTIOT et al. 2015).

Text-fig 30. Scatter diagrams of H, W and U, and H/D, W/D, and U/D for *Hemiprionites* species [n = 85] (all from Palomino Ridge, UAZ5; except for *H. klugi* from South China). Dot
111

symbols indicate *Hemiprionites walcotti* specimens; square symbols indicate *Hemiprionites klugi* holotype; cross symbols indicate *Hemiprionites typus* specimens with depression; and circle symbols indicate *Hemiprionites typus* specimens without depression (wd).

Text-fig 31. Scatter diagrams of H, W and U, and H/D, W/D, and U/D for *Arctopriionites resseri* (open symbols indicate specimens from Palomino Ridge, UAZ₅ [n = 7]; grey symbols indicate specimens from Utah, UAZ₅ [n = 1]; data from BRAYARD et al. 2013).

Text-fig 32. Scatter diagrams of H, W and U, and H/D, W/D, and U/D for *Meekoceras gracilitatis* (open symbols indicate specimens from Palomino Ridge, UAZ₄ [n = 10]; grey symbols indicate specimens from Utah, UAZ₄ [n = 2] and Crittenden Springs, Nevada [n = 101]; data respectively from BRAYARD et al. 2013 and JENKS et al. 2010).

Text-fig 33. Scatter diagrams of H, W and U, and H/D, W/D, and U/D for *Paranannites aspenensis* (open symbols indicate specimens from Palomino Ridge, UAZ₄ [n = 1]; grey symbols indicate specimens from Crittenden Springs [n = 39]; data from KUMMEL & STEELE 1962).

Text-fig 34. Scatter diagrams of H, W and U, and H/D, W/D, and U/D for *Paranannites cf. baudi* from Palomino Ridge (open symbols, UAZ₄ [n = 2]) and *Paranannites baudi* from Oman (grey symbols [n = 13]; data from BRÜHWILER et al. 2012a).

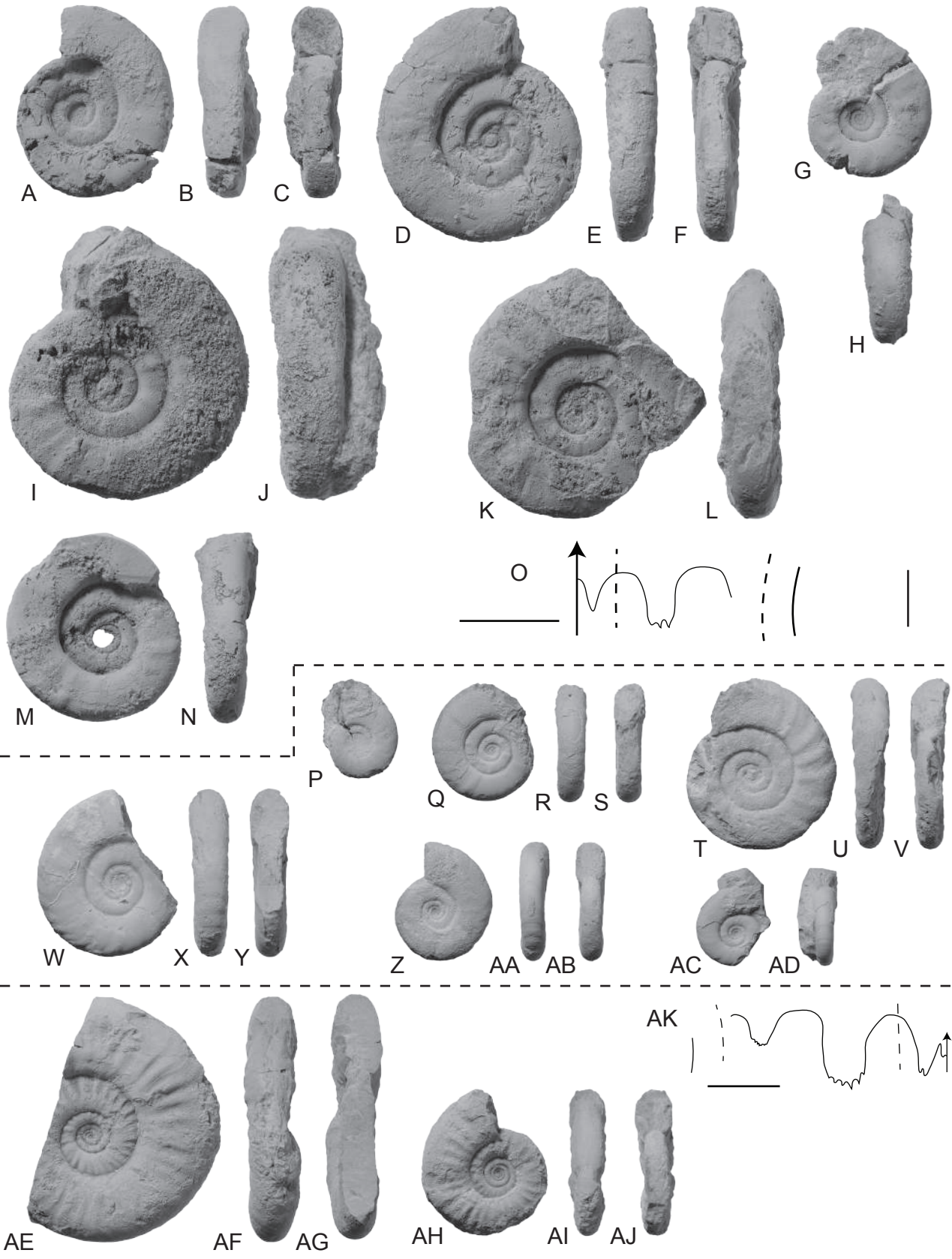
Text-fig 35. Scatter diagrams of H, W and U, and H/D, W/D, and U/D for *Owenites koeneni* (open symbols indicate specimens from Palomino Ridge, UAZ₄ [n = 7]; grey symbols indicate specimens from Utah, UAZ₄ [n = 1]; data from BRAYARD et al. 2013).

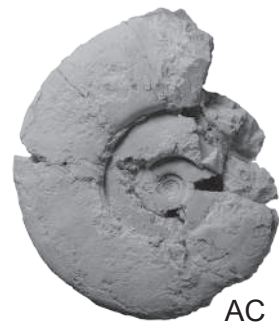
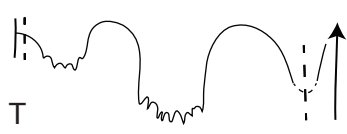
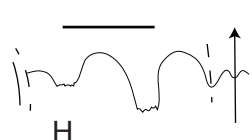
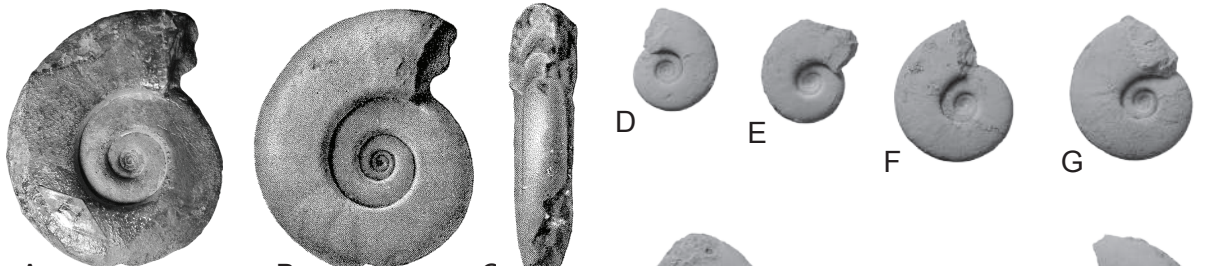
Text-fig 36. Scatter diagrams of H, W and U, and H/D, W/D, and U/D for *Owenites carpenteri* (open symbols indicate the single specimen from Palomino Ridge, UAZ₄; grey symbols indicate specimens from Utah, South China, Tibet, Spiti and Oman; data respectively from BRAYARD et al. 2013, BRAYARD & BUCHER 2008, BRÜHWILER et al. 2010b, 2012a, c; [n = 17]).

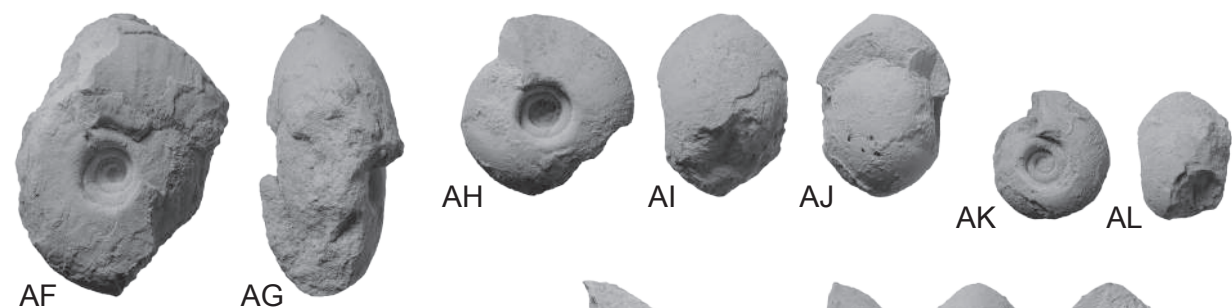
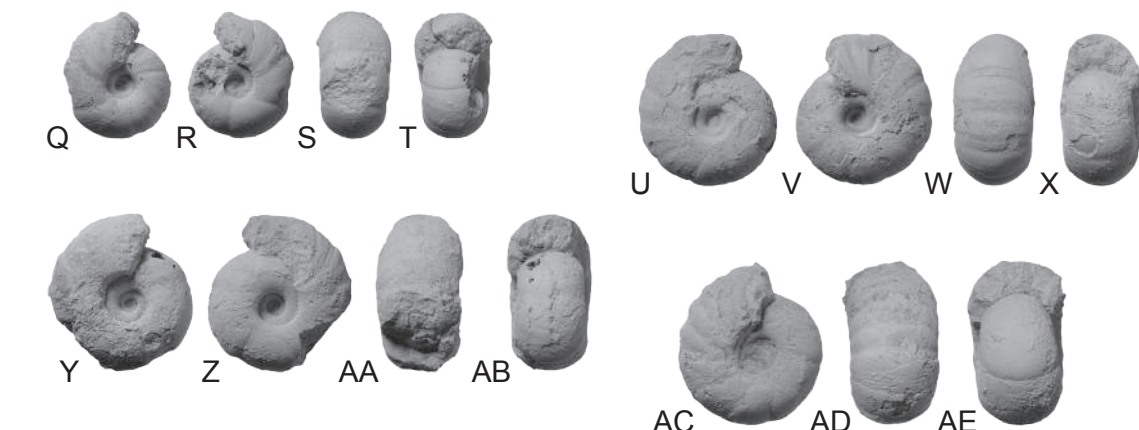
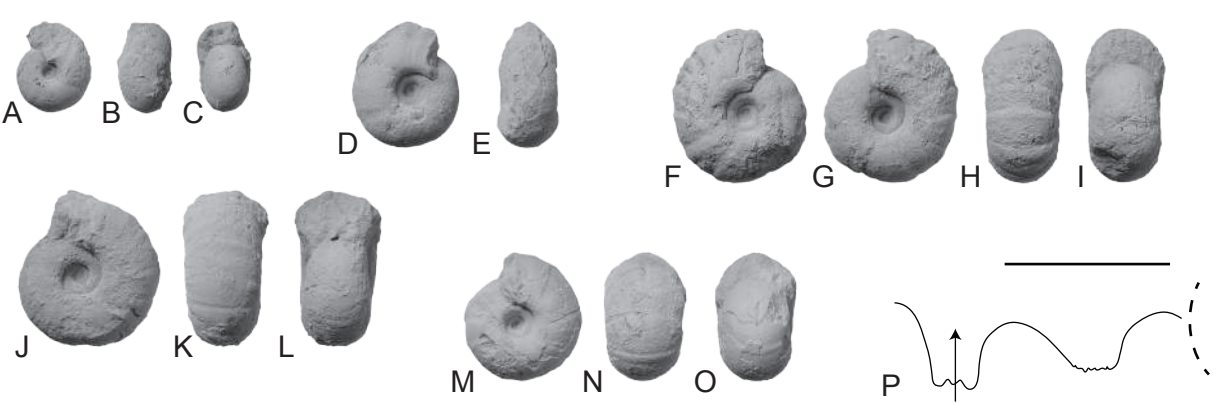
Text-fig 37. Scatter diagrams of H, W and U, and H/D, W/D, and U/D for ?*Galfettites* sp. indet. from Palomino Ridge, UAZ₄ [n = 16].

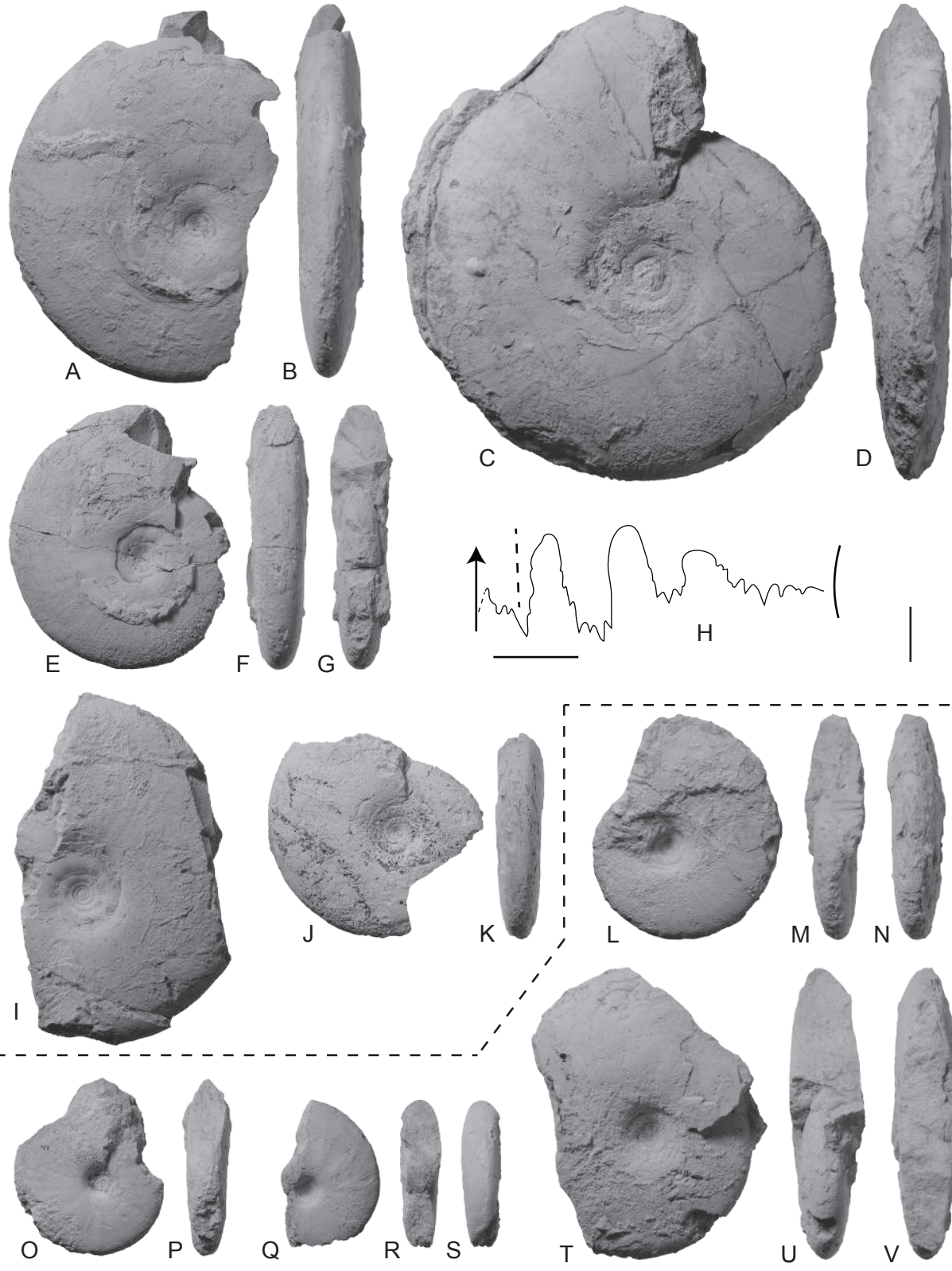
Text-fig 38. Scatter diagrams of H, W and U, and H/D, W/D, and U/D for *Pseudosageceras multilobatum* (open symbols indicate specimens from Palomino Ridge, UAZ₄ [n = 5]; grey symbols indicate specimens from Utah, Siberia, South China, Crittenden Springs, Madagascar, the Caucasus, Tibet, Oman and Pakistan; data respectively from BRAYARD et al. 2013, DAGYS & ERMAKOVA 1990, BRAYARD & BUCHER 2008, KUMMEL & STEELE 1962, COLLIGNON 1933, SHEVYREV 1968, BRÜHWILER et al. 2010b, 2012a, b; [n = 56]).

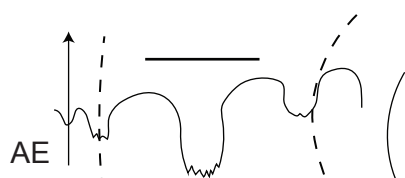
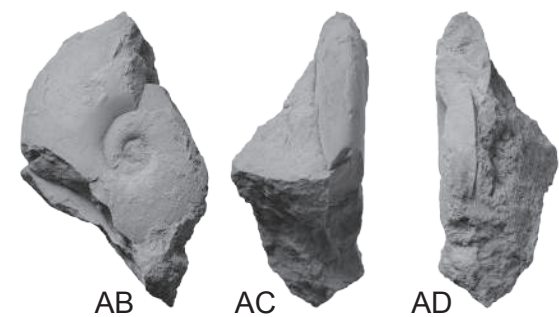
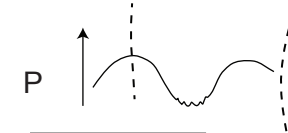
Text-fig 39. Scatter diagrams of H and W, and H/D and W/D for *Aspenites acutus* (open symbols indicate specimens from Palomino Ridge, UAZ₄ [n = 4]; grey symbols indicate specimens from Utah, South China, Crittenden Springs, Tibet, Oman and Spiti; data respectively from BRAYARD et al. 2013, BRAYARD & BUCHER 2008, KUMMEL & STEELE 1962, BRÜHWILER et al. 2010b, 2012a, c; [n = 54]).

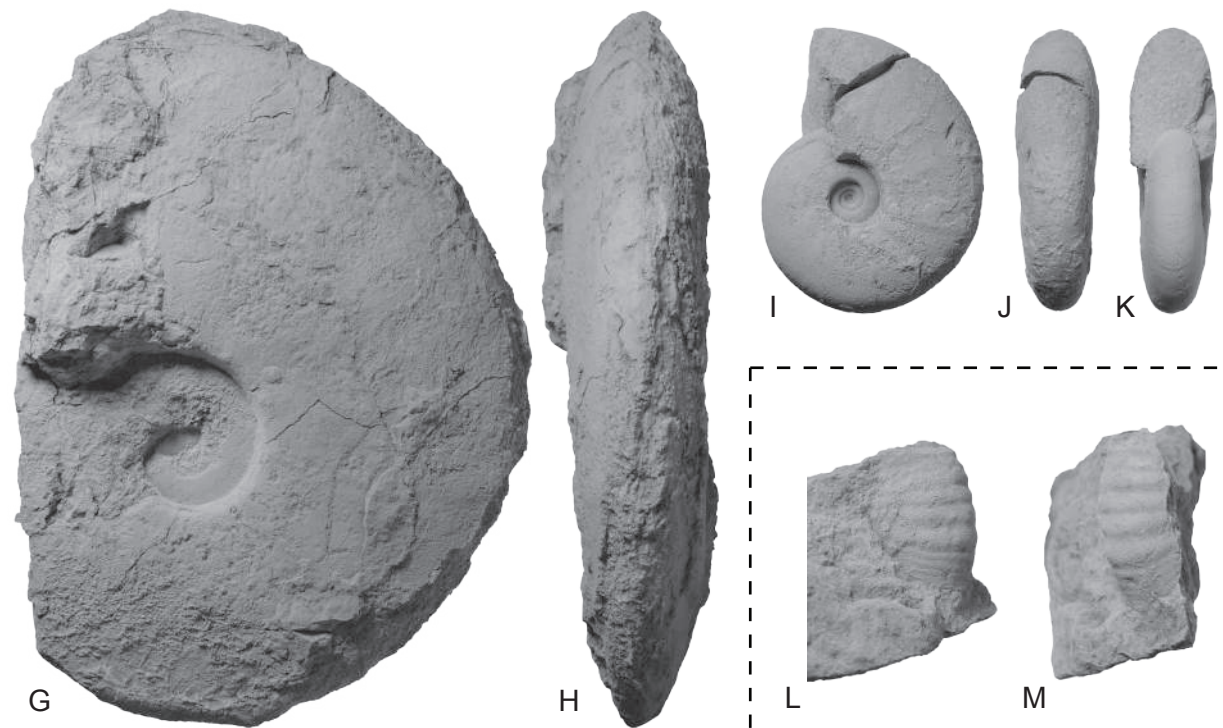
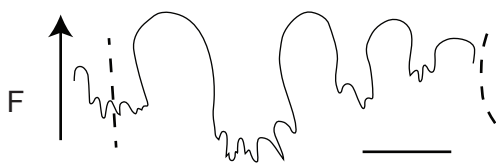


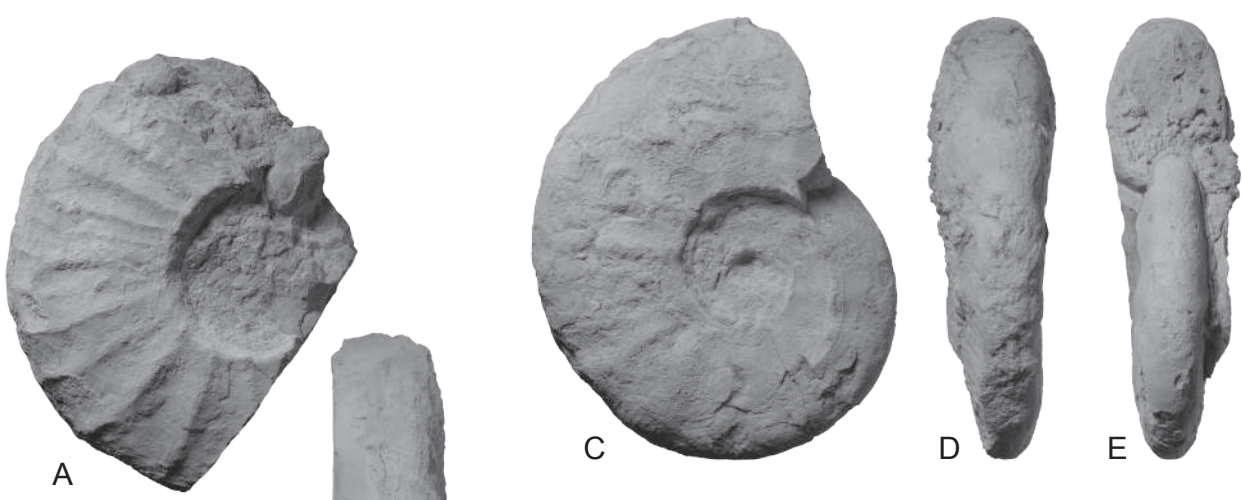










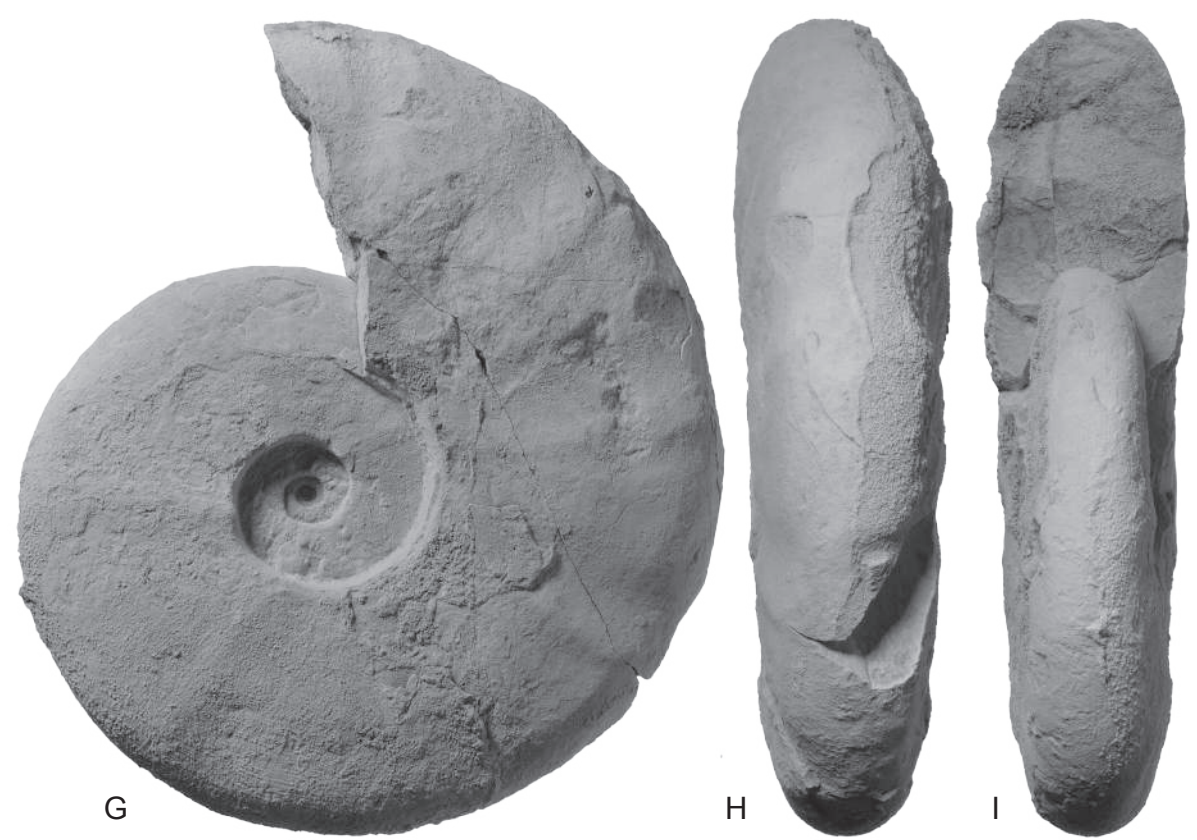
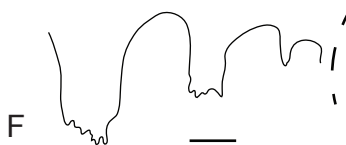


C

D

E

B

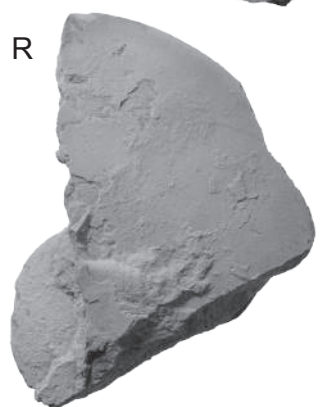
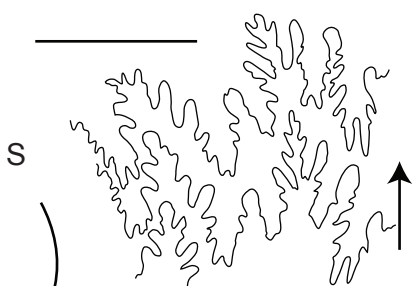
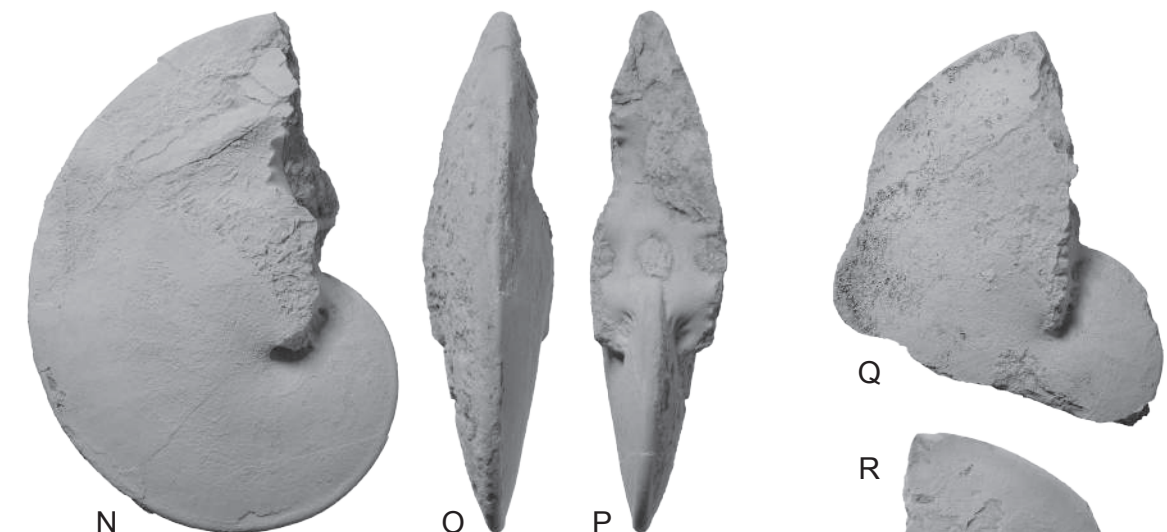
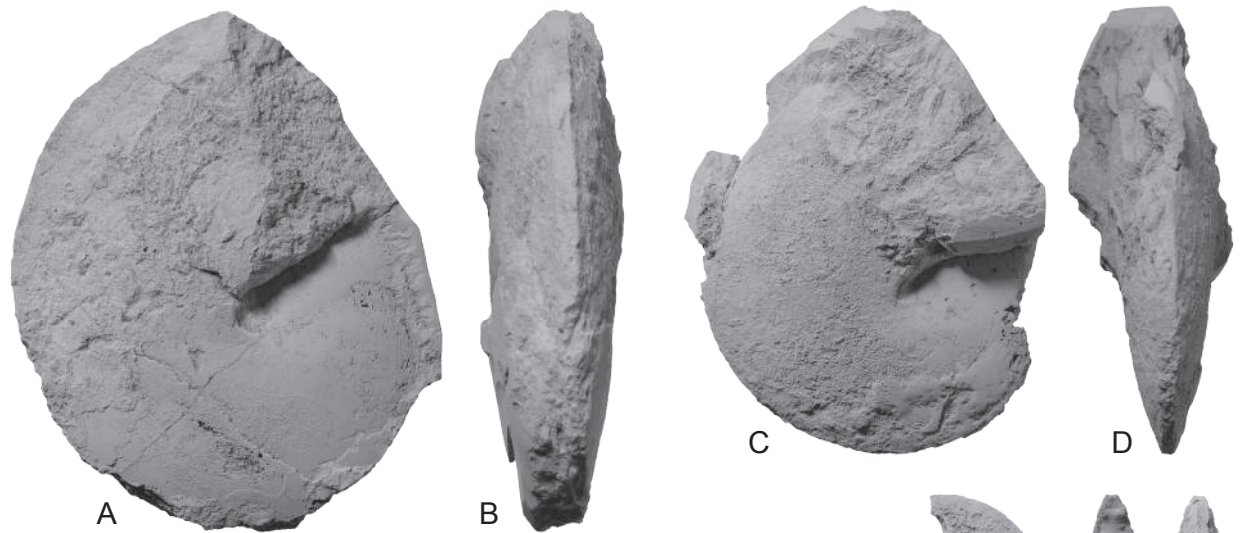


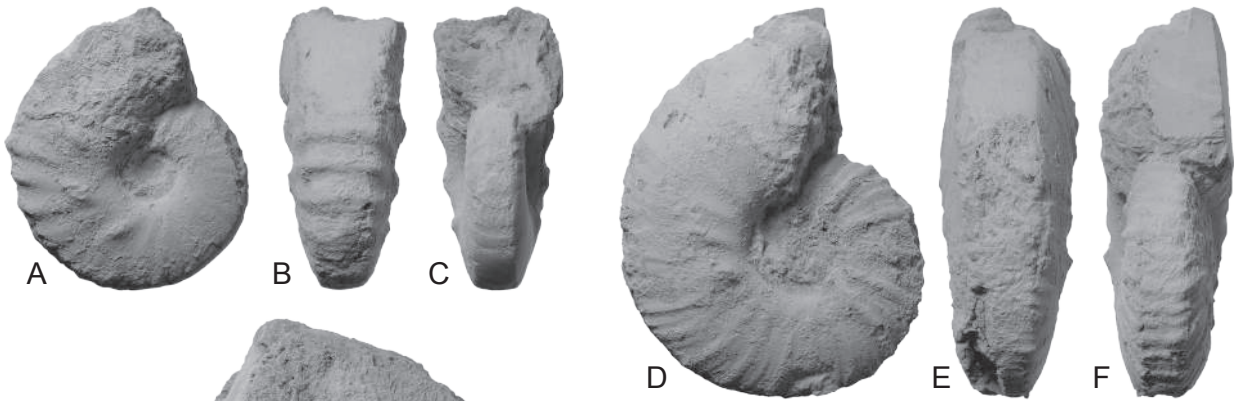
G

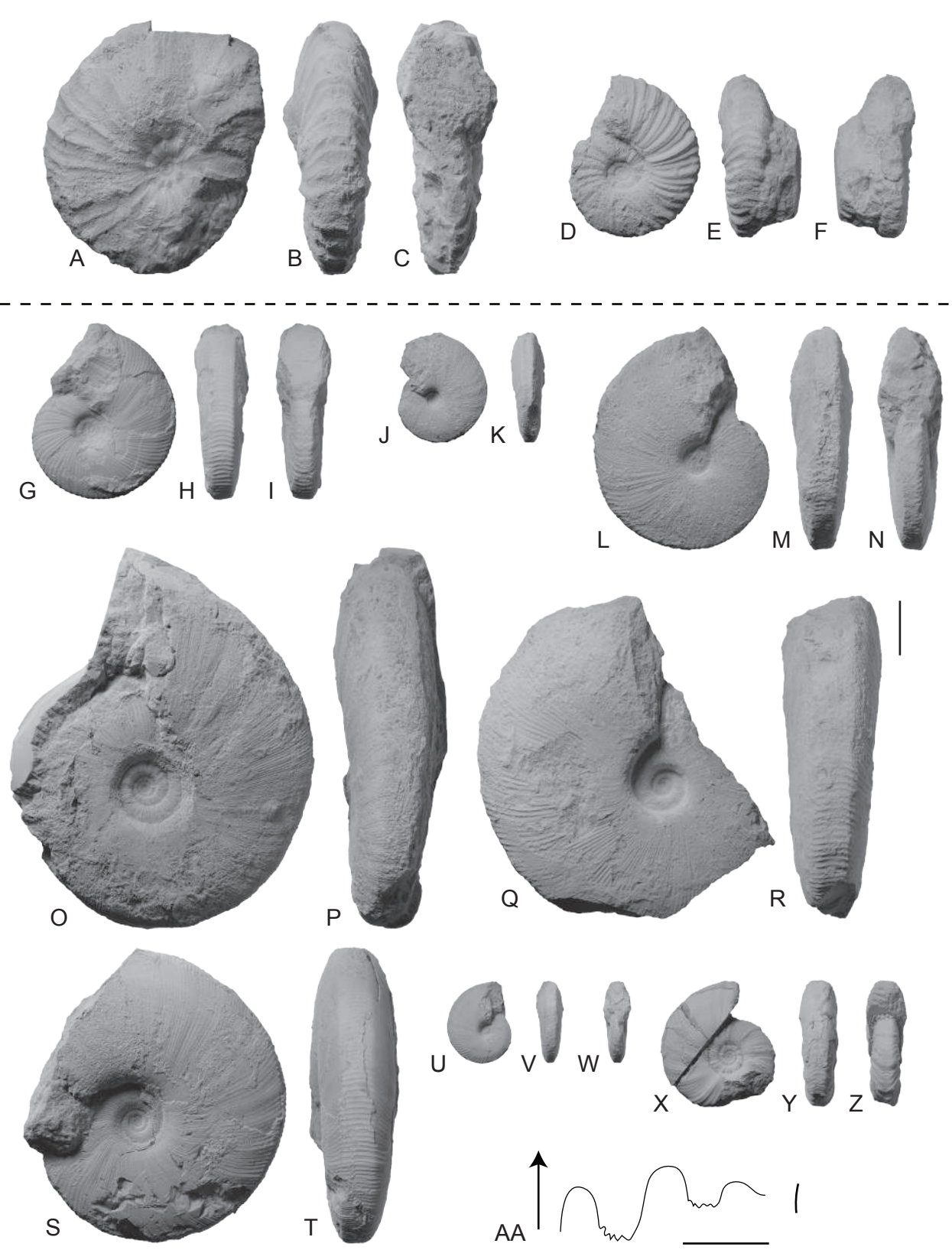
H

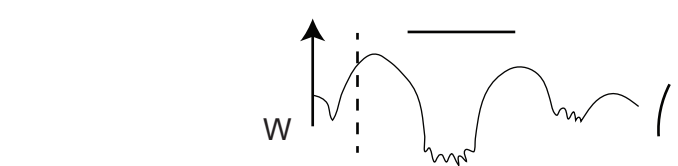
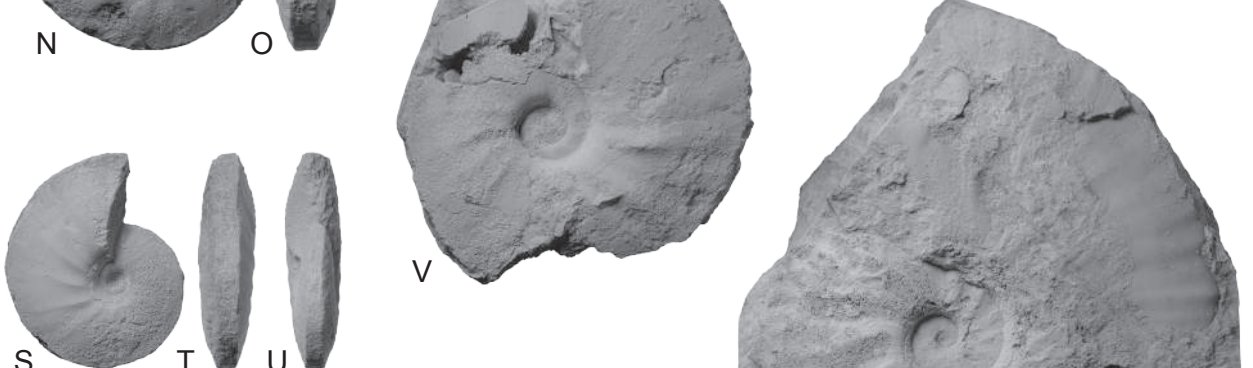
I

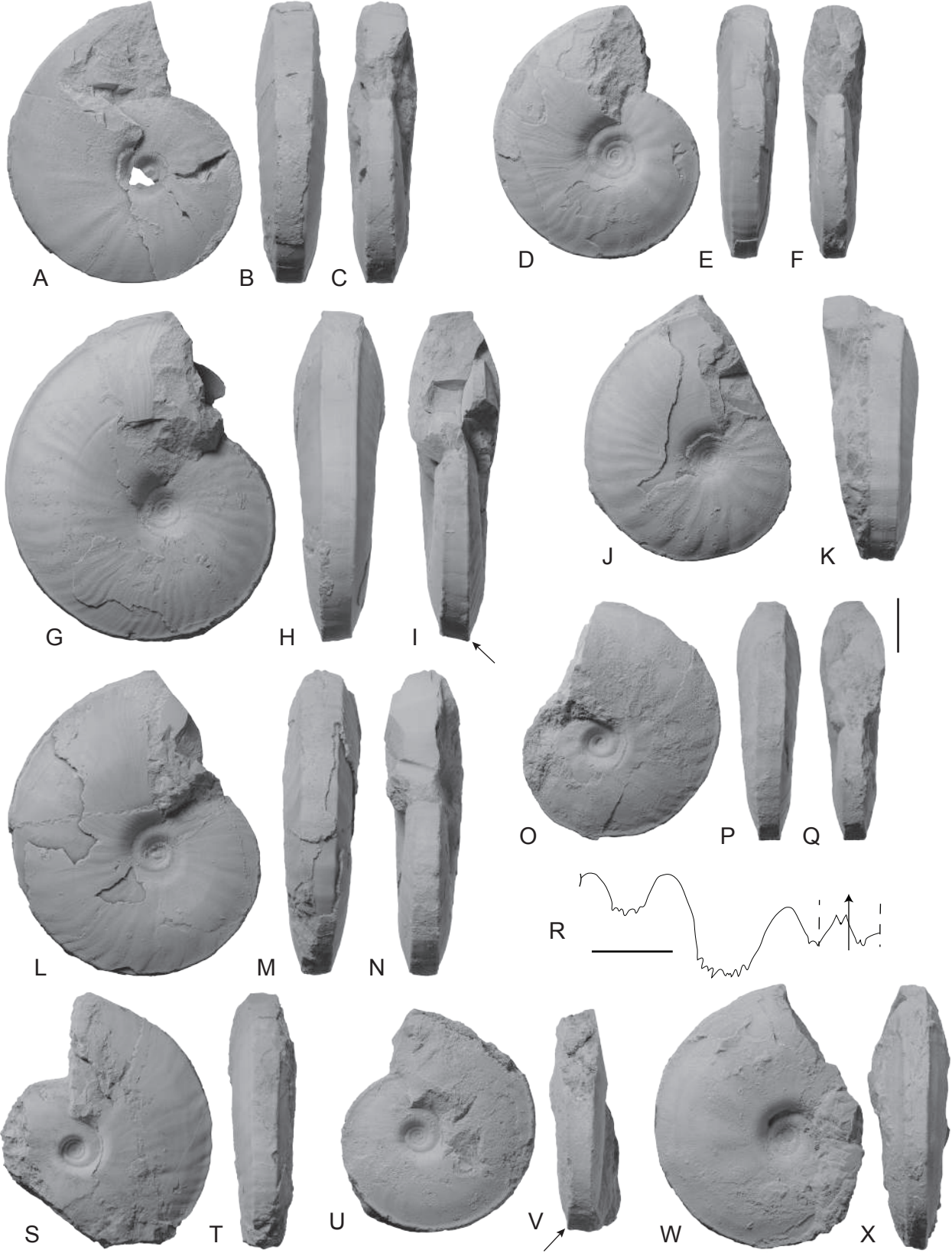


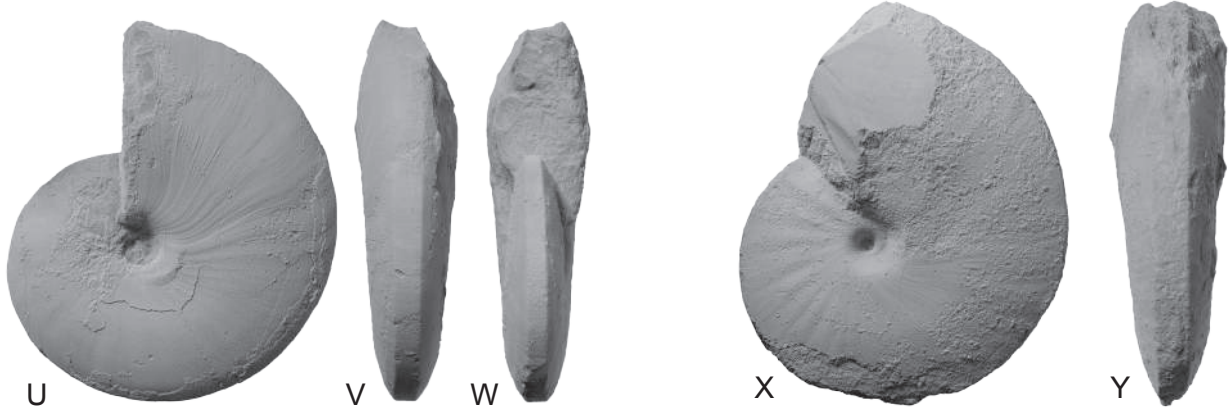
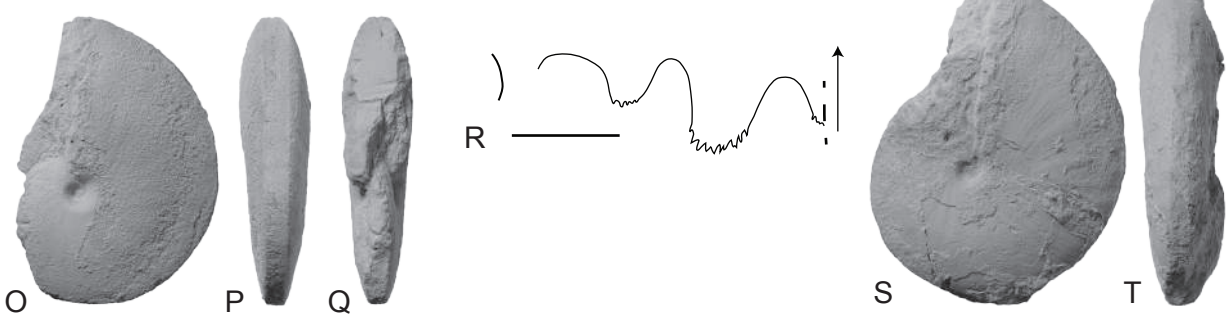
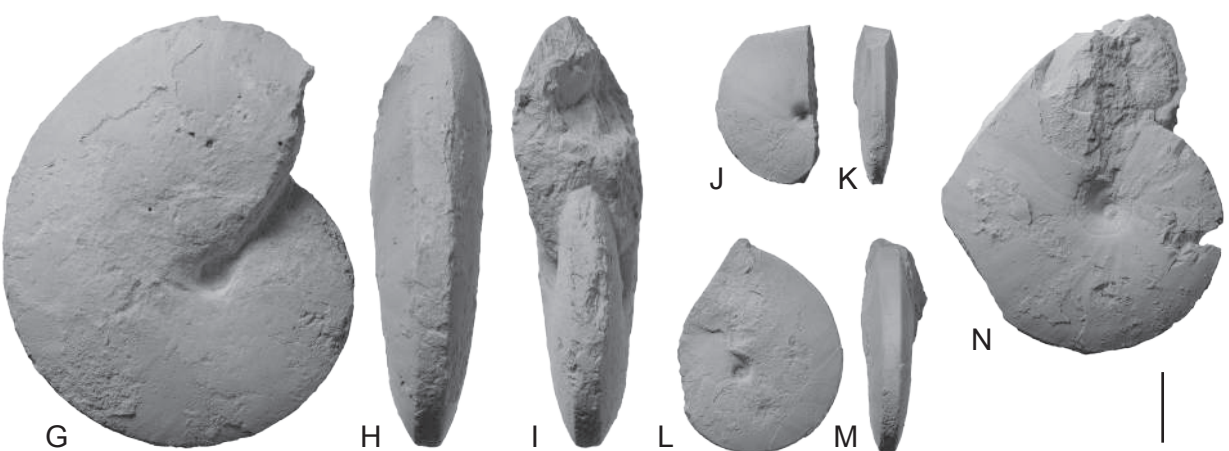














A



B



C



D



E



F



G



H



I



J



K



L



Q



N



O



P



R



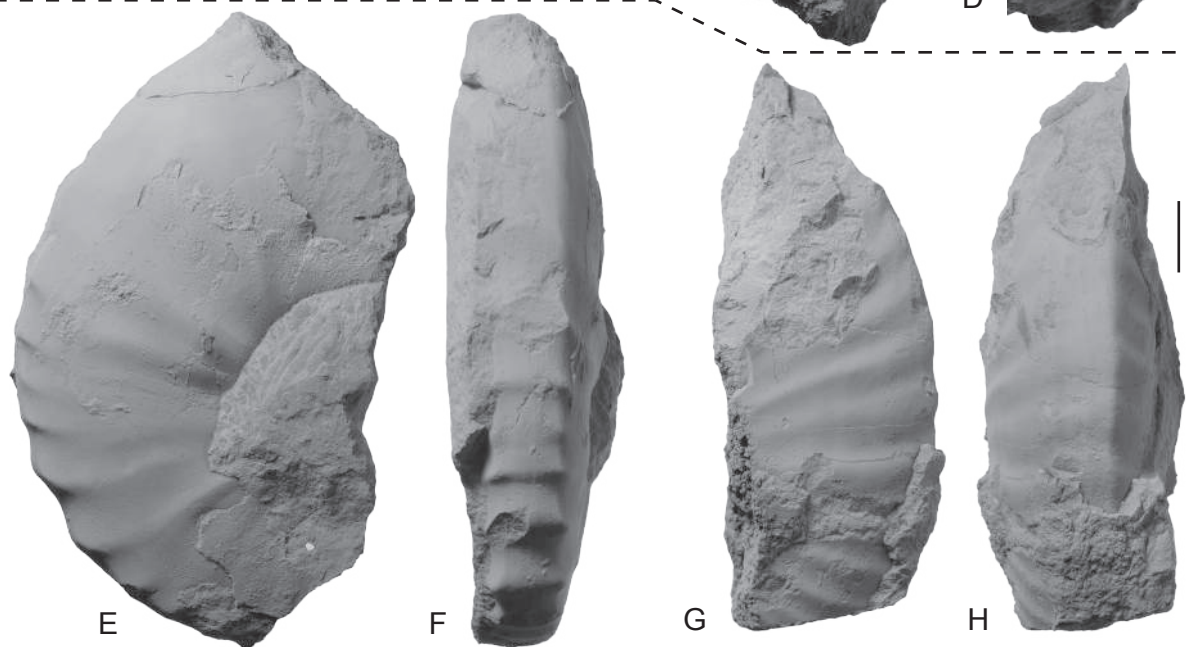
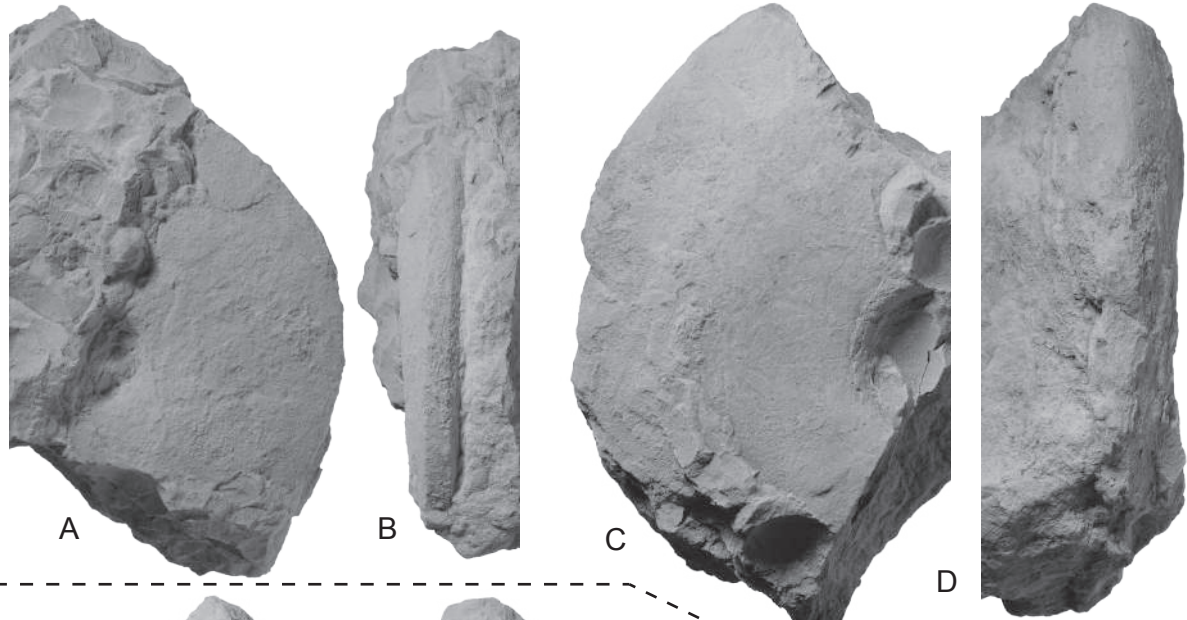
S

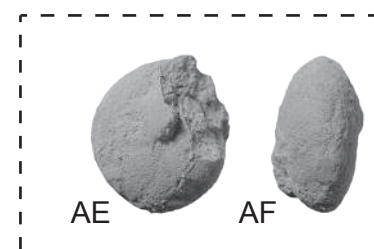
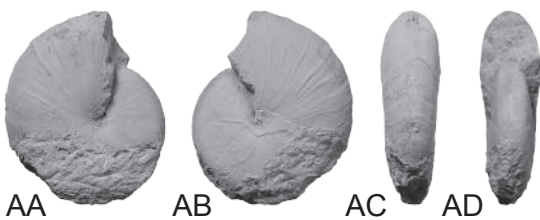
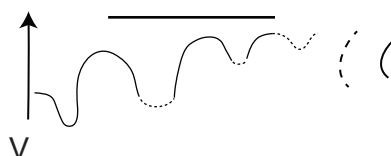
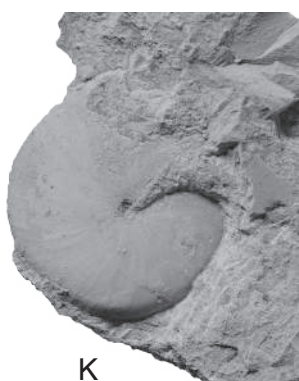
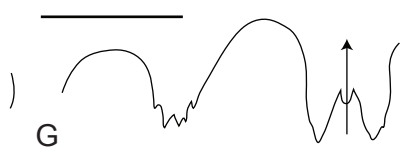
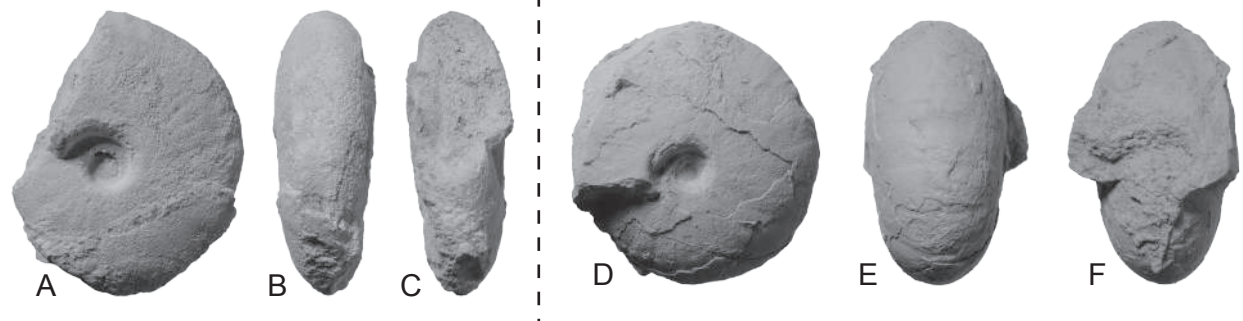


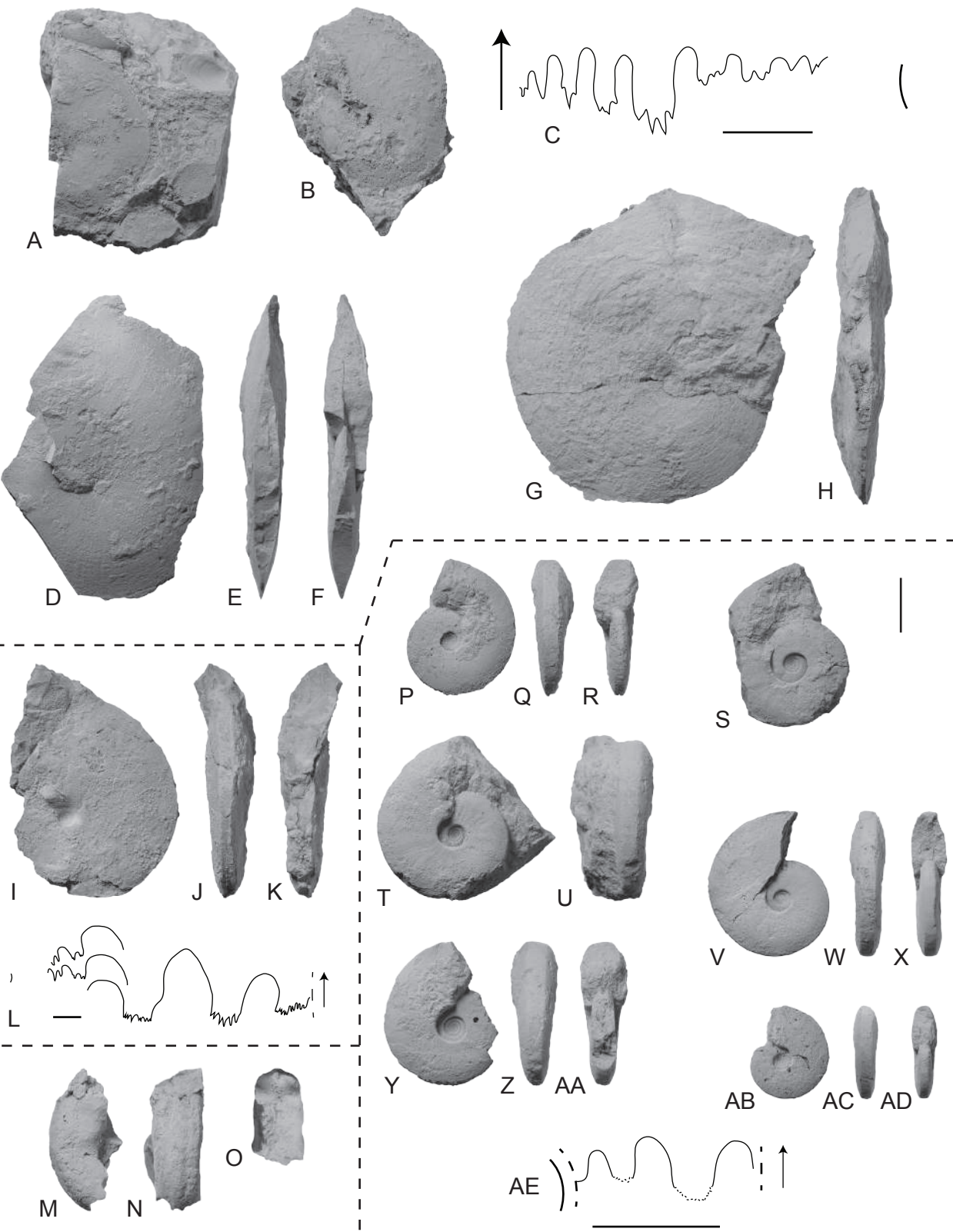
T



U









A



B



C



D



E



G



H



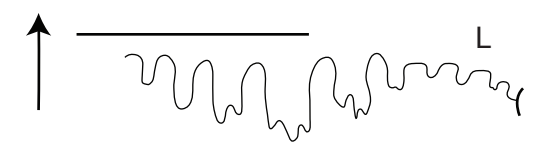
F



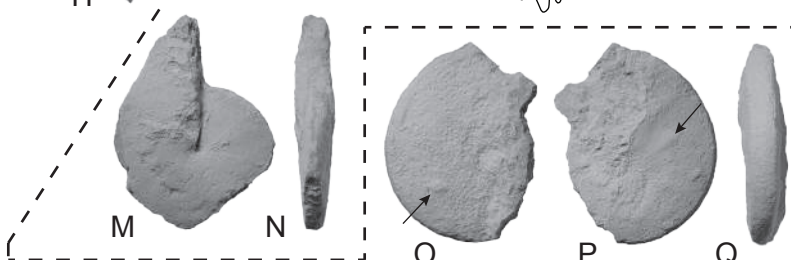
J

K

I



L



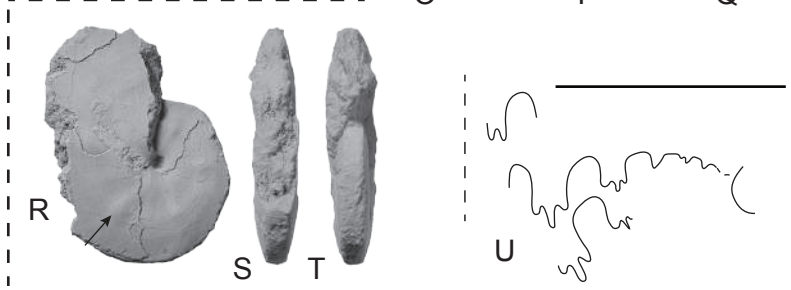
M

N

O

P

Q



R

S

T

U

Early Triassic

Induan

Olenekian

$$247.05 \pm 0.16$$

Ovtcharova et al. 2015

Spathian

$$250.55 \pm 0.4$$

Galfetti et al. 2007

$$250.55 \pm 0.4$$

Smithian

Galfetti et al. 2007

$$251.22 \pm 0.2$$

Dienerian

Griesbachian

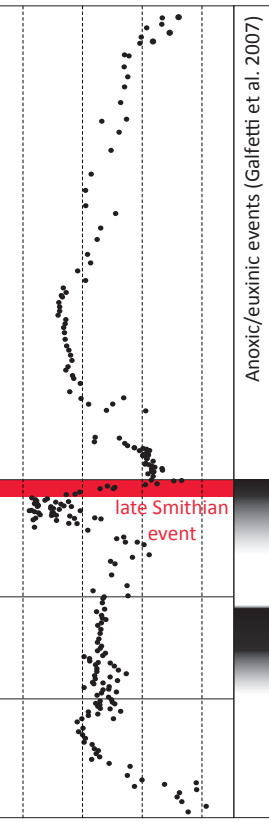
$$251.88 \pm 0.03$$

Burgess et al. 2014

Permian

ea. mi. I. ea. mi. I.

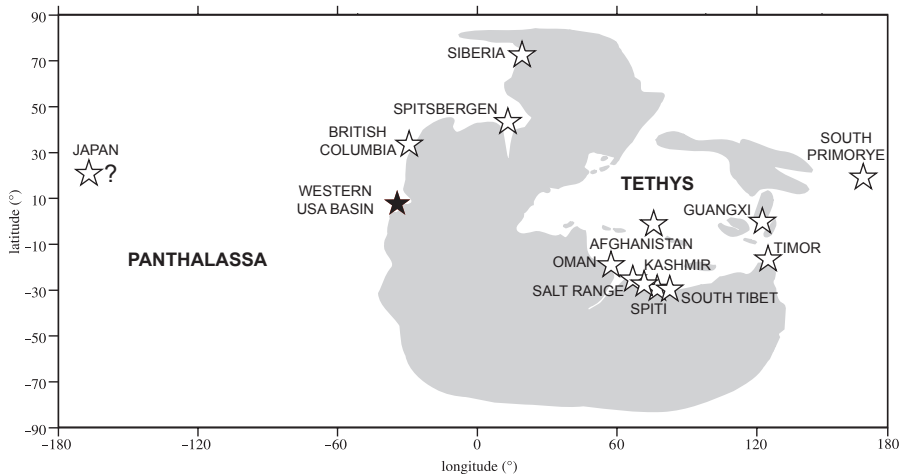
Ammonoid Zones

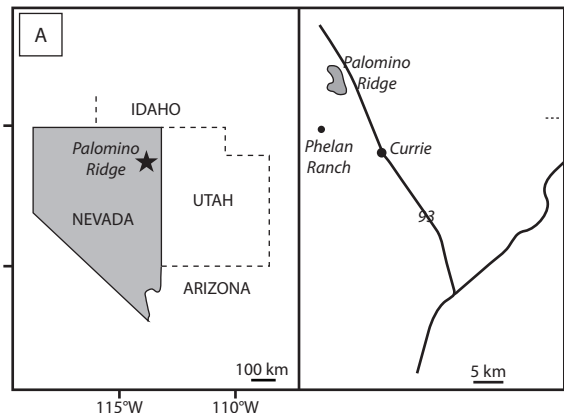


$\delta^{13}\text{C}_{\text{carb}}$ (VPDB) [‰]

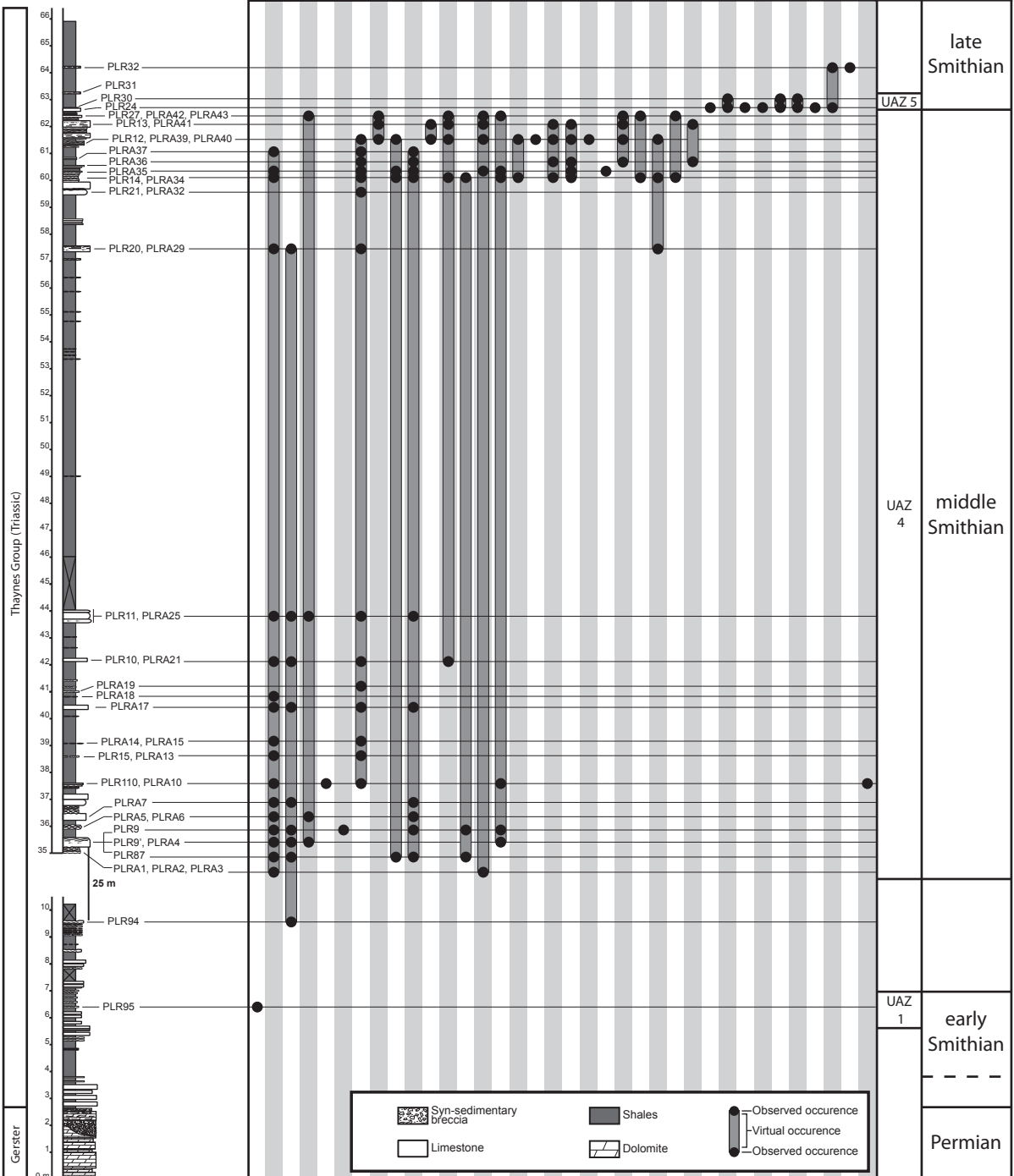
late Smithian event

Anoxic/euxinic events (Galfetti et al. 2007)

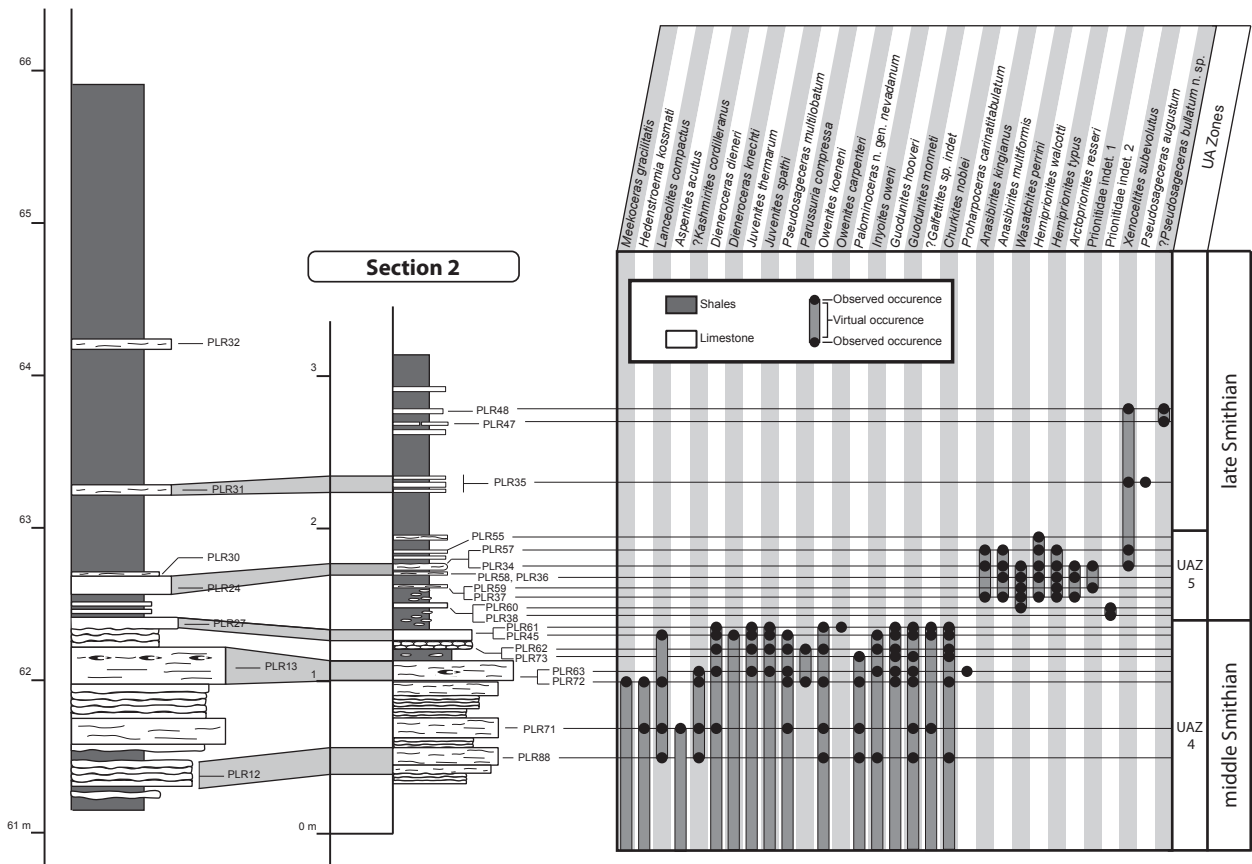




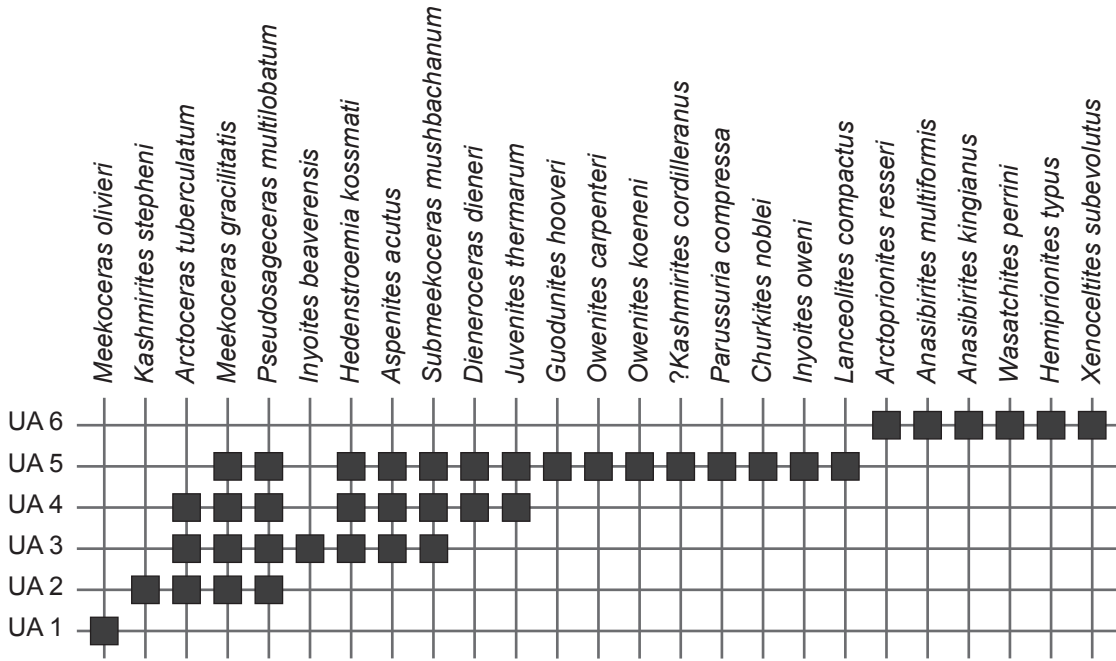
Section 1



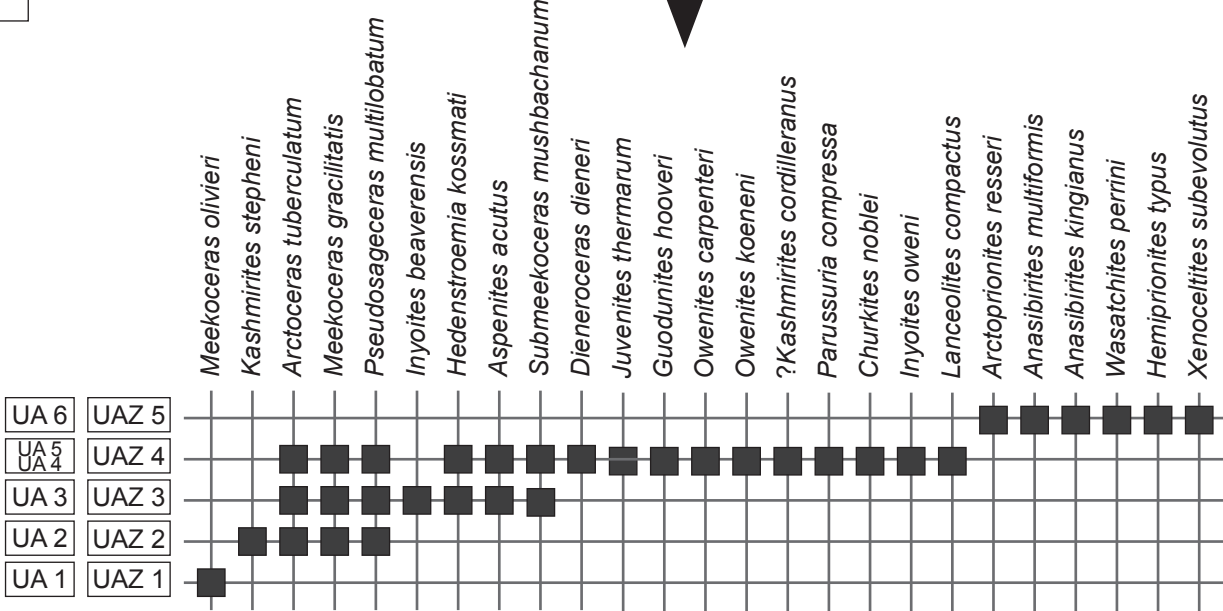
Section 1 (uppermost part)

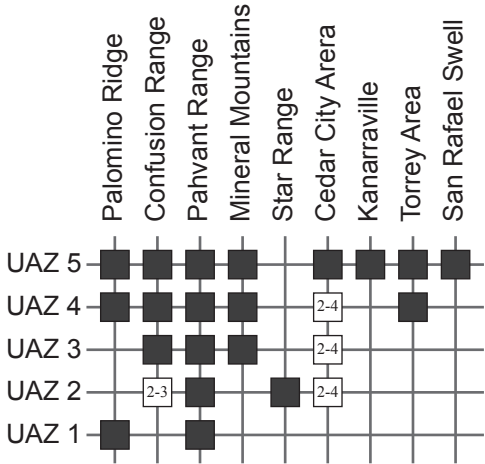


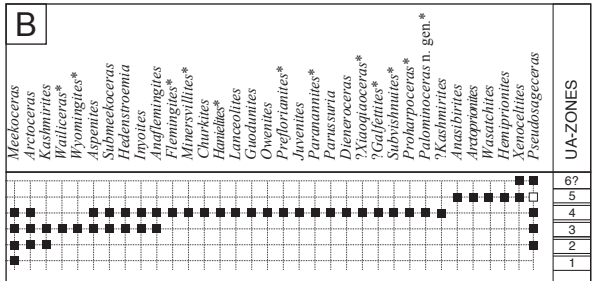
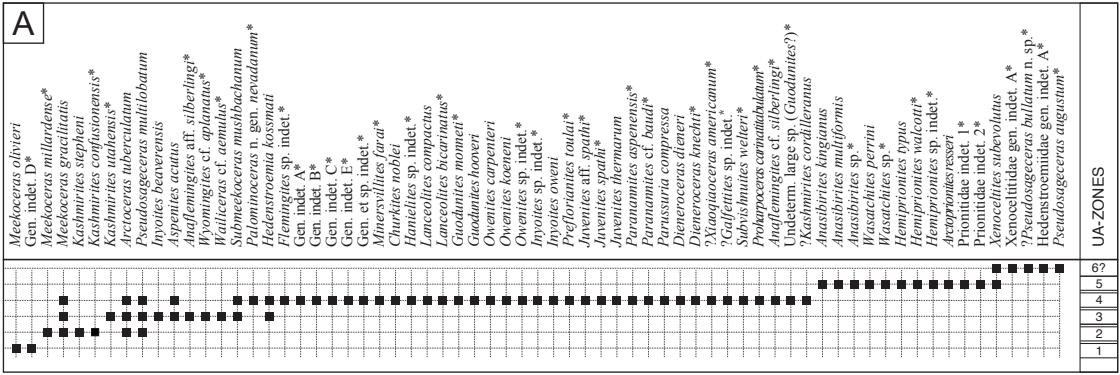
A



B







LATE
MIDDLE
EARLY

UA-Zones

western USA

NIM

UAZ 6?

S-14

LATE

UAZ 5

S-13

MIDDLE

UAZ 4

S-12

S-11

S-10

S-9

S-8

UAZ 3

S-7

EARLY

UAZ 2

S-6

S-5

S-4

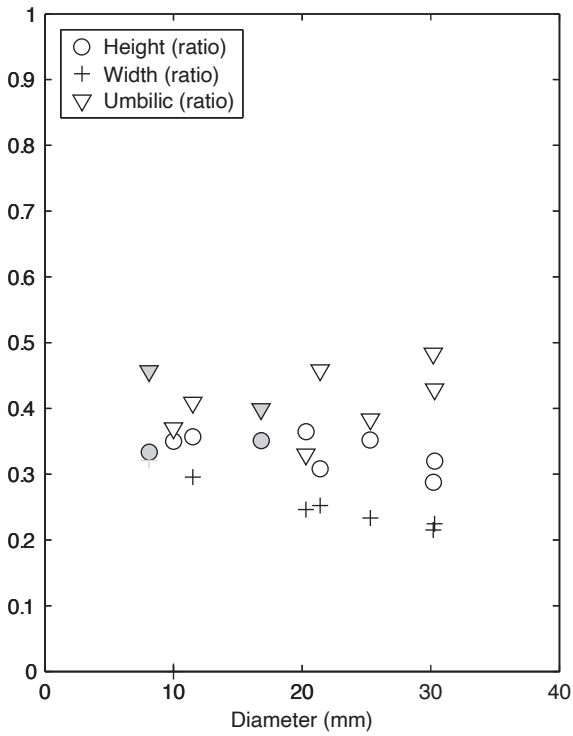
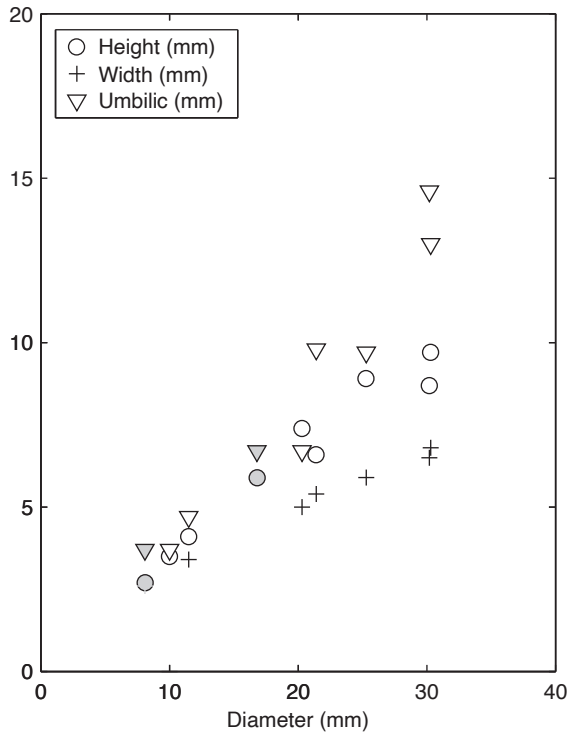
S-3

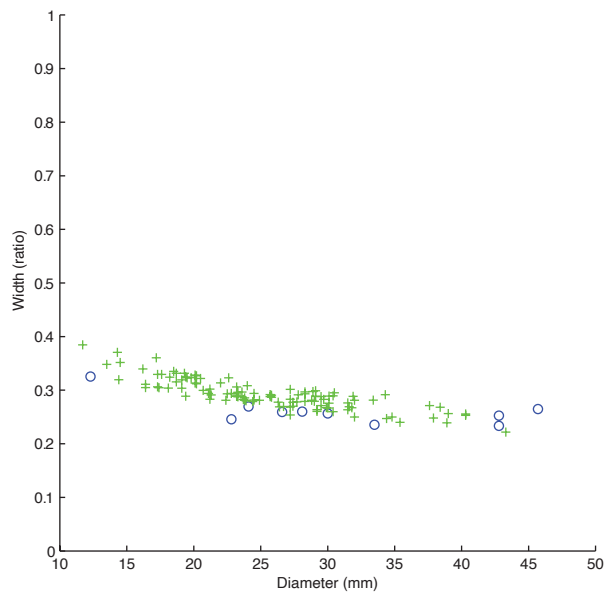
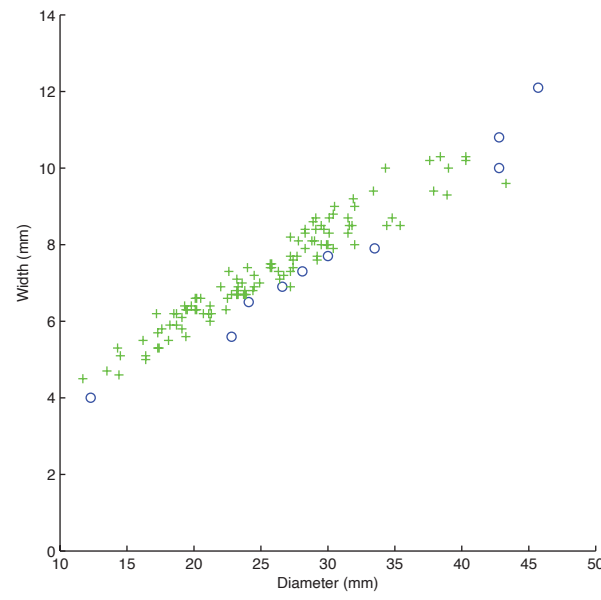
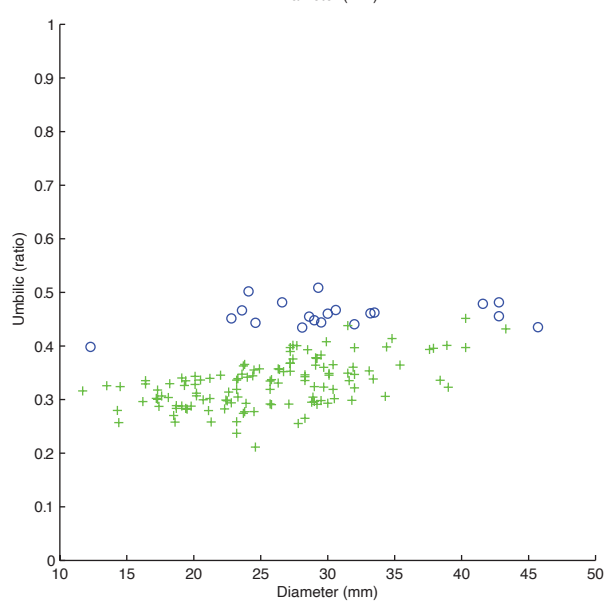
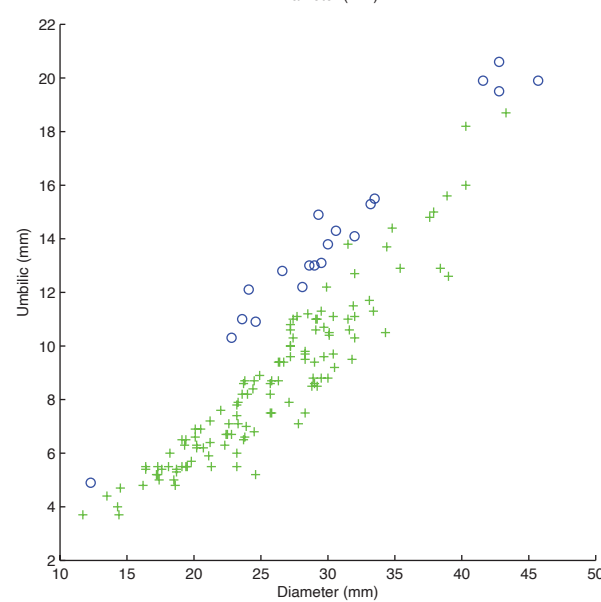
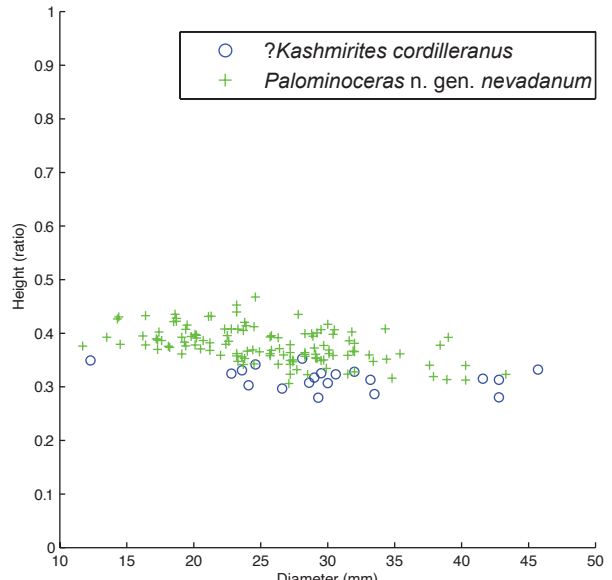
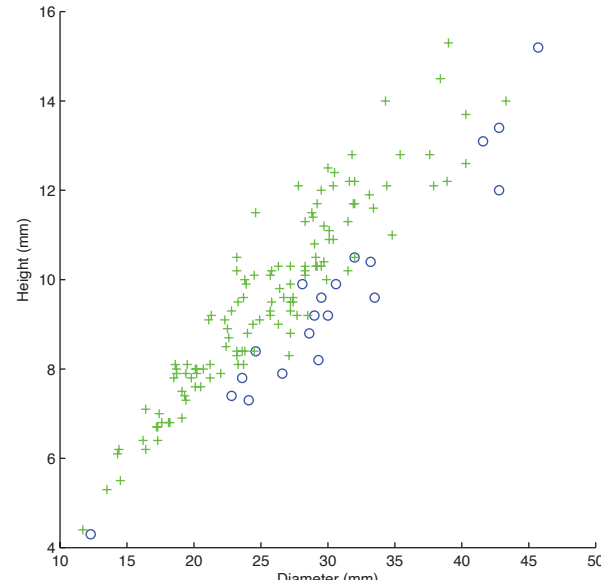
UAZ 1

S-2

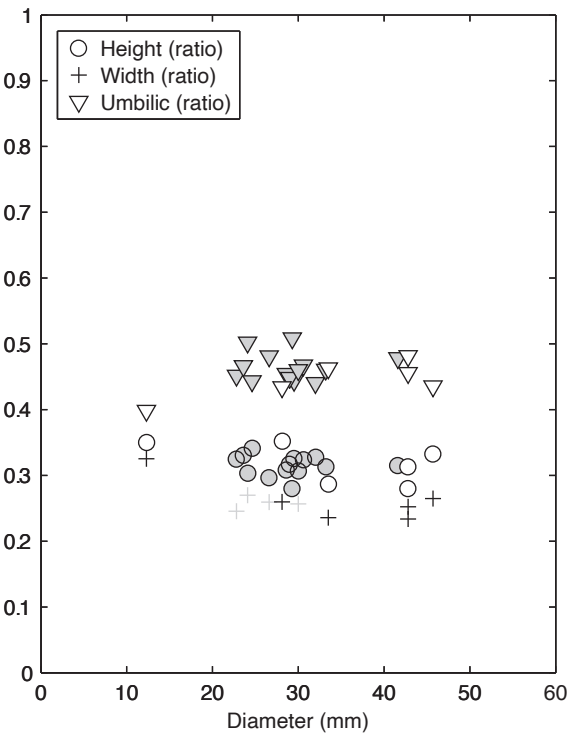
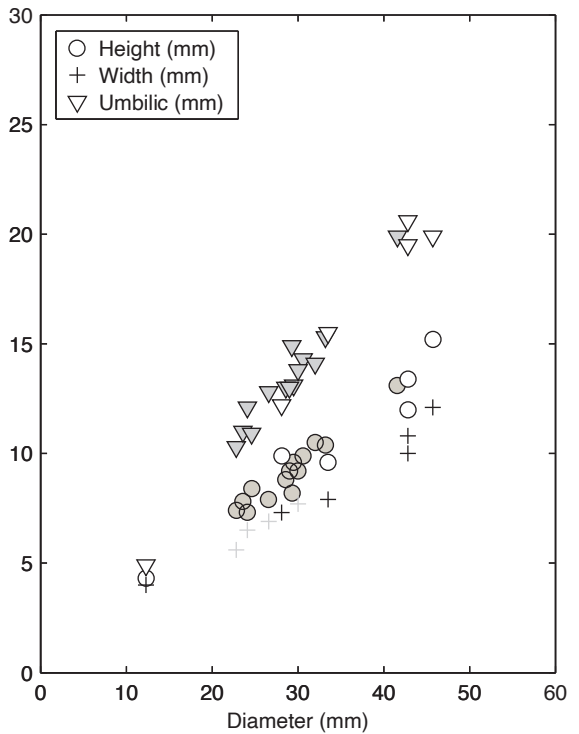
SMITHIAN

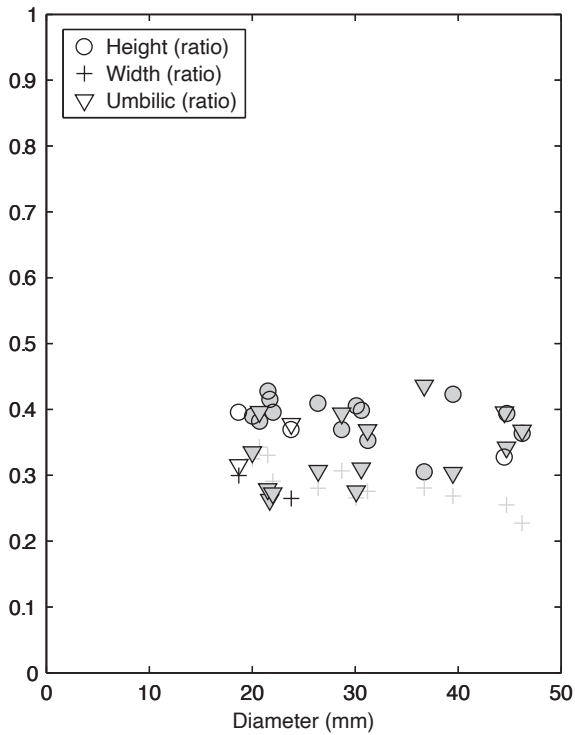
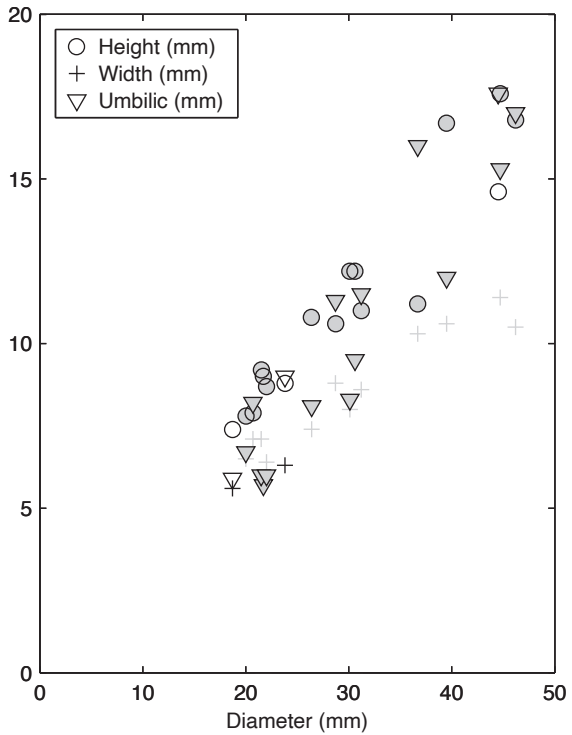
S-1

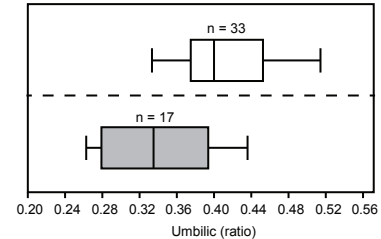
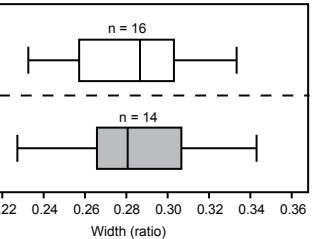
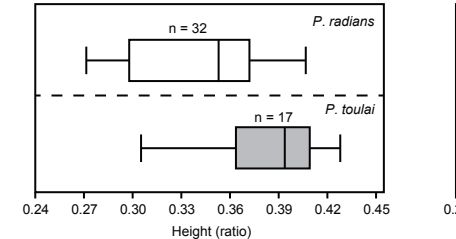


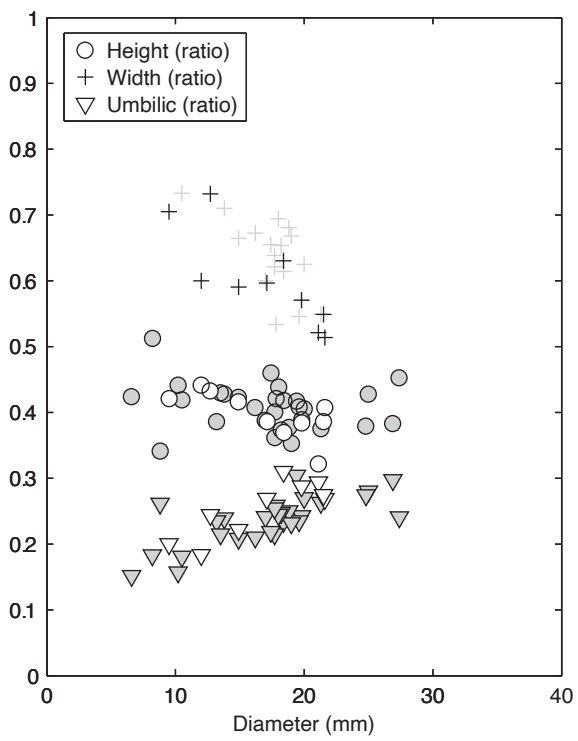
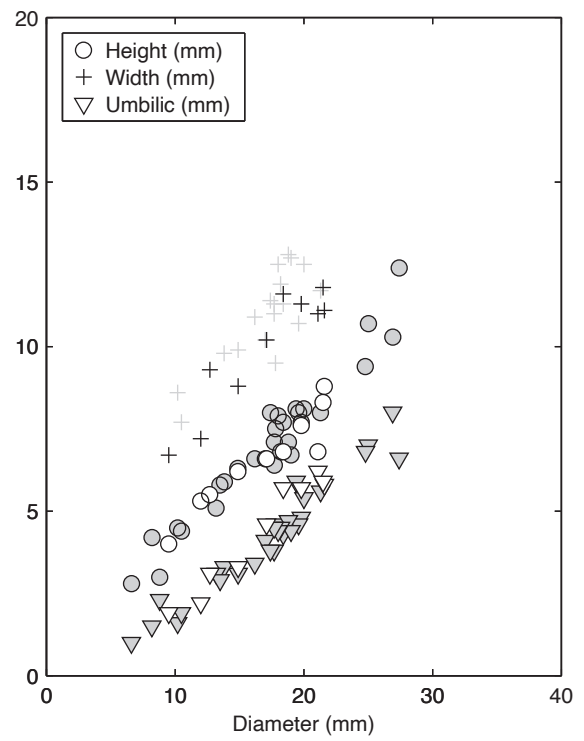


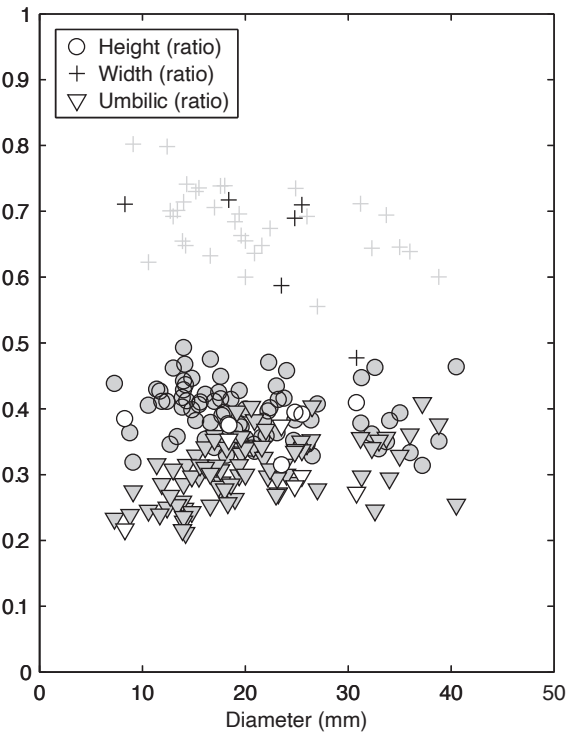
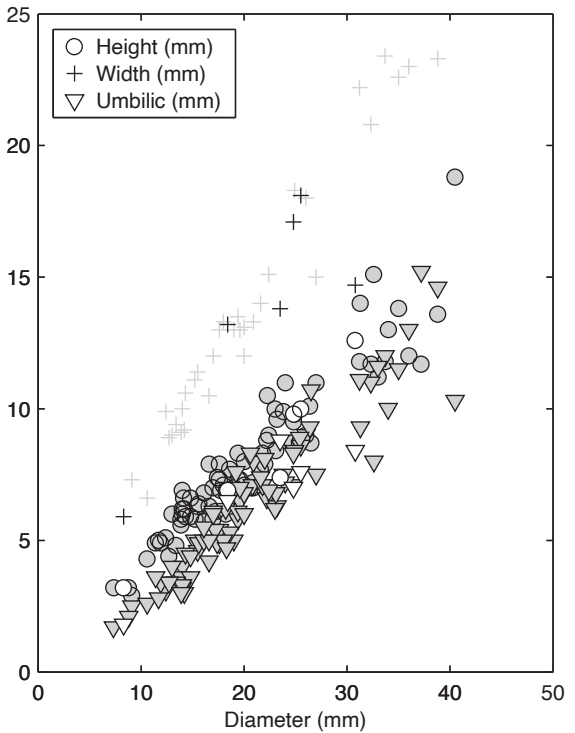
?Kashmireites cordilleranus
Palominoceras n. gen. nevadanum

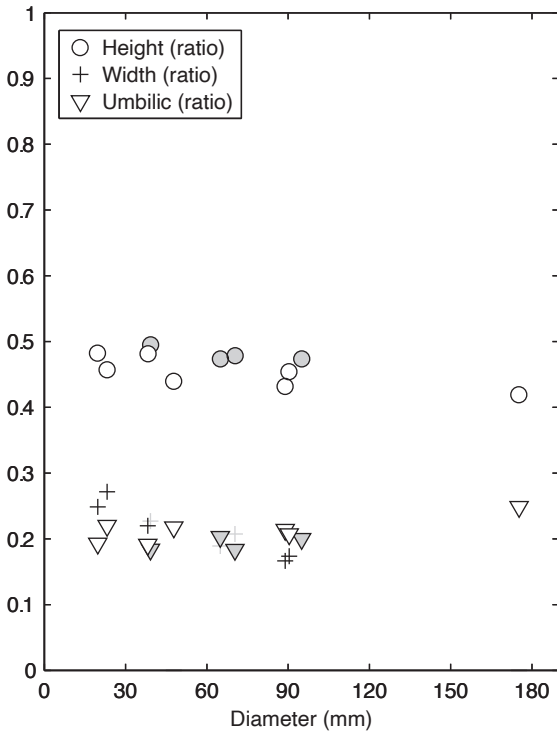
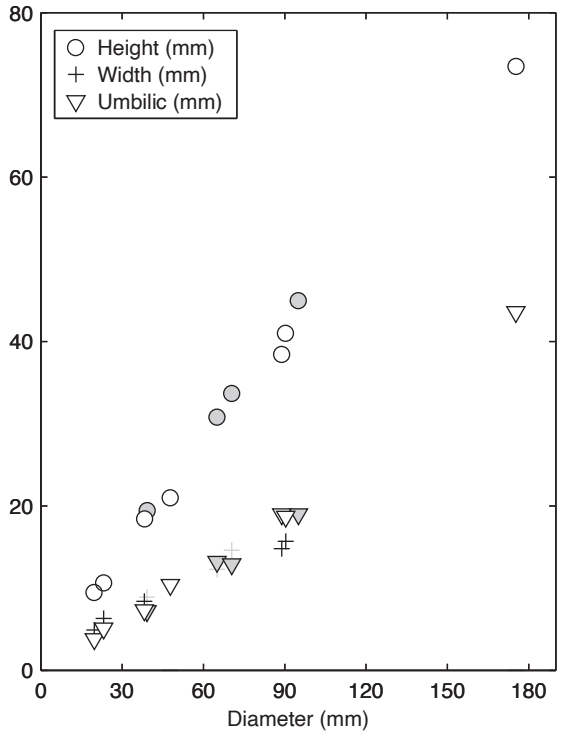


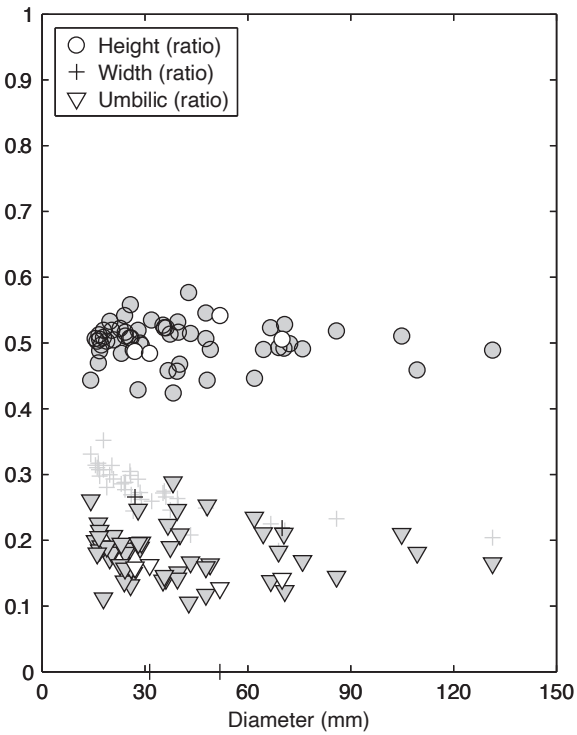
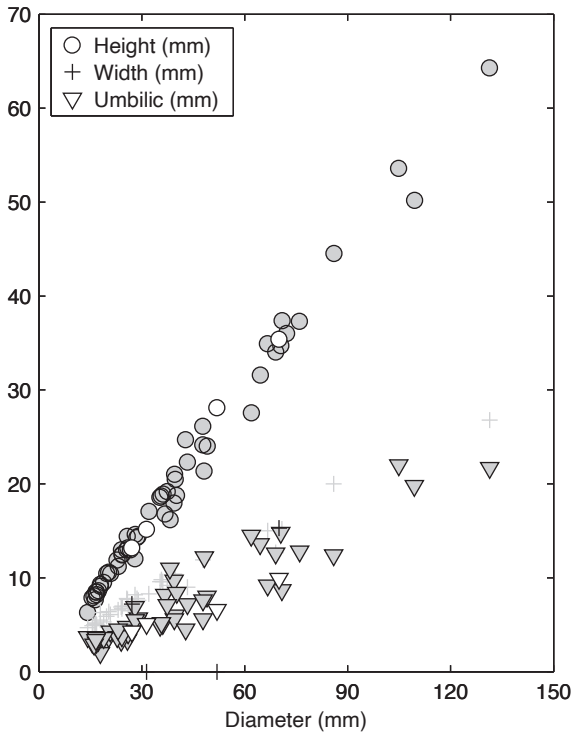


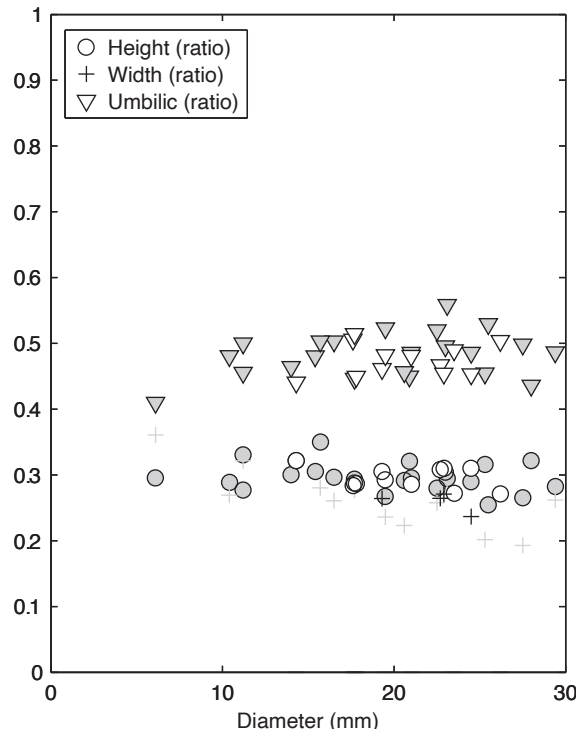
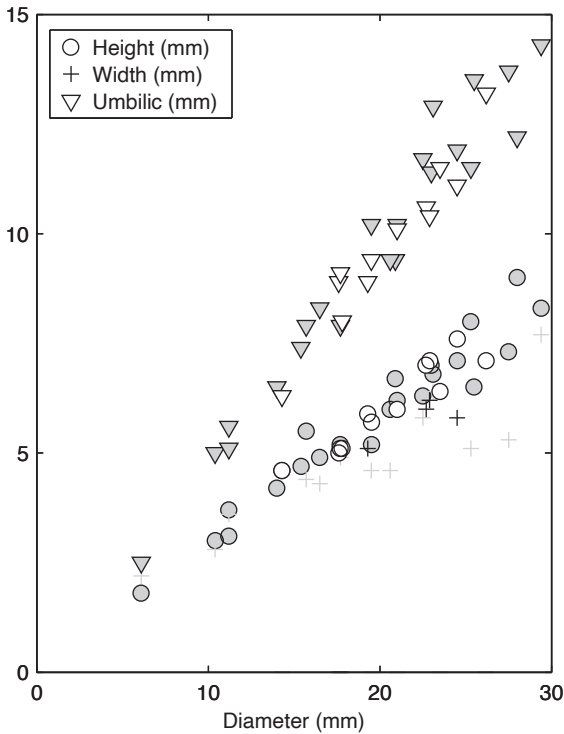


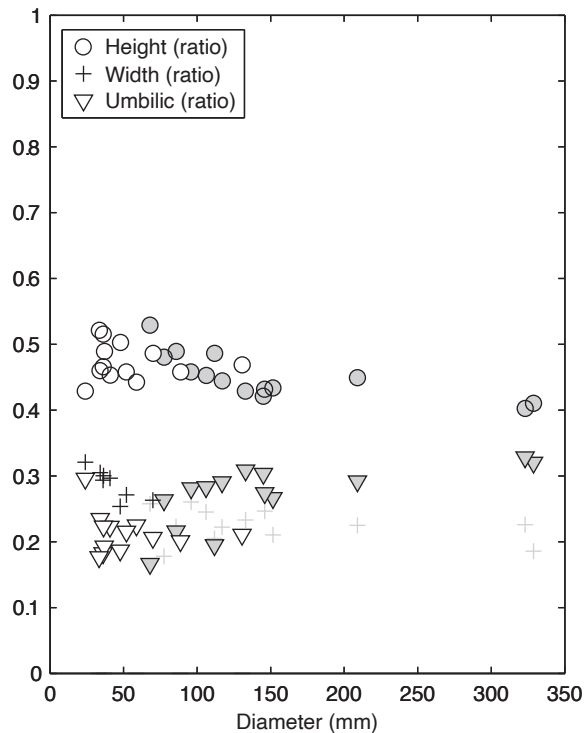
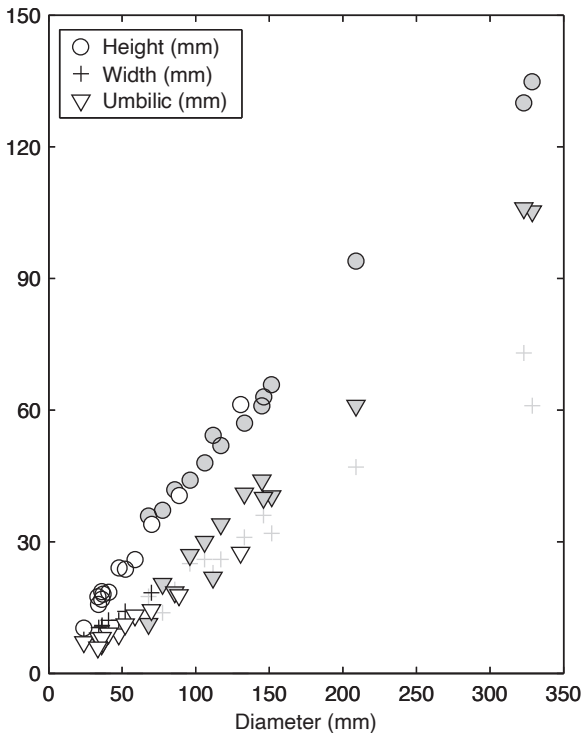


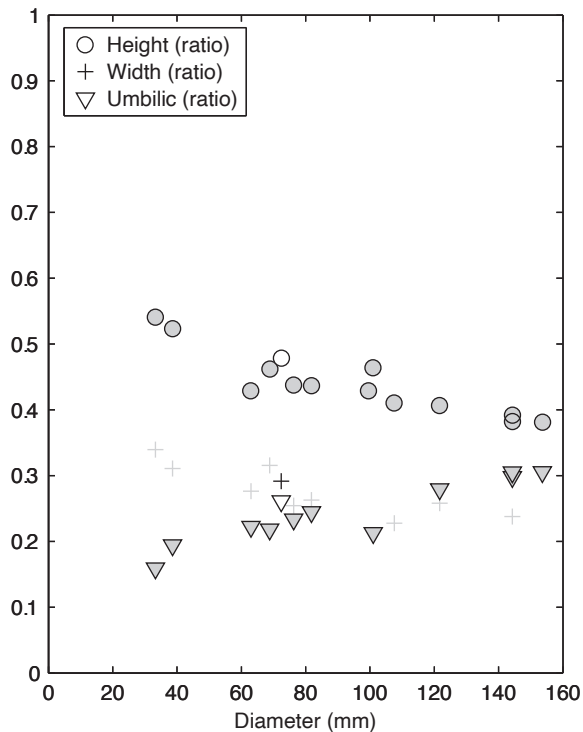
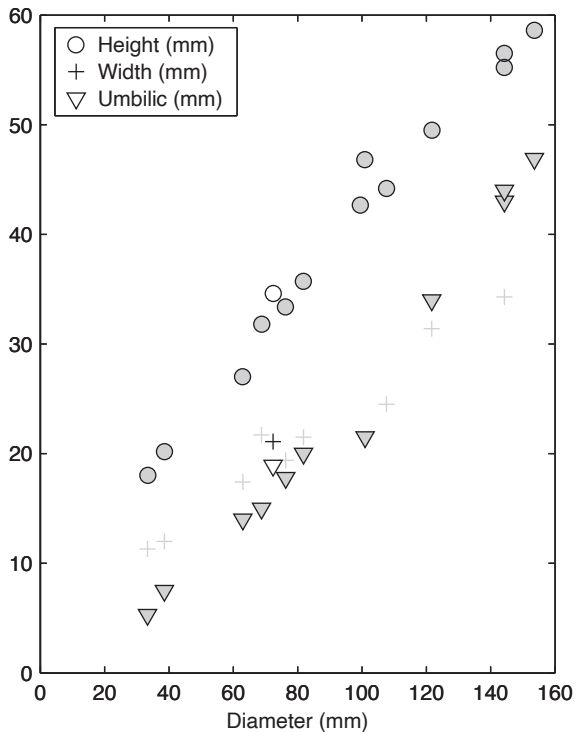


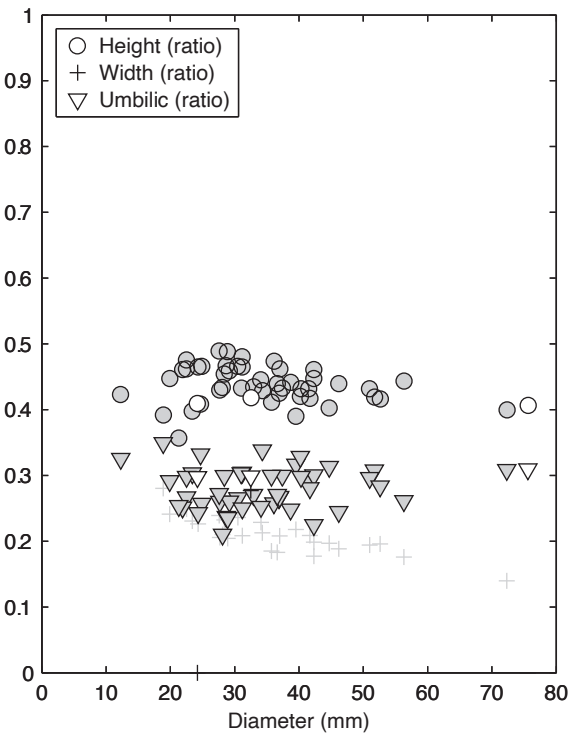
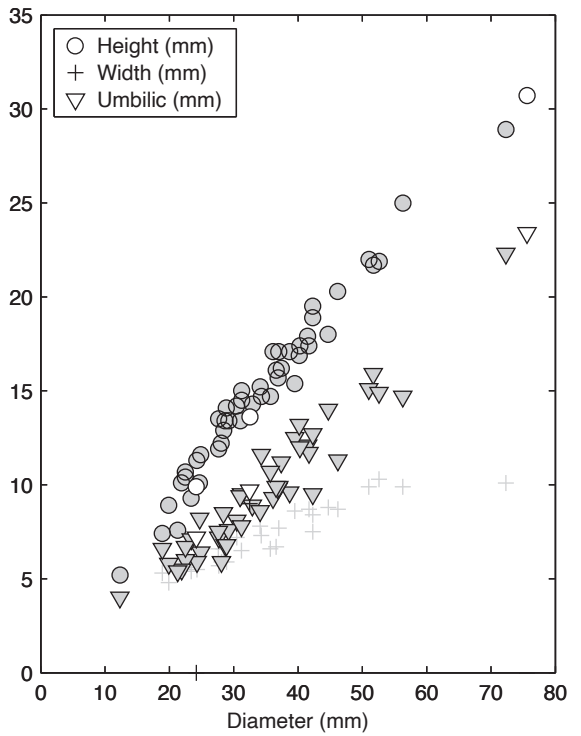


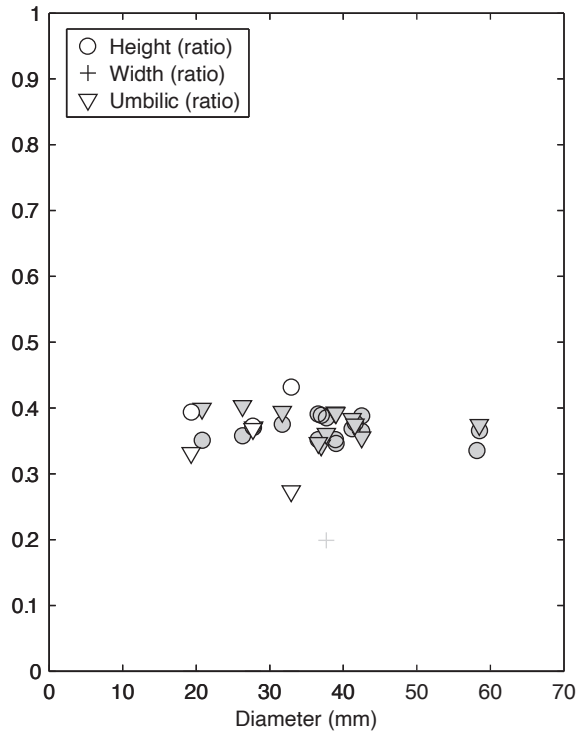
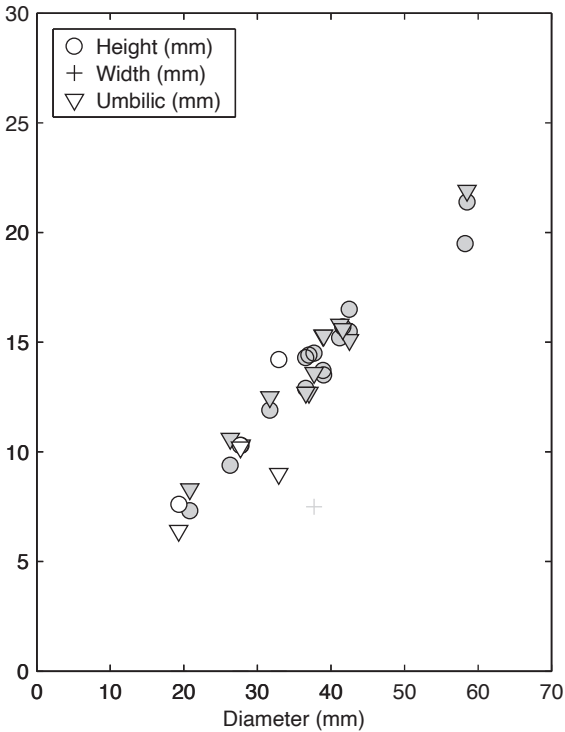


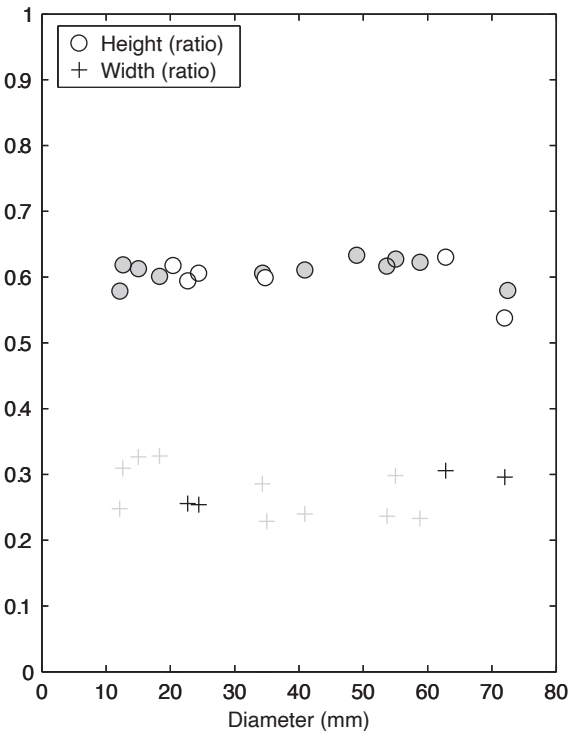
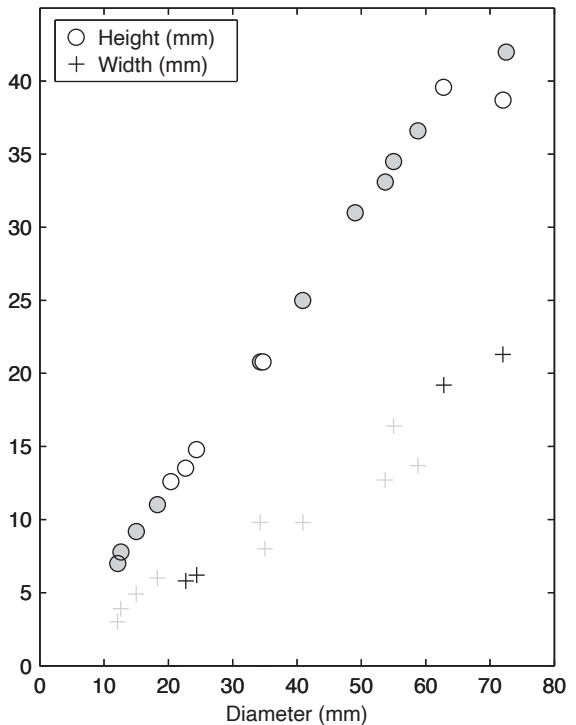


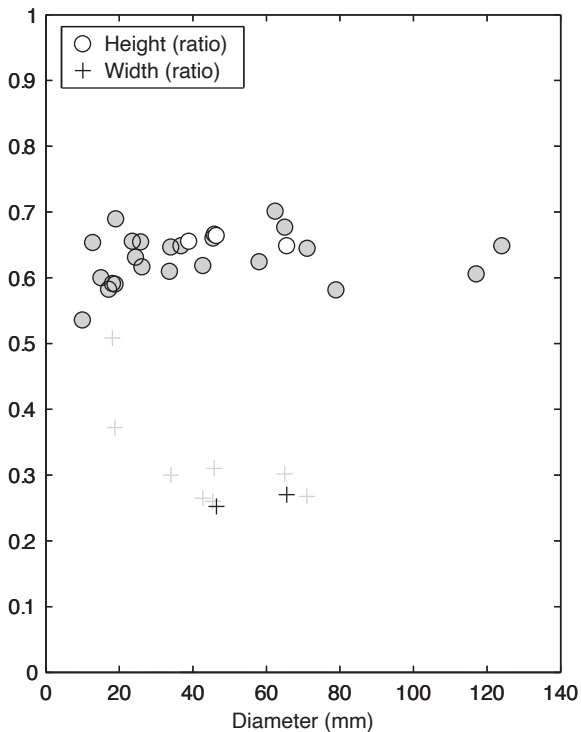
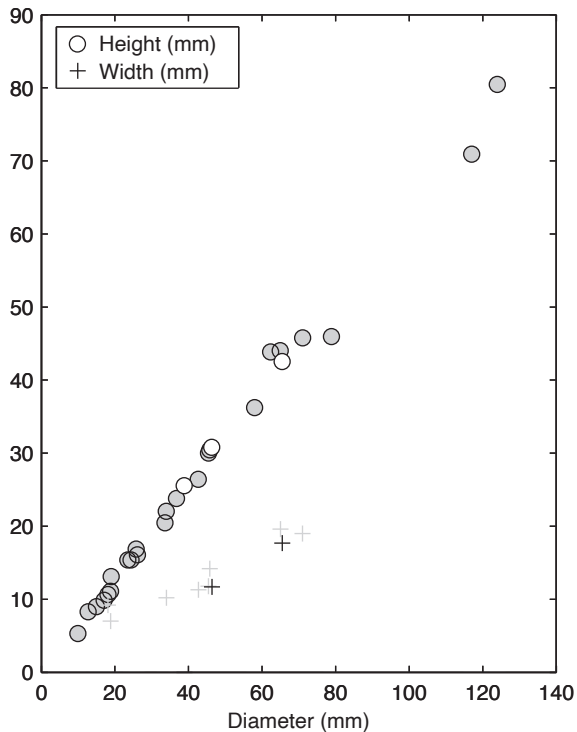


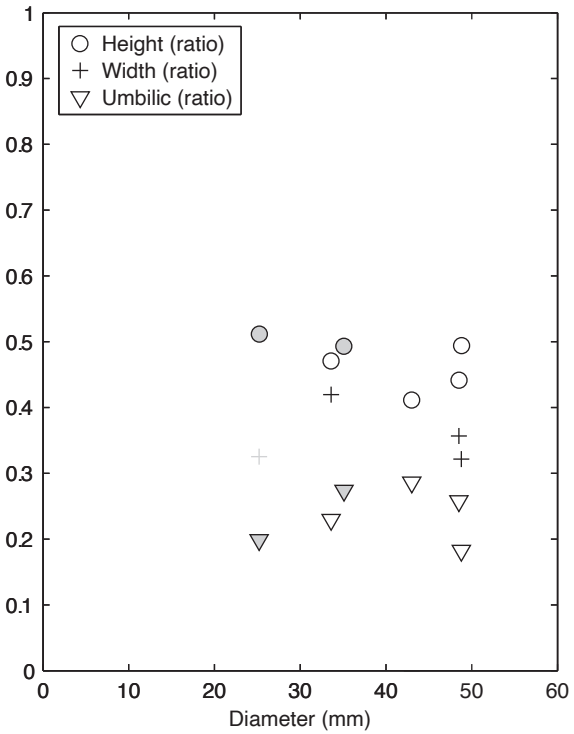
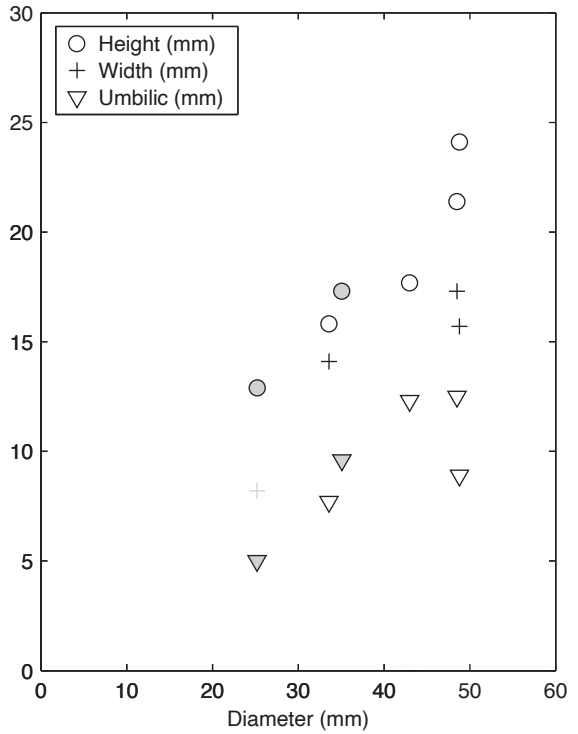


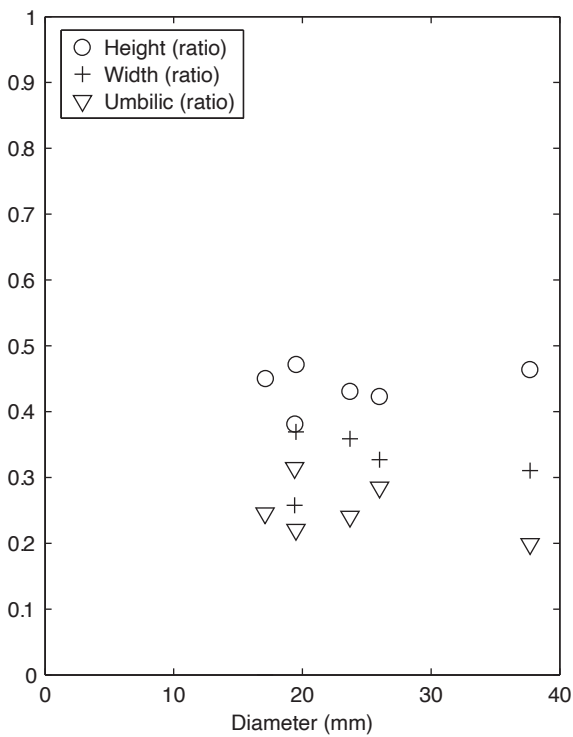
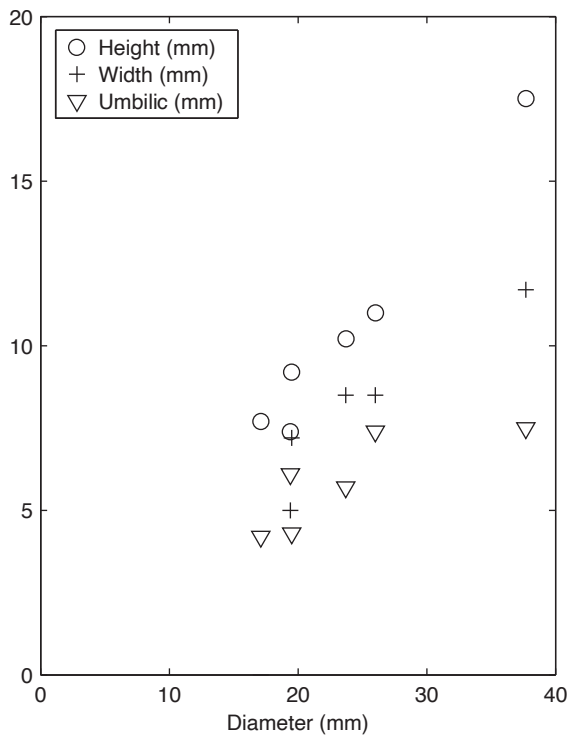


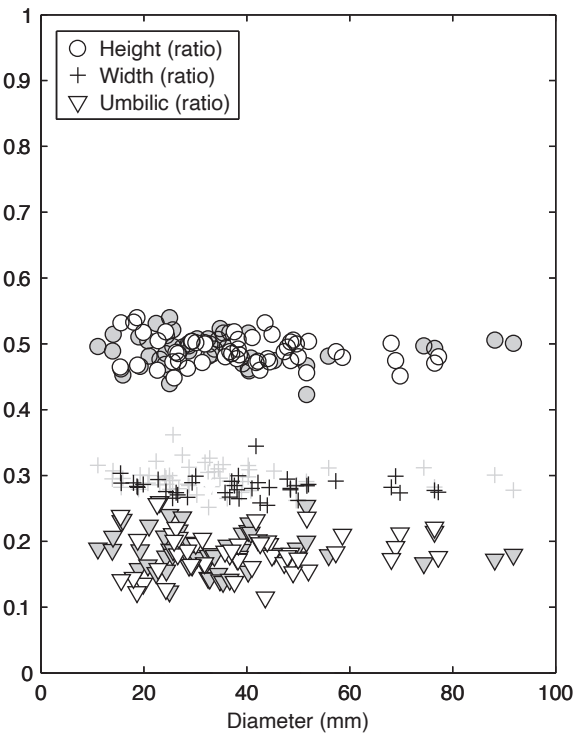
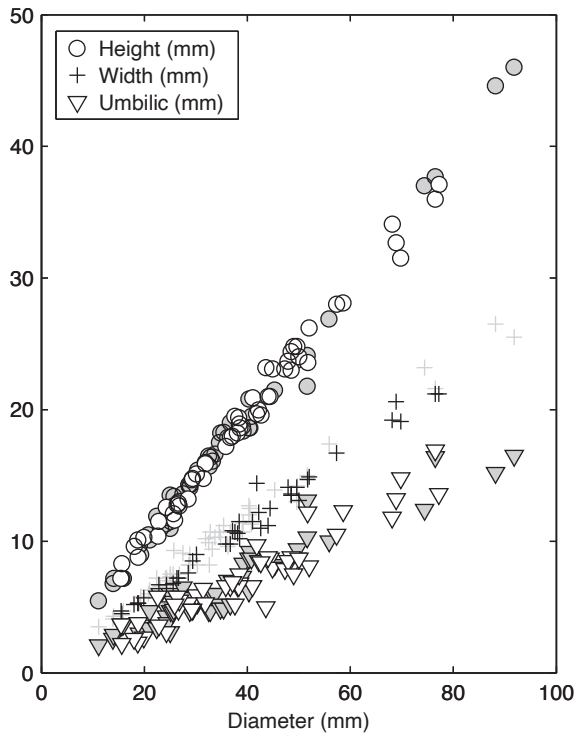


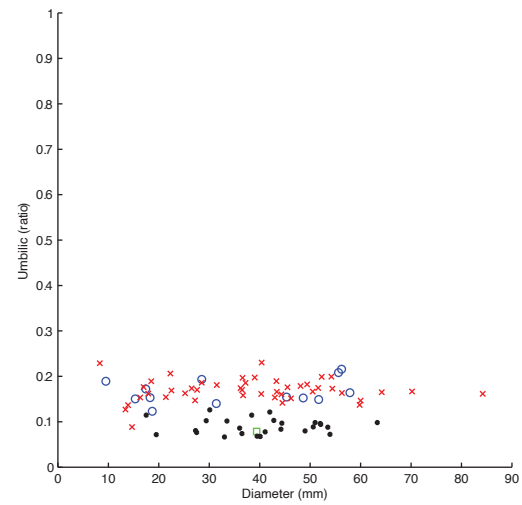
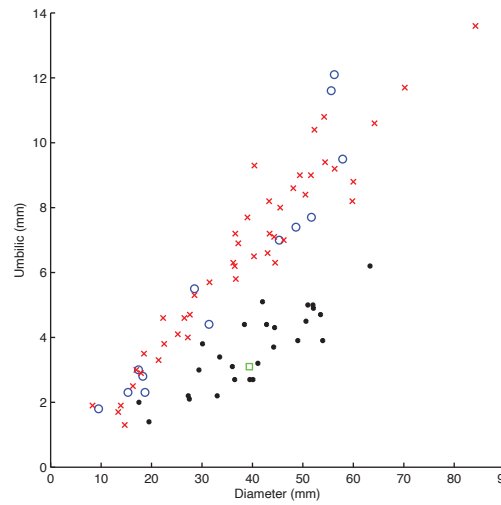
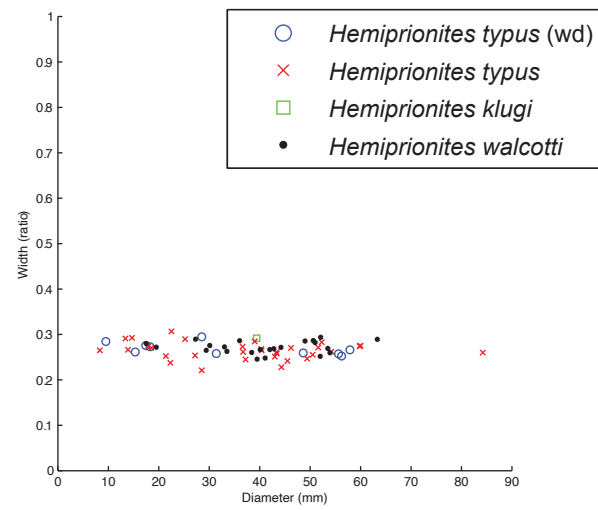
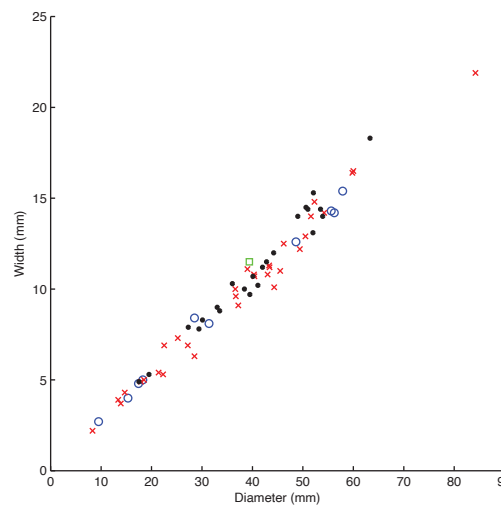
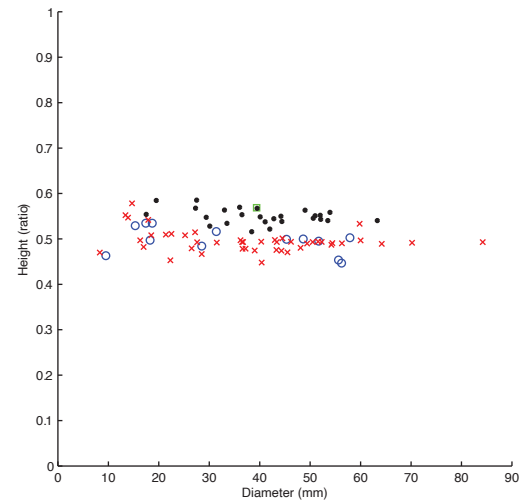
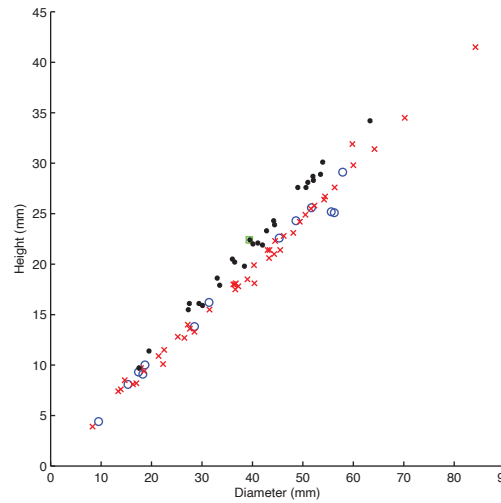












○	<i>Hemiprionites typus (wd)</i>
×	<i>Hemiprionites typus</i>
□	<i>Hemiprionites klugi</i>
●	<i>Hemiprionites walcotti</i>

